

VARIATIONS IN METAMORPHIC GRADE IN METAPELITES
IN TRANSECTS ACROSS THE QUETICO SUBPROVINCE
NORTH OF THUNDER BAY, ONTARIO

by

BARABRA ELLEN SEEMAYER ©

A thesis submitted in partial fulfillment of the requirements
for the degree of Master of Science

Department of Geology
Faculty of Arts and Science
Lakehead University
Thunder Bay, Ontario
February, 1992

ProQuest Number: 10611849

All rights reserved

INFORMATION TO ALL USERS

The quality of this reproduction is dependent upon the quality of the copy submitted.

In the unlikely event that the author did not send a complete manuscript and there are missing pages, these will be noted. Also, if material had to be removed, a note will indicate the deletion.



ProQuest 10611849

Published by ProQuest LLC (2017). Copyright of the Dissertation is held by the Author.

All rights reserved.

This work is protected against unauthorized copying under Title 17, United States Code
Microform Edition © ProQuest LLC.

ProQuest LLC.
789 East Eisenhower Parkway
P.O. Box 1346
Ann Arbor, MI 48106 - 1346



National Library
of Canada

Bibliothèque nationale
du Canada

Acquisitions and
Bibliographic Services Branch

Direction des acquisitions et
des services bibliographiques

395 Wellington Street
Ottawa, Ontario
K1A 0N4

395, rue Wellington
Ottawa (Ontario)
K1A 0N4

Your file *Votre référence*

Our file *Notre référence*

The author has granted an irrevocable non-exclusive licence allowing the National Library of Canada to reproduce, loan, distribute or sell copies of his/her thesis by any means and in any form or format, making this thesis available to interested persons.

L'auteur a accordé une licence irrévocable et non exclusive permettant à la Bibliothèque nationale du Canada de reproduire, prêter, distribuer ou vendre des copies de sa thèse de quelque manière et sous quelque forme que ce soit pour mettre des exemplaires de cette thèse à la disposition des personnes intéressées.

The author retains ownership of the copyright in his/her thesis. Neither the thesis nor substantial extracts from it may be printed or otherwise reproduced without his/her permission.

L'auteur conserve la propriété du droit d'auteur qui protège sa thèse. Ni la thèse ni des extraits substantiels de celle-ci ne doivent être imprimés ou autrement reproduits sans son autorisation.

ISBN 0-315-78947-6



TABLE OF CONTENTS

	<u>PAGE</u>
Abstract.....	i
Acknowledgements.....	iii
List of Figures.....	iv
Introduction.....	1
Previous Geological Work.....	9
Geology of the Study Area.....	15
Introduction.....	15
Block A.....	20
Block B.....	34
Block C.....	37
Block D.....	52
Mineralogy of Metapelites.....	56
Feldspars.....	58
Chlorite.....	58
Biotite.....	58
Muscovite.....	61
Staurolite.....	61
Garnet.....	62
Cordierite.....	64
Andalusite.....	64
Sillimanite.....	65
Metamorphism.....	65
Low Grade Metamorphism in Pelites.....	67
Medium Grade Metamorphism in Pelites.....	72
High Grade Metamorphism in Pelites.....	75
Granulites.....	79
Quantitative Analyses of Minerals.....	80
Geothermobarometry.....	86
Baric Types.....	92
Discussion and Interpretation.....	93
A Model for Archean Crustal Evolution.....	93
A General Model.....	95
Evolution of Rocks in the Study Area.....	100
Conclusions.....	110
References.....	114
Appendices.....	119

ABSTRACT

The Quetico subprovince is a northeast-southwest striking linear belt of migmatites, gneisses, and metasedimentary rocks. These Archean rocks form part of the southern Superior Province. This study involves an examination of variations in metamorphic grade along cross-strike transects in an area north of Thunder Bay, Ontario.

The rocks of the Quetico subprovince include metasedimentary rocks with well preserved primary structures, knotted schists, gneisses, migmatites, and anatectic granitic rocks. Metamorphic porphyroblasts include muscovite, biotite, garnet, staurolite, cordierite, andalusite, and sillimanite. Chemical analyses of garnets, geothermobarometry, and mineral assemblage data were used to determine variations in metamorphic grade in transects across the subprovince.

Mineral assemblages characteristic of low to high grade metamorphism are exposed along an across-strike transect. Metamorphic grade rises gradually from low grade (521°C) to high grade (714°C) northwards along Highway 527. North of the peak conditions, the grade drops off sharply. Garnet-biotite geothermometry confirms this pattern. Maximum pressure reached in the study area is approximately 5 kbar.

The model proposed to account for the distribution of metamorphic assemblages and minerals involves transpression of the Quetico accretionary prism between the Wabigoon volcanic cratonic margin to the north and the docking Wawa volcanic complex to the south. Buckling and folding of the sedimentary rocks was accompanied by thrusting. Erosion has exposed high grade migmatitic and anatectic rocks within the Quetico fold belt which developed as a result of thermal relaxation of depressed isotherms. The boundaries between metavolcanic and metasedimentary terranes are structurally complex. Boundaries may be best described as geometrically complex zones up to several kilometres in extent in which various rock types representative of the adjacent terranes have been folded, faulted, and intruded.

ACKNOWLEDGEMENTS

I would like to thank Dr. Manfred Kehlenbeck for suggesting and supervising this study as well as for his untiring support, advice, and encouragement. Thanks are also extended to Drs. Ken Card and John Percival at the Geological Survey of Canada who acted as external readers and whose constructive criticism and helpful comments greatly improved this thesis, and to Dr. Graham Borradaile whose suggestions helped clarify the manuscript. Dr. John Percival supplied the PTmeter program and Dr. Mikkel Schau of the G.S.C. guided me through it. Dr. Garth Platt supplied the MINFILE program. Anne Hammond and Reino Viitala cheerfully prepared thin sections and polished sections and Sam Spivak provided drafting advice. Al Mackenzie at Lakehead University and Ron Chandler at University of Manitoba provided assistance and advice on quantitative mineral analysis.

I would like to thank the geology faculty of Lakehead University for their instruction and helpfulness over the years, and my fellow students for sharing their interest and joy in geology. Heartfelt thanks go to my parents for their constant love, support, and encouragement throughout my strange endeavors, and to Brian, for keeping me happy.

Finally, I gratefully acknowledge NSERC for providing two years of financial support in the form of PGS1 and PGS2 Postgraduate Scholarships.

LIST OF FIGURES

- Fig. 1 General geological map of the study area
- Fig. 2 Sample location map
- Fig. 3 Geological map of the study area
- Fig. 4 Index map of the study area
- Fig. 5 Turbidite bed showing Bouma sequence
- Fig. 6 Primary sedimentary features
- Fig. 7 Poles to bedding
- Fig. 8 Major fold asymmetry
- Fig. 9 Intrafolial folds
- Fig. 10 Ptygmatic fold
- Fig. 11 Refolded folds
- Fig. 12 Sheath folds
- Fig. 13 Poles to foliations
- Fig. 14 Lineations
- Fig. 15 Coarse-grained fibrous sillimanite
- Fig. 16 Polymetamorphic schist
- Fig. 17 Feldspar compositions
- Fig. 18 Metamorphic mineral assemblage map
- Fig. 19 P-T petrogenetic grid
- Fig. 20 Mineral assemblages
- Fig. 21 Garnet plot: $(\text{MnO} + \text{CaO})$ vs $(\text{FeO} + \text{MgO})$
- Fig. 22 Garnet-biotite geothermometry
- Fig. 23 Variations in temperature in a transect across strike
- Fig. 24 Proposed evolution of the Quetico subprovince
- Fig. 25 Geologic cross-section of the study area

INTRODUCTION

The Archean rocks of the Superior Province of the Canadian Shield have been subdivided into a number of linear, east-west trending subprovinces (Fig. 1). These subprovinces are distinguished from one another by variations in lithology, structure, metamorphism, geophysical and metallogenetic characteristics, and ages of rock units and tectonic events (Card, 1990). On a regional scale the subprovinces can generally be identified on the basis of lithology. "Greenstone belts" or "greenstone-granite terranes" such as the Wabigoon and Wawa subprovinces are composed of metavolcanic, volcanoclastic, and minor sedimentary rocks and have been extensively intruded by granitic rocks. "Gneiss belts" or "metasedimentary terranes" such as the Quetico and English River subprovinces, on the other hand, include metasedimentary rocks, gneisses, migmatites, and anatectic rocks of predominantly magmatic and/or migmatitic origin (Mackasey et al., 1974).

In the western Superior province, the age of deformation and metamorphism for the subprovinces decreases from north to south (Langford and Morin, 1976; Card, 1990). Volcanic and plutonic rocks in the Sachigo subprovince give ages of up to 3023 Ma (Card, 1990). The age of emplacement of granitic plutons within the Superior province ranges from 2.65 to 2.90 b.y., which is generally synchronous with the time of extensive volcanism (Goodwin and West, 1974). Throughout the southern Superior province, volcanism and plutonism was active during the interval between 2750 and 2680 Ma

Fig. 1 General geology of the western part of the Archean Superior Province (after Card and Ciesielski, 1986).

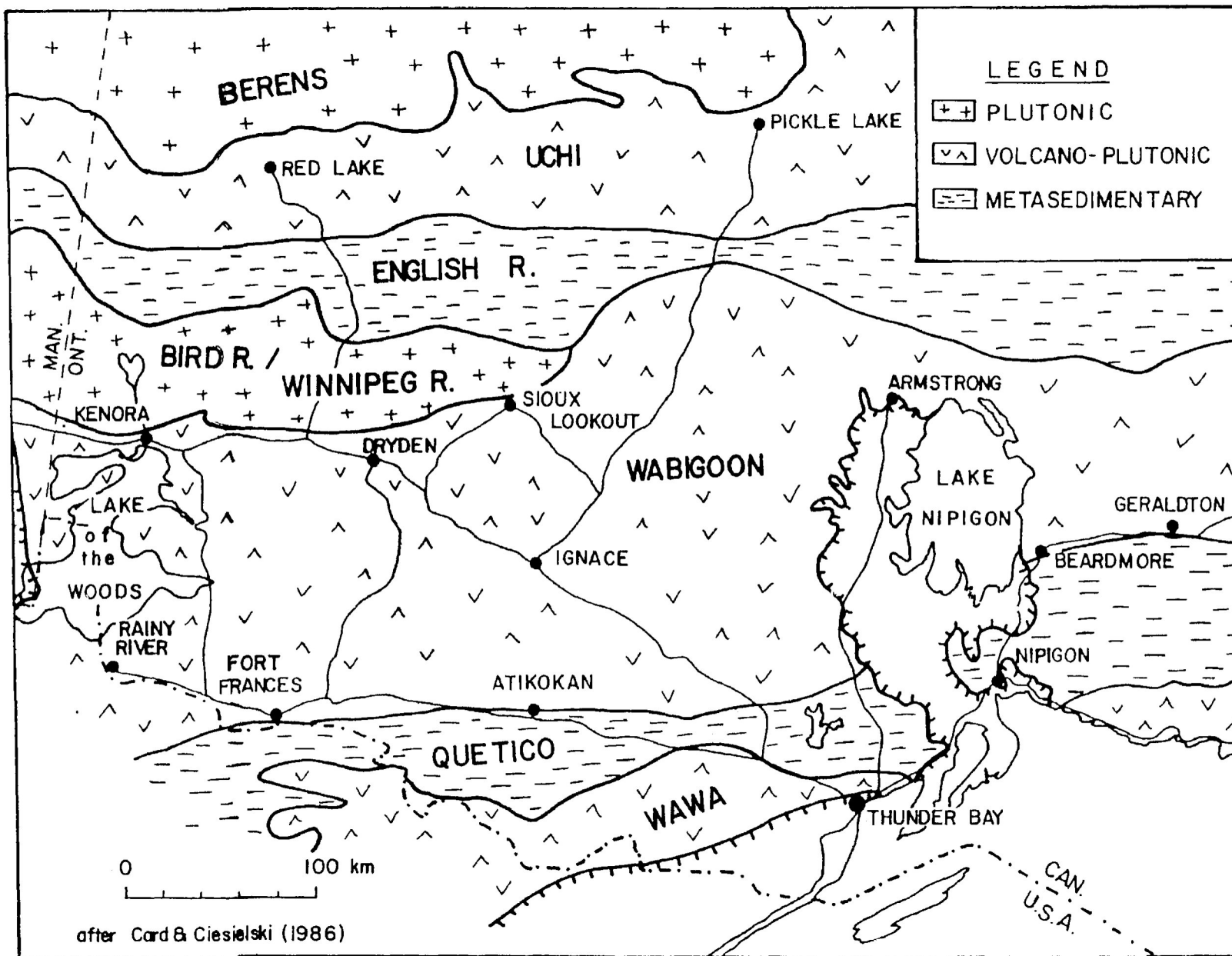


Fig. 1

(Percival and Sullivan, 1988). Davis et. al. (1989) determined an absolute time span for igneous activity in the Rainy Lake area from 2686 to 2728 Ma and found that Quetico subprovince sediments were deposited between 2698 and 2688 Ma. Card and Ciesielski (1986), Percival (1989), Williams (1990), and Card (1990), among others, have suggested that the subprovinces represent a series of accreted volcanic arcs and their associated accretionary prisms.

Several workers have noted that the subprovinces exhibit contrasting structural styles and metamorphic regimes. For example, Borradaile (1982) stated that the dominant tectonic style of the Wabigoon greenstone belt near Flanders, Ontario is one of steeply plunging, sideways closing, single-generation isoclinal folds with curvilinear hinges. Sheath folds with coplanar primary cleavage surfaces were documented in this same area near the faulted northern boundary of the Quetico subprovince (Borradaile et. al., 1988). To the south primary folds become more homoaxial until small-scale polyphase deformation becomes evident in the interior of the subprovince.

Ayres (1978) pointed out that the metavolcanic rocks of the greenstone belts are metamorphically zoned. The highest metamorphic grades occur in rocks adjacent to granitic batholiths which provided the heat source for much of their metamorphism. Narrow zones of amphibolite facies metamorphism and discontinuous zones of hornblende hornfels are found adjacent to the batholiths. Greenschist facies conditions are reflected in

metavolcanic rocks farther away from the intrusions. Low grade assemblages are common in the metasedimentary rocks of a gneiss belt where they are in contact with low grade metavolcanic rocks of an adjacent greenstone belt. Where the subprovince boundary is marked by a fault, however, there is an abrupt increase to higher metamorphic grade in the metasedimentary rocks (Ayers, 1978; Borradaile and Spark, 1991). Card and Ciesielski (1986), Percival (1989), and Card (1990) pointed out that mineral assemblages of rocks from the Quetico subprovince show that greenschist facies metamorphism near the subprovince margins is replaced by low-pressure amphibolite facies and locally granulite facies metamorphism toward central portions of the subprovince. Detailed examinations of metamorphism in parts of the Quetico terrane include those by Kehlenbeck (1976), Pirie and Mackasey (1978), Percival et. al. (1985), and Percival (1989).

The exact nature of the subprovince boundaries remains uncertain. In some places boundaries are clearly marked by faults. For example, the Quetico Fault between Rainy Lake and Lac des Milles Lacs separates the Quetico and Wabigoon subprovinces. In other places it is impossible to delineate boundaries by a single line on a geological map. Due to tectonic stacking, possibly coupled with primary lateral facies changes, outcrops of sedimentary and volcanic rocks often alternate over several kilometres in cross-strike traverses near the suspected boundary. Because of this relationship the contact between sedimentary and volcanic rocks as such is a poor criterion for boundary definition.

It therefore seems reasonable to suggest that, in general, subprovince boundaries are structurally complex, lithologically diverse transition zones between adjacent subprovinces. These zones may also be characterized by systematic changes in metamorphic grade.

The purpose of this study is to determine variations in metamorphic grade along a transect across metasedimentary and migmatitic rocks of the "Quetico subprovince". It is expected that an examination of mineral compositions and assemblages from metapelites will provide data which will permit conclusions on the presence or absence of systematic variations in grade across the strike of the rocks.

The area selected for study is located north of Thunder Bay, Ontario. Access to the area is excellent, via several highways and minor roads which cross the strike of the rocks at a high angle. Field work completed during the summer of 1990 and spring of 1991 included detailed examination and sampling of representative outcrops in several transects (Fig. 2). Structural elements were recorded and attitudes measured. Critical mineral assemblages were noted in outcrop and in thin section. A scanning electron microscope with energy-dispersive analytical equipment and an electron microprobe were used to determine the compositions of metamorphic minerals. Samples were collected from rocks of similar bulk composition and consequently the mineral data should reflect

Fig. 2 Sample location map.

changes in metamorphic grade rather than variations in bulk composition of the rocks.

PREVIOUS GEOLOGICAL WORK IN THE QUETICO SUBPROVINCE

The Quetico subprovince has been variously referred to as a metasedimentary, gneissic, or migmatitic terrane, in contrast with the adjacent Wabigoon and Wawa metavolcanic "greenstone-plutonic" terranes. The northeast-southwest striking Quetico subprovince extends for 1200 km from its contact with Paleozoic strata in western Minnesota to the Kapuskasing Structure in the east. The subprovince ranges in width from 10 to 100 km. Linear gravity and aeromagnetic lows characterize much of the subprovince, although metasedimentary rocks produce slight gravity highs relative to the granitoid regions (Kehlenbeck and Cheadle, 1990). The depth to the Moho beneath the Quetico subprovince is in the range 35-42 km (Percival, 1989).

Summaries of geochronological work in the Quetico subprovince have been published by Percival and Sullivan (1988), Davis et. al. (1989), Percival (1989), and Davis et. al. (1990). Davis et. al. (1989) found detrital zircons from Coutchiching metagreywackes near Rainy Lake to range in age from 3059 \pm 3 Ma to 2704 \pm 3 Ma, indicating the presence of some old material in the sediment source region. A felsic sill provided a lower age limit of 2692 \pm 2 Ma. Since single zircon data from Quetico metasedimentary rocks showed a similar age distribution to those of the Coutchiching, Davis et.

al. (1989) suggested that Quetico and Coutchiching rocks are correlative.

Davis et. al. (1990) performed U-Pb analyses on single detrital zircon grains from the northern boundary of the Quetico subprovince in northwestern Ontario. Zircons from Quetico metasedimentary rocks gave ages from 2698 \pm 3 Ma, the older limit of deposition, to 3009 \pm 4 Ma. A late, cross-cutting intrusion provided a lower limit of 2688 \pm 4 Ma. Deposition and metamorphism of the metasedimentary rocks was therefore bracketed within a 10 \pm 5 Ma time span.

Although zircons give evidence of source rocks of up to 3009 \pm 4 Ma in age, the majority give ages in the 2709 - 2698 Ma range. This corresponds to the time of emplacement of late intrusions and associated volcanic rocks of the Kakagi Lake - Savant Lake greenstone belt to the north and are therefore suggestive of a sediment source from the Wabigoon subprovince. Davis et. al. (1990) did not rule out zircon contribution from the Shebandowan-Wawa subprovince to the south, and indicated that the southeast part of the Superior province may also have contributed detritus which was transported longitudinally in the Quetico sedimentary basin.

Percival and Sullivan (1988) reported detrital zircon ages of 3100, 2880, and 2702 Ma in Quetico rocks. White, pink, and pegmatitic granites yielded ages of 2671, 2667, and 2652 Ma,

respectively. Based on their results Percival and Sullivan (1988) suggested that the sedimentary rocks of the accretionary prism became contiguous with the adjacent volcanic arcs by about 2685 Ma ago and were affected by common transpressional deformation at 2684-2679 Ma. Major plutonism in the Quetico subprovince occurred between 2671 and 2665 Ma, significantly later than the peak plutonism of 2680 Ma in the Wawa subprovince and the even earlier igneous activity of the Wabigoon subprovince (Percival and Sullivan, 1988).

Delineation of subprovince boundaries depends on the criteria used to distinguish individual subprovinces. Boundaries based on lithology may be in different positions than those determined by metamorphic or structural character of the rocks. In the west, the Quetico-Wabigoon boundary is clearly marked by faults. The Rainy Lake-Seine River fault separates the Quetico subprovince from the Rainy Lake wrench zone, a wedge-shaped fault-bounded block of unknown affinity situated between the Quetico and Wabigoon subprovinces (Tabor and Hudleston, 1991). West of Atikokan the Rainy Lake-Seine River fault merges with the Quetico Fault, which separates Quetico metasedimentary rocks from volcanic and sedimentary rocks of the Wabigoon subprovince. At the present level of erosion, the approximately east-west trending Quetico Fault zone forms the northern boundary of the Quetico subprovince for over 200 km between Rainy Lake and Lac des Milles Lacs. East of Lac des Milles Lacs the fault cuts rocks of the Quetico

subprovince. Dextral displacement along the fault has been estimated at 100 km (Mackasey et. al., 1974).

Kehlenbeck (1976) described the structure and metamorphism of a sequence of schists and gneisses about 55 km north of the city of Thunder Bay. He concluded that the supracrustal, regionally metamorphosed rocks in this area were intruded by paligenetically generated magmas of basement gneisses and suggested that a polymetamorphic zone of approximately 8 km in width represented the Quetico-Wabigoon boundary. Kehlenbeck (1986) also examined rocks in the vicinity of the Quetico-Wabigoon boundary in the Beardmore-Geraldton area to the east. He found the transition zone to be marked by a series of fault-bounded, internally-folded panels. The shear sense along panel boundaries is dominantly dextral and the hinge lines of the folds are strongly curvilinear. Overall structural facing directions vary from upward-facing in the west, through sideways-facing, to downward-facing in the east. However, structural facing directions between adjacent panels also vary. Because of this alternation in structural facing direction, Kehlenbeck (1986) concluded that folds of more than one generation existed prior to their disruption by shears.

Devaney and Williams (1989) examined the Quetico-Wabigoon boundary in the Beardmore-Geraldton area. They interpreted the fold belt described by Kehlenbeck (1986) as a tectono-stratigraphically distinct, thrust-imbricated supracrustal stack. Their "Beardmore-Geraldton Terrane" (BGT) consists of three metasedimentary belts and three metavolcanic belts. The BGT

sedimentary belts were thrust-imbricated, together with their basaltic volcanic basement, into the present steeply-dipping succession. Based on similarities in lithology, top indicators, and regional context, Devaney and Williams (1989) suggested the sedimentary belts could be correlated with each other as well as with the Quetico sedimentary terrane. They concluded that the BGT represents a southward-prograding sedimentary basin deposited on a basaltic basement which has become thrust imbricated into belts of repeated sedimentary-volcanic couplets forming a transition zone between the Quetico and Wabigoon subprovinces.

Williams (1990) placed the BGT within the Wabigoon subprovince on the basis of structure and lithologic criteria. He suggested the Wabigoon-Quetico and Quetico-Wawa subprovince boundaries were originally shallowly-dipping reverse dip-slip shear zones.

Sawyer (1983) and Borradaile and Spark (1991) examined the Wawa-Quetico boundary in the Planet-Huronian Lakes area. Sawyer (1983) mapped a series of isograds which approximately parallel the subprovince boundary and described multiple episodes of penetrative deformation. This view was disputed by Borradaile and Spark (1991) who found only one penetrative deformation in the rocks of the same area. Younging directions in both the Quetico metasedimentary and Shebandowan metavolcanic rocks are consistently northward and rocks on both sides of the boundary possess a single subvertical, east-west striking penetrative cleavage. No obvious discrete boundary structure such as a broad shear zone was found, although there is

a transition from a metabasaltic Wawa sequence to a metagreywacke Quetico sequence as well as a steep greenschist-to-amphibolite facies metamorphic gradient. Borradaile and Spark (1991) documented a slight obliquity in the orientations of magnetic and mineral lineations. Based on analyses of magnetic and strain fabrics, they suggested a dextral transpressive kinematic model for this area with compression normal to the subprovince boundaries.

Kehlenbeck (1983) discussed multiple folds in sedimentary rocks near the Quetico-Wawa boundary in the Hazelwood Lake area north of Thunder Bay. In a description of refolded fold geometry he commented on the difficulty of drawing a simple boundary line between the subprovinces. The location of the boundary may vary by several kilometres depending on whether it is placed on the basis of lithology or structural style.

Previously published geological maps available at various scales cover all or parts of the present study area. The recently published Ontario Geological Survey map 2542, **Bedrock Geology of Ontario** (1991) covers the west-central part of Ontario at a scale of 1:1 000 000. The Atikokan-Lakehead map sheet covers an area from Lake Nipigon in the east to Flanders in the west and from Ignace in the north to the Canada-United States border the south at a scale of 1 inch to 4 miles (Pye and Fenwick, 1964). Gorham Township, in the southern half of the study area, was mapped at a scale of 1 inch to 1 mile (Macdonald, 1939) and the Starnes-Eyres Lake map, covering the northern part of the study area west of

Eaglehead Lake, was mapped by Kaye (1969) at a scale of 1 inch to 1 mile.

A number of HBSc and MSc theses have been written at Lakehead University which cover sections of this study. Noteworthy are those by Kyryluk (1973), Lehto (1975), Chiew (1976), Perry (1976), Peden (1978), and Kennedy, (1980).

GEOLOGY OF THE STUDY AREA

INTRODUCTION

The geological map of the study area (Fig. 3) is based on previously published data by MacDonald (1938), the Ontario Geological Survey (1991), Kehlenbeck (1976, 1983, and pers. comm.), and Seemayer (1989). Additional data were collected by the writer during the 1990 and 1991 field seasons. For the purposes of this discussion the geological map has been sub-divided into four blocks. The reader is referred to the index map (Fig. 4) for location of these subdivisions. The blocks are designed to aid in the description of the regional geology. They are not intended to represent any specific geological terrane, nor are the boundaries between blocks suggestive of subprovince boundaries. Rock names used here correspond to those listed in the geological map legend of Fig. 3.

BLOCK A

Fig. 3 Geological map of the study area.
The cross-section X-Y is discussed in Fig. 23.

GEOLOGICAL MAP

-  Metavolcanic rocks
-  Migmatite
-  Mylonite
-  Silicic to Intermediate intrusives
-  Metasedimentary rocks
-  Schists, foliats, & gneisses
-  Leucogranite
-  Porphyritic quartz monzonite
-  dip < 45°
-  unconformity

based on data by
 MACDONALD, 1938
 O.G.S., 1991
 KEHLENBECK, 1976 & 1988
 SEEMAYER, 1989 to 1991
 KEHLENBECK, pers. comm.

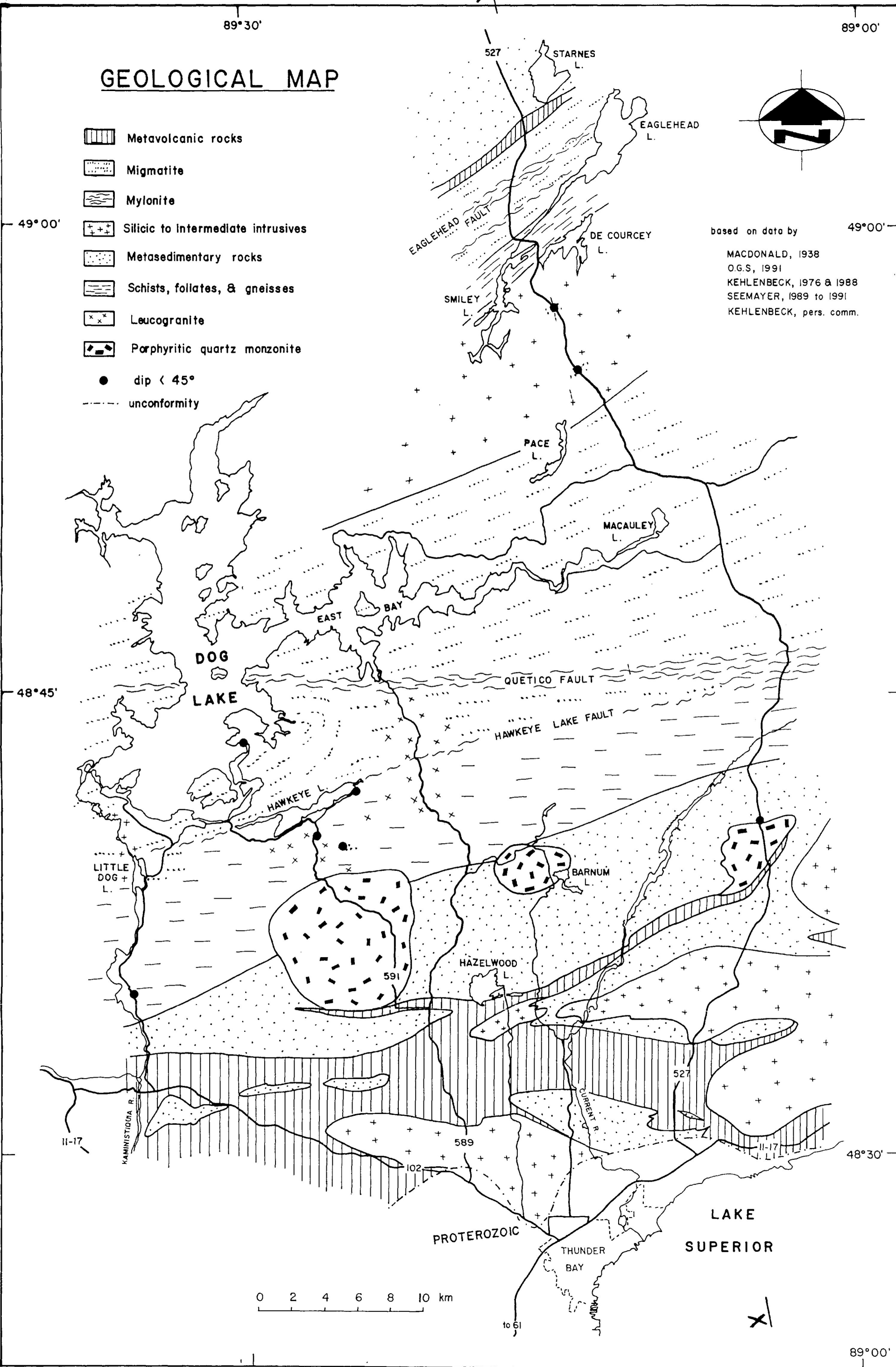
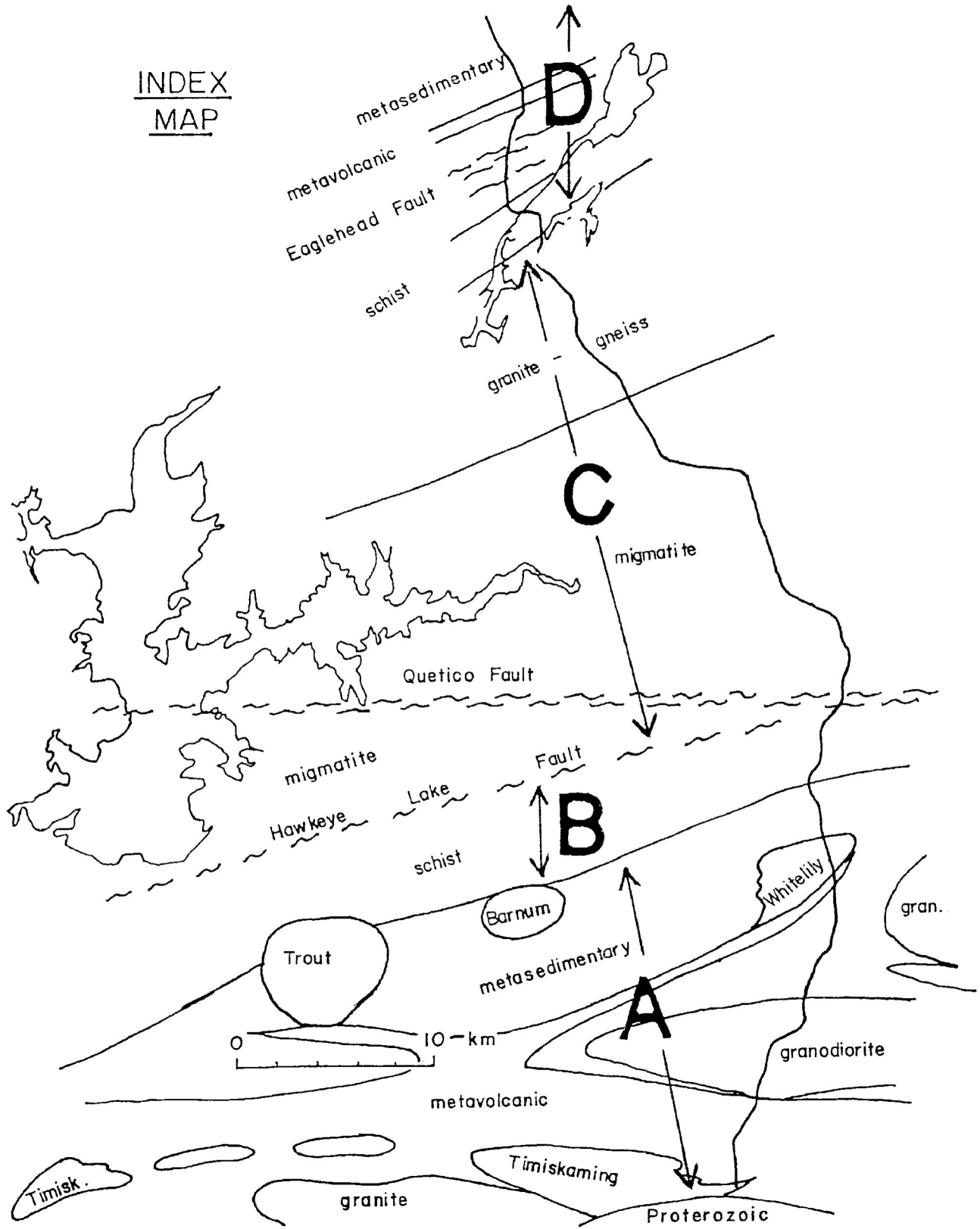


Fig. 3

Fig. 4 Index map of geology of the study area. Block boundaries are for discussion purposes only and do not represent any specific geological features.



Block A encompasses the southern portion of the map area and is lithologically the most diverse of the four zones. It is underlain by a variety of metavolcanic rocks and a sequence of slates and greywackes. These rocks form the host to several igneous intrusions ranging in composition from granite to quartz monzonite. Several exposure areas of late Archean clastic rocks are confined to fault-bounded basins which are separated from one another by metavolcanic rocks. These Timiskaming-type sequences are identified on Fig. 4. The rocks of Block A are unconformably overlain by sedimentary rocks of the Proterozoic Gunflint formation.

Greenish-grey low grade metavolcanic rocks dominate in the southern part of the area (Fig. 3). They are composed of porphyritic and massive mafic flows, pillow lavas, and felsic volcaniclastic rocks interlayered with subordinate sedimentary rocks. A pervasive, subvertical, east-west striking cleavage is present in most exposures. Gravity modelling by Kehlenbeck and Cheadle (1990) has shown that the volcanic unit is a basin-like mass extending to depths of 6 to 10 km. The metavolcanic rocks were faulted to produce a number of fault-bounded pull-apart basins which were infilled by late Archean Timiskaming-type clastic sequences. Complex fault motions resulted in transpression of the basins and development of an internal crenulation cleavage (Seemayer, 1989).

The northern half of Block A is dominated by metasedimentary slates and greywackes (Fig. 3). The rocks are grey in colour and

show well-preserved primary structures. Turbidites with bed thicknesses of approximately 10 cm are common and complete Bouma sequences are occasionally found (Fig. 5). Local way-up is usually readily determinable from primary sedimentary features such as herringbone cross-stratification, ball and pillow structures, scours, ripple marks, and graded bedding (Fig. 6). Fig. 7 shows a stereoscopic projection of poles to bedding from these rocks. It is evident that the predominant bedding plane strikes west-southwest and dips steeply to the northwest. The same steeply dipping subvertical cleavage of the metavolcanic rocks is also present in the metasedimentary rocks where it is subparallel to bedding in many exposures. The metasedimentary sequence was modelled as a trough-like body varying in depth between 3 and 8 km (Kehlenbeck and Cheadle, 1990). The contact between the volcanic and sedimentary units dips steeply to the south.

The metasedimentary rocks are essentially composed of quartz-plagioclase-biotite with minor amounts of muscovite and chlorite. Accessory minerals include apatite and opaque minerals. Quartz-feldspar arenites at Hazelwood Lake appear unmetamorphosed except for a well developed cleavage. Porphyroblasts of muscovite, andalusite, garnet, and cordierite are common in metasedimentary rocks near intrusive contacts and are the products of contact metamorphism.

The distribution of metavolcanic and metasedimentary rocks and their contacts in the central part of Block A results in an overall pattern which bears a striking resemblance to a Type 2 fold

Fig. 5 Turbidite bed from south of the Quetico Fault, showing younging to the north north-east. This particular example shows the complete Bouma sequence (from bottom to top):

- A. massive to graded sand
- B. parallel-laminated sand
- C. cross-laminated or convoluted sand
- D. parallel-laminated fine sand and silt
- E. massive mud

Fig. 6 Primary sedimentary features:

- a) Ball and pillow structure (Hwy. 527).

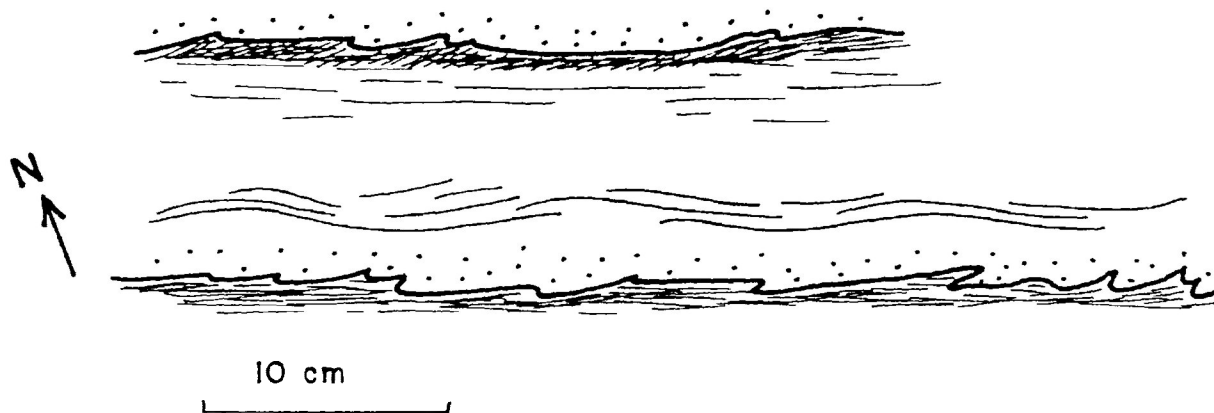


Fig. 6a

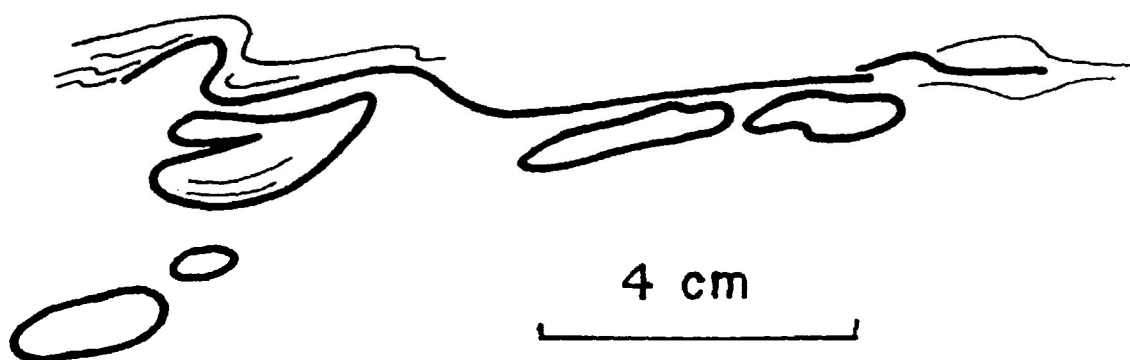


Fig. 6 Primary sedimentary features (continued):

b) Graded bedding (Hwy 527).

c) Herringbone cross-stratification (Hwy. 527).

Fig. 6b



Fig. 6c

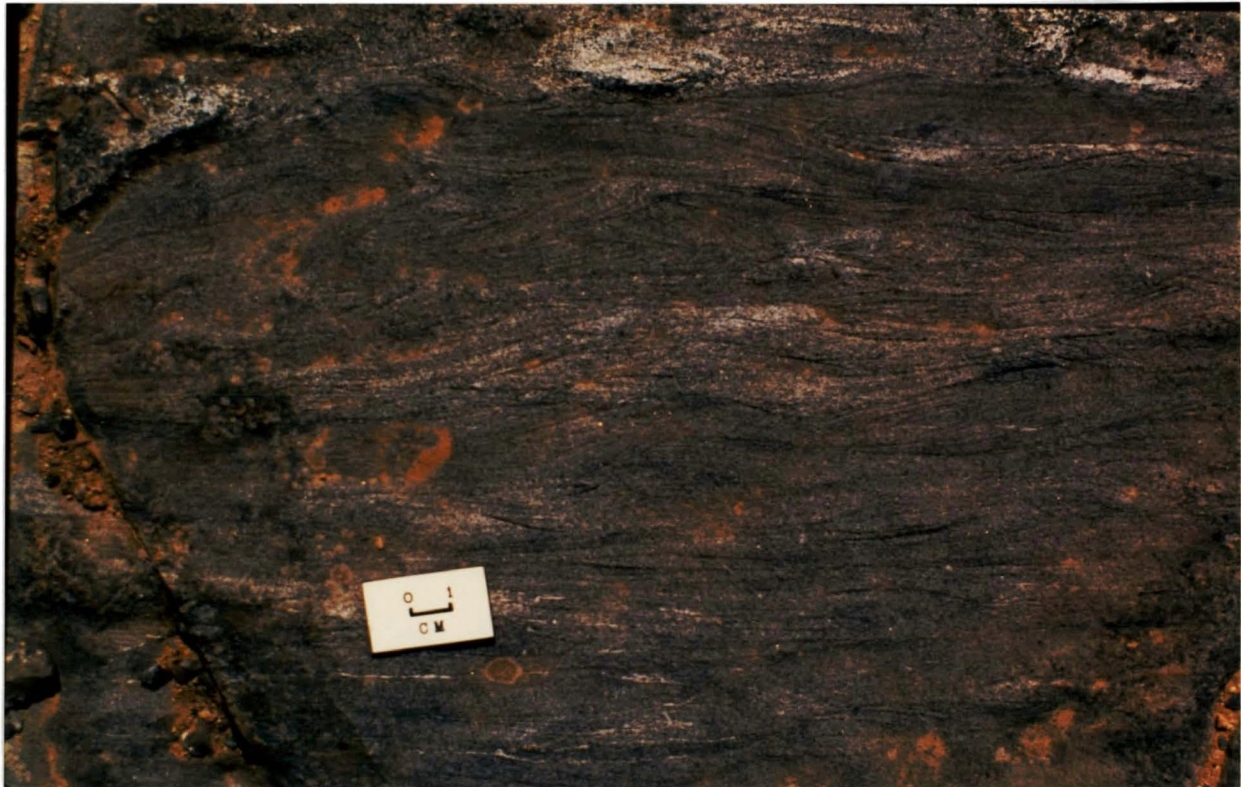
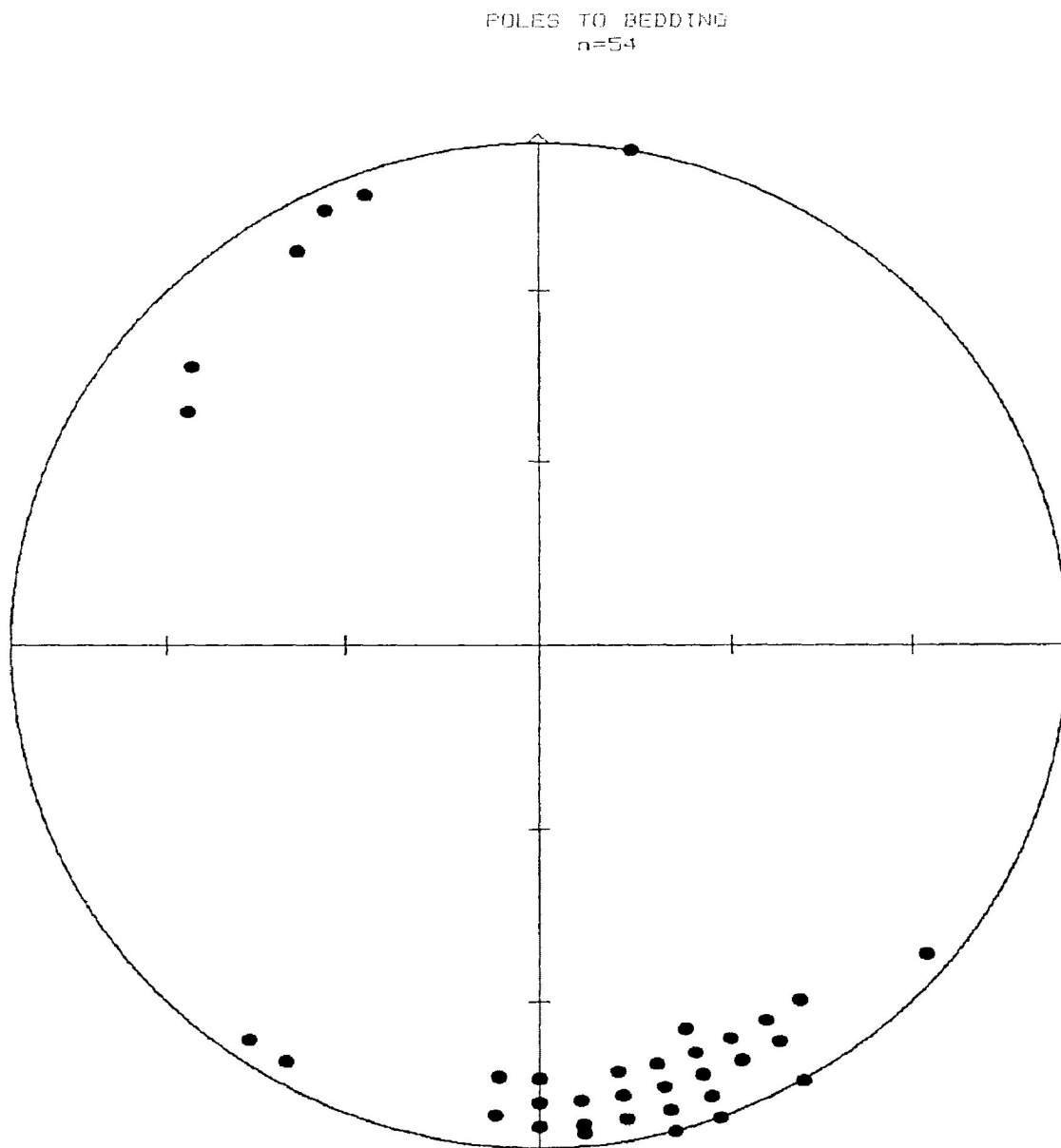


Fig. 7 Poles to bedding. The trend and plunge of the maximum position is 166-07, corresponding to a common plane of 256-83.

Fig. 7



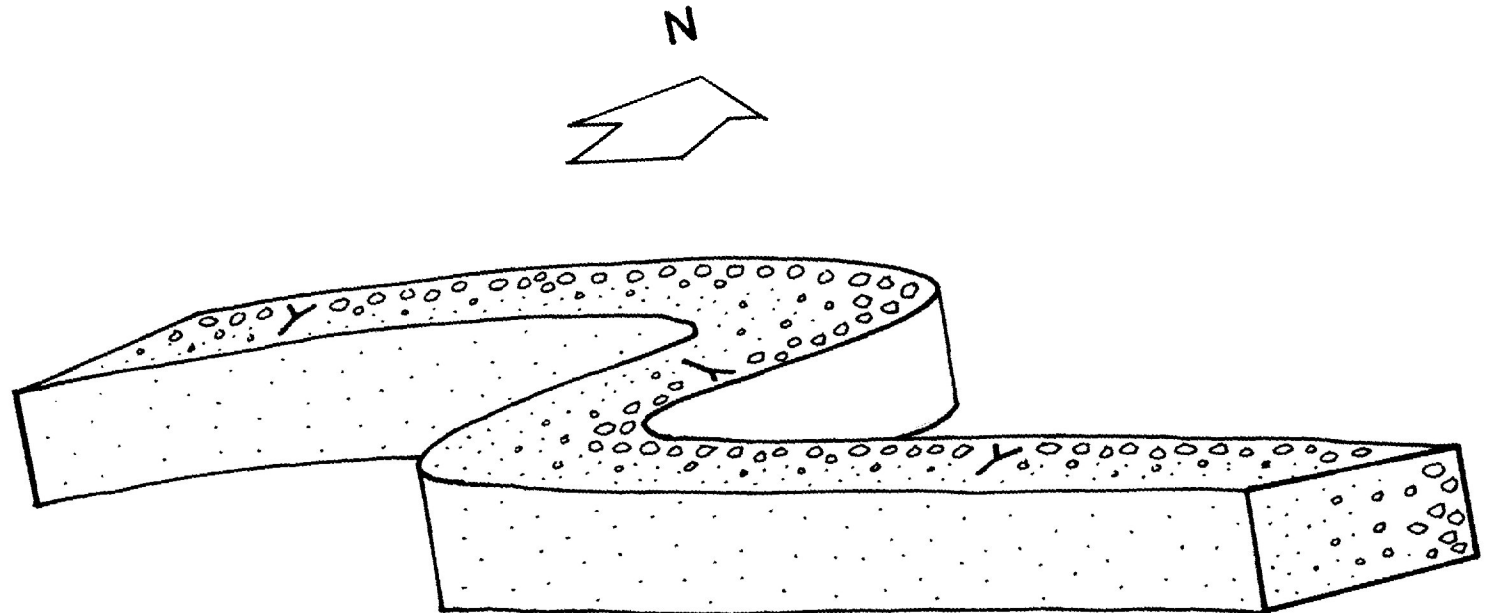
interference pattern (Ramsay, 1967). Although primary way-up indicators are rare in the metavolcanic rocks, a few pillowed lavas exist from which reliable top indicators have been recorded. These data are in support of large scale folds (Kehlenbeck, pers. comm.).

Multiple folding of a sequence of low grade slates and metagreywackes near Hazelwood Lake is reflected by reversals in local way-up of the beds and, more importantly, by reversals in the structural facing directions. The pervasive cleavage is axial planar to the second generation folds (Kehlenbeck, 1983). The fact that these rocks are stratigraphically conformable with the metavolcanic rocks to the south suggests that both sequences share a common fold history.

In the eastern part of Block A no folds have been observed in outcrops of the metasedimentary rocks and the younging direction is consistently to the southeast. Since these rocks appear to be laterally continuous with the folded sequence at Hazelwood Lake, the dominance of southerly younging here may be the result of overall F_2 fold asymmetry. In strongly asymmetric folds the chance of exposures on the long limb is greatly increased compared to exposures on the shorter limbs or in the hinge zones of the folds (Fig. 8). Interestingly, in the Kashabowie area 80 km to the west younging appears to be overwhelmingly northward and structural facing to the east in the metasedimentary as well as in the

Fig. 8 Major fold asymmetry. Large scale folds may not be recognized because on more commonly exposed long limbs way-up is overwhelmingly in one direction.

Fig. 8



adjacent volcanic rocks along both the northern and southern margins of the Quetico subprovince (Borradaile and Spark, 1990).

North of the quartz monzonite intrusions the character of the metasedimentary rocks changes. There is a marked transition from rocks in which primary sedimentary features are readily apparent to a sequence of homogeneous, fine-grained, biotite-rich, foliated rocks in which these structures are obscured. The rocks, however, possess a relict layering which on occasion appears in the form of intrafolial folds (Fig. 9). Extension in the plane of the foliation has produced boudins in more competent quartz-plagioclase-amphibole-carbonate layers. Where the relict layers are not parallel to the foliation they are folded and the foliation is axial planar to the folds. Since no field evidence for a tectonic contact with the metasedimentary rocks to the south has been located, it is suggested that this foliated sequence of rocks may represent an advanced stage of transposition of primary layering into the pervasive cleavage and that a transitional relationship exists with the rocks to the south. Individual outcrops appear to confirm this suggestion. Although not continuous, exposures to the south reflect less evidence of transposition of bedding planes and minor folds and local primary sedimentary structures are well preserved.

Both metavolcanic and metasedimentary rocks of Block A are host to late, unfoliated, granitic to dioritic intrusions. Reddish-pink to greenish in colour, the intrusives are composed of

Fig. 9 Layering preserved as intrafolial folds. Fold limbs
 have been transposed into the foliation.

Fig. 9

quartz, plagioclase, microcline, hornblende, and biotite. Although shown as continuous bodies on the general geology map, the intrusions enclose folded and metamorphosed blocks of schist and foliate which may represent roof pendants or inclusions of the country rocks. Angular, mafic-rich blocks within the schists may represent former dikes or mafic flows which resisted partial melting. Gravity modelling (Kehlenbeck and Cheadle, 1990) has shown that the south-central granite of Block A extends to 7 km depth while one of the intrusions exposed along Highway 527 forms a thin sheet rather than a deep plug. High temperature metamorphic effects are noticeable in rocks enclosed by or near the intrusions.

Three late, unfoliated, porphyritic quartz monzonite plutons intrude the metasedimentary rocks. From east to west they are the Whitelily Lake, Barnum Lake, and Trout Lake plutons. The Whitelily Lake pluton forms an intrusive contact with the northernmost exposure of volcanic rocks in Block A along the Highway 527 transect (Fig. 3). Kehlenbeck and Cheadle's (1990) gravity survey modelled all three intrusions as narrowing at depth, suggesting diapiric emplacement. The late plutons overprinted the regional metamorphism with local contact effects preserved in hornfelsic textures (Kehlenbeck, 1977).

BLOCK B

Rocks in Block B are best described as well foliated schists which retain evidence of a layered sedimentary protolith. Traces of incipient anatexis are the distinguishing characteristic of the

rocks. Intrusions of granodioritic to leucogranitic composition are exposed over large areas in the central and western parts of Block B (Fig. 3).

Although no sharp break between the rocks of Block A and Block B was observed in the field, the distinguishing feature of the rocks of Block B is layer-parallel, wispy quartz-feldspar lenses which mark the onset of anatexis. The first appearance of layer-parallel coarse white pegmatites up to a few decimetres thick in these rocks also coincides with the beginning of partial melting.

South of the Quetico Fault along Highway 527, the layered schists are granular in texture which gives them a metasedimentary appearance, even though no primary sedimentary features by which bedding could be established were found. The dominant subvertical foliation strikes approximately east-west.

Similar rocks are found in the western part of Block B south of Dog Lake. Here isolated occurrences of shallowly-dipping units have been observed; these are marked by solid circles on Fig. 3. Locally, a garnet-bearing, fragmental metasedimentary rock of overall greywacke composition is exposed on the north and south shores of Little Dog Lake, where it is in contact with an unfoliated granodiorite intrusion.

The brownish grey pelitic to semipelitic schists of Block B are compositionally similar to the metasedimentary rocks of Block

A to the south. The bulk of the rock is composed of quartz-plagioclase-biotite. Andalusite porphyroblasts are absent but the high temperature polymorph sillimanite was observed in at least one sample. Almandine garnet is the most common metamorphic porphyroblast, while the first appearance of cordierite and staurolite signals the beginning of medium grade regional metamorphism. Knots composed of staurolite cores with cordierite rims suggest a metamorphic path of increasing temperature or decreasing pressure for these rocks (Winkler, 1976).

Gneisses in which regional metamorphism has produced compositional layers of mica-rich and K-feldspar-rich composition are common south of Hawkeye Lake. These migmatitic outcrops within the gneisses are marked on Fig. 3 with a dotted pattern. Products of extensional and compressional strains are present as pinch-and-swell structures and folds, respectively. In many outcrops examples of both are observed in layers of appropriate orientation with respect to the bulk strain.

The migmatitic gneisses, closely associated with large areas of leucogranite, are exposed south and east of Hawkeye Lake (Fig. 3). The medium-grained, homogeneous, non-foliated leucogranite is composed mainly of quartz and feldspars. Xenoliths or roof pendants of biotite foliate and stromatic to agmatitic migmatite are commonly enclosed. The contacts of the inclusions are generally sharp, suggesting that little resorption has taken place. A late unfoliated granodiorite is exposed along the north and west

shores of Little Dog Lake. Kehlenbeck and Cheadle's (1990) gravity model of this area shows that the gneisses and leucocratic rocks dip to the south beneath the metasedimentary rocks.

BLOCK C

Block C is composed of the migmatites and granitic rocks typical of the Quetico subprovince. The southern part of Block C is dominated by stromatic migmatites while the northern part is composed largely of granitic gneisses containing inclusions of migmatite. Block C is cut by a major shear zone, the Quetico Fault.

A wedge of migmatites, "megascopically composite rocks comprising alternating layers or lenses of granitoid and schist or gneiss" (Brown, 1973), is fault-bounded to the south by the Hawkeye Lake Fault and to the north by the Quetico Fault (Fig. 3). North of the Quetico Fault is a much larger expanse of migmatitic rock. Although structures range from schlieric to agmatitic, stromatic migmatites are the most common. White leucosome layers are mainly composed of quartz, plagioclase, and perthite or microcline. Brown to black schistose melanosome is made up of biotite, quartz, and plagioclase. Porphyroblasts of garnet, cordierite, and sillimanite and mineral assemblages devoid of muscovite but including alkali feldspar reflect regional high grade metamorphic conditions. As pointed out by Breaks et. al. (1978) almandine, cordierite, and sillimanite are all atypical in granitic rocks. Occurrence of these alumina-rich minerals in the migmatitic rocks of the central

part of the study area is therefore suggestive of diatexis of pelitic source rocks.

Leucosome and melanosome make up approximately equal proportions of the stromatic migmatites. A single outcrop may illustrate a complete range of rock types from biotite schist, foliate, and gneiss, to tonalitic gneiss and quartz-feldspar-mica pegmatite. Schlieren and forellen of paleosome are found enclosed in coarse white pegmatites which are commonly many metres in outcrop extent. In some outcrops of migmatite, competent angular blocks and disrupted layers of amphibolite have been observed. Thin sections of these rocks show that they are metamorphosed olivine gabbros and ultramafic rocks. These rocks are clearly different from the migmatites and may represent tabular igneous bodies of mafic to ultramafic composition.

Extensional structures such as pinch-and-swell and boudinage parallel to the east-west layering attests to the relative competence of the leucosome with respect to the melanosome. Ptygmatic veins folded about subvertical, east-west striking axial planes suggest a north-south compression with a shortening of up to 78% (Fig. 10).

Although many outcrops of migmatites show evidence for at least two episodes of folding, the folds cannot be traced for any distance in the field. Refolded quartz veins cutting folded layered rocks (Fig. 11) and sheath folds (Fig. 12) confirm complex

Fig. 10 A ptygmatic fold from north of the Quetico Fault. An estimate of overall shortening can be made from this near-profile view by comparing the initial and final lengths of the vein:

$$\begin{aligned} e &= (l-l_0) / l_0 \\ &= (19.5-90) / 90 \\ &= -.78 \end{aligned}$$

Therefore, this vein has undergone approximately 80% shortening.

Fig. 10

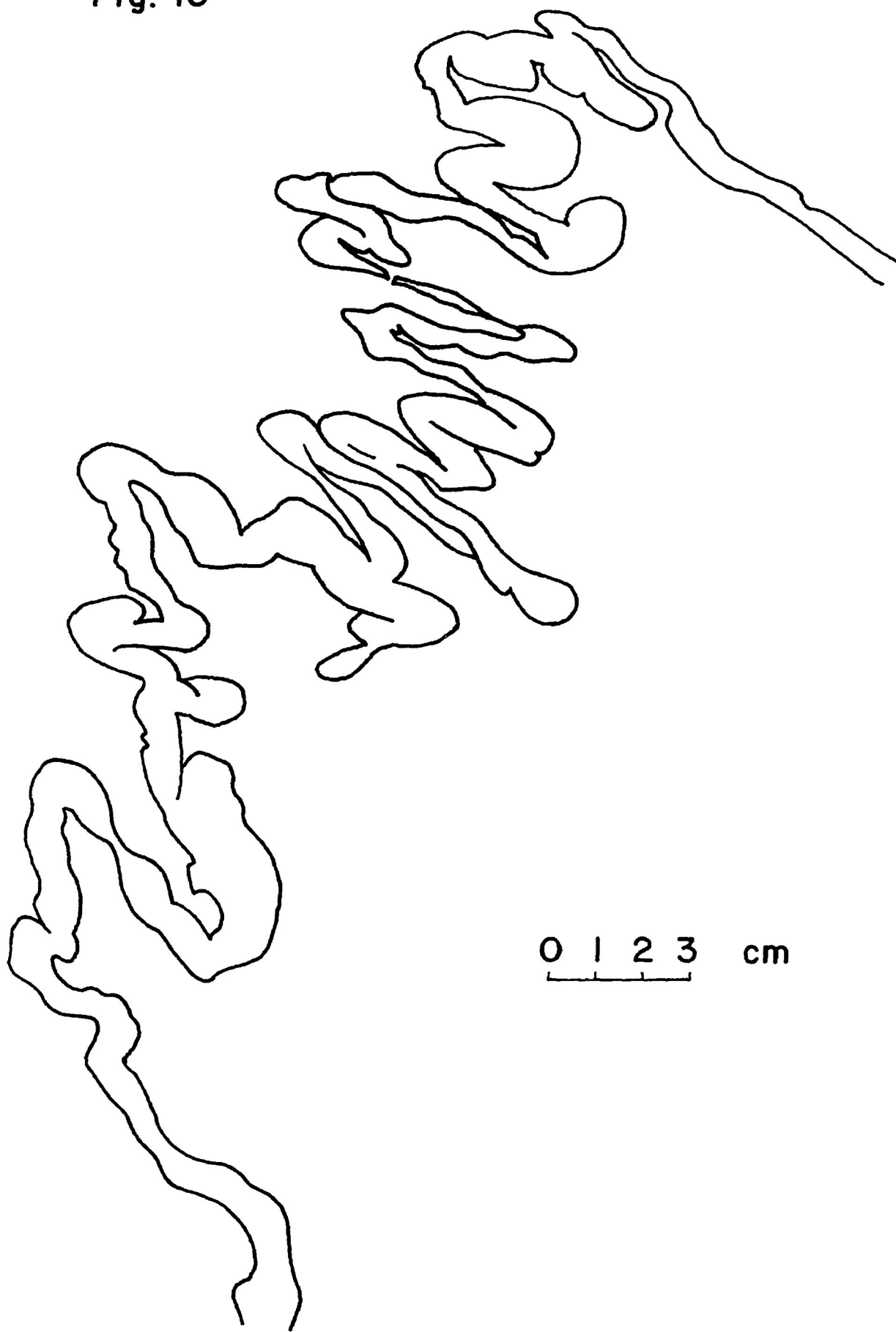


Fig. 11 Refolded quartz vein in folded metasedimentary rocks.
Hwy. 527.

Fig. 12 Sheath folds in migmatite, Hwy 589.

Fig. 11**Fig. 12**

heterogeneous folding within the central parts of the subprovince. Outcrop-scale folds in the high-grade rocks are generally isoclinal with subvertical hinge lines. Isoclinal fold hinges whose limbs have been transposed into the foliation are common within melanocratic layers of stromatic migmatites. This suggests that the entire sequence of Quetico migmatites has been greatly shortened even before metamorphic segregation occurred. Later folds which also fold leucosome are open and have variably plunging hinge lines.

Fig. 13, a plot of poles to foliations including cleavage and migmatitic layering, illustrates that the dominant layering of the rocks within the study area is subparallel to the bedding of metasedimentary rocks in Block A. In most outcrops the layering of the foliated rocks is subvertical; however, a number of exposures where shallow dips occur in layered rocks have been observed. The locations of these outcrops are marked on Fig. 3 as solid circles. In most cases the shallowly dipping layers are accompanied by a subvertical cleavage or schistosity. The low dip of layering together with a shallowly plunging intersection lineation suggests that these outcrops may represent remnants of former recumbent folds, fold nappes, or thrust nappes. The overall distribution of poles along a great circle in the stereo plot is the result of large scale folding of the foliated rocks. The trend and plunge of the beta-axis of the folds is 074-31 (Fig. 13). Fig. 14 is a plot of linear structures including mineral lineations, quartz rods, and mullion structures. Fold hinge lines are shown by the solid

Fig. 13 Poles to foliations, including migmatitic layering. The average planar orientation is 255-85. The distribution of the data defines a great circle girdle and an eastward plunging β -axis.

Fig. 13

POLES TO FOLIATIONS
n=70

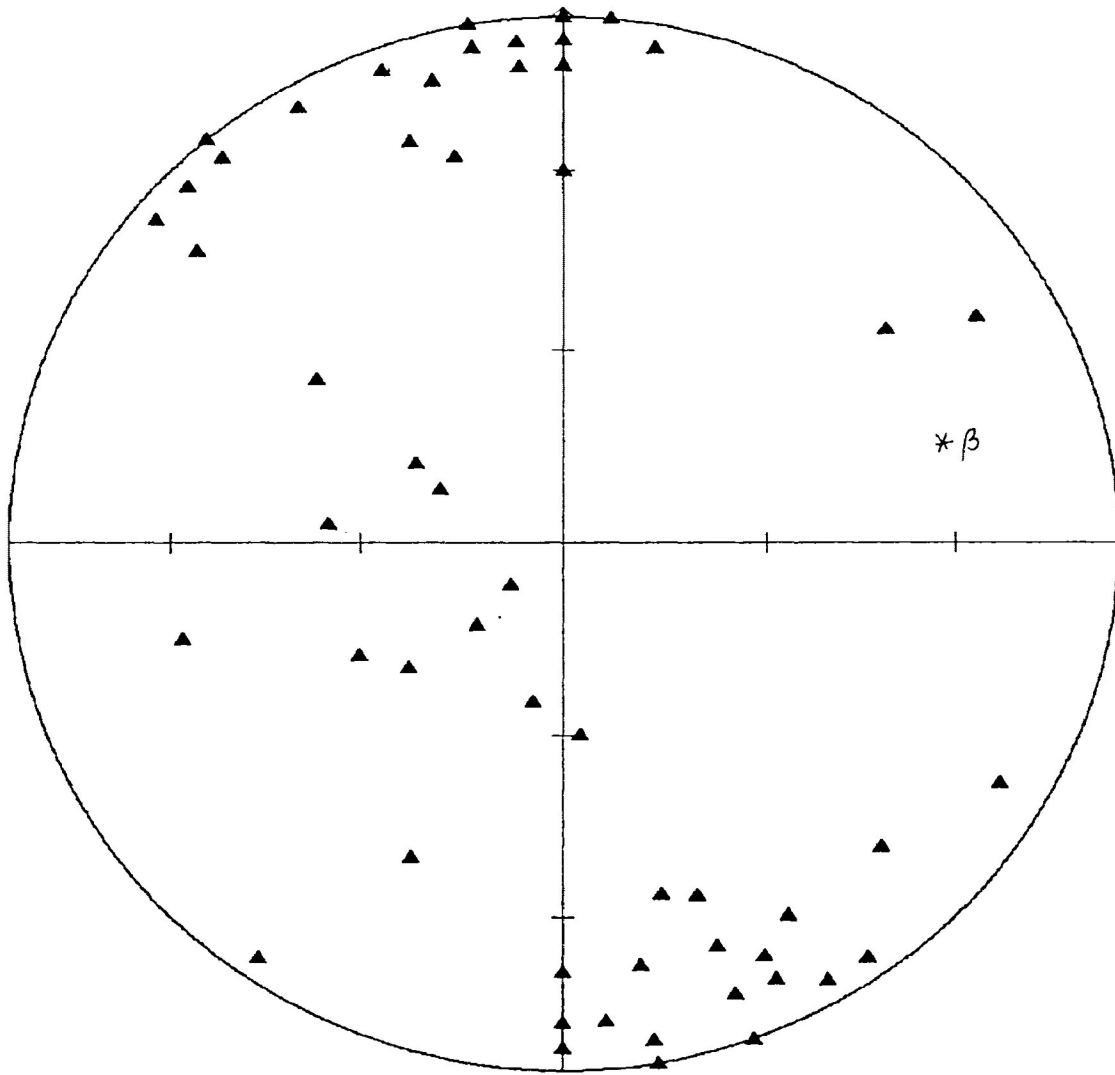
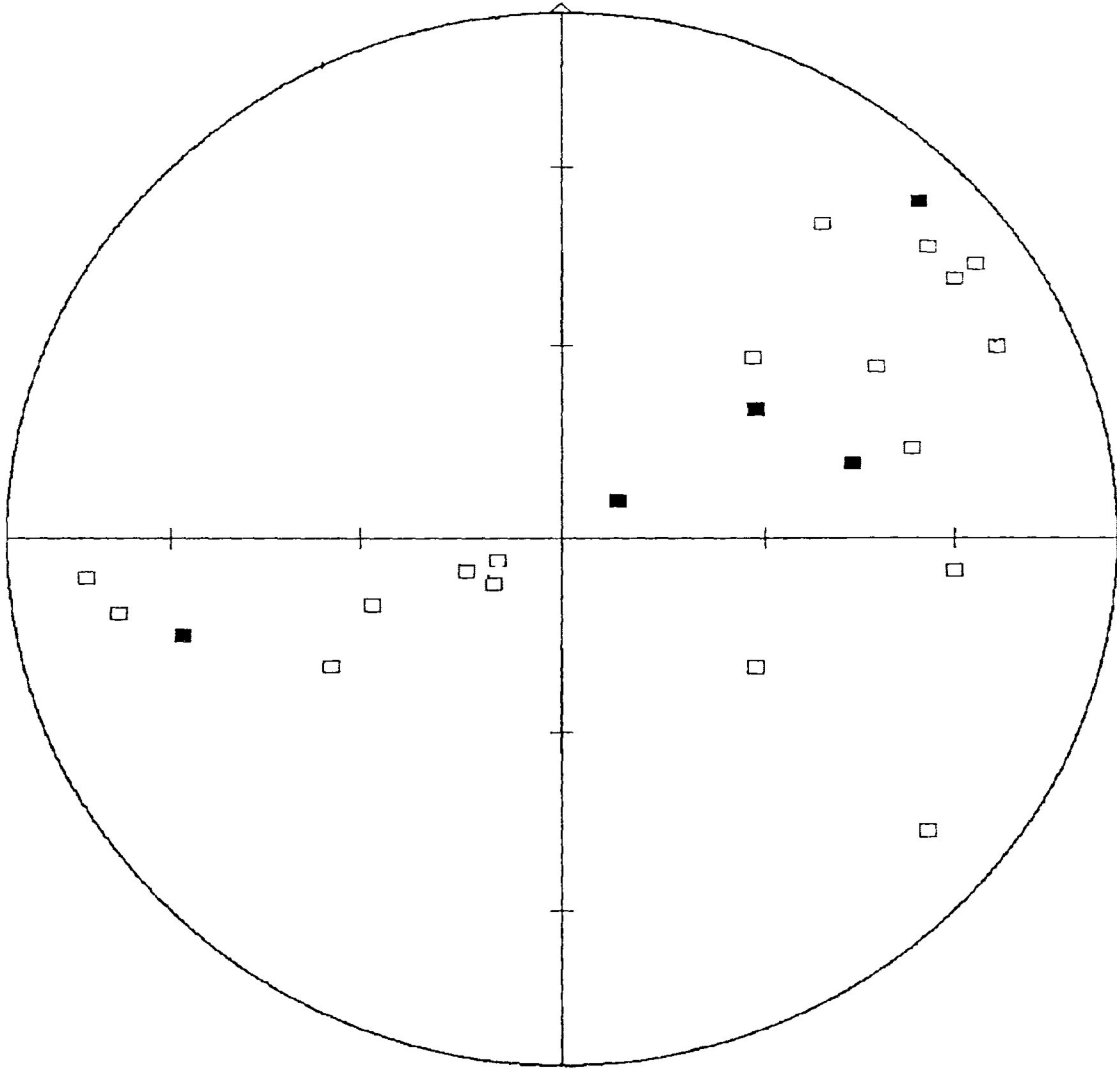


Fig. 14 Lineations including mineral lineations, quartz rods, and mullion structures. Fold hinges are indicated by the solid square symbol.

Fig. 14

LINEATIONS
n=24



squares. The distribution of hinge lines appears to lie in the general plane of the foliation. The wide variation in plunge of the hinge lines from very steep to very gentle may be due to refolding of earlier folds or sheath folding.

Evidence for a late shortening parallel to the east-west schistosity and the development of a crenulation cleavage about north-south striking axial planes is found in coarse, crenulated sillimanite from central outcrops in the Quetico subprovince (Fig. 15).

Homogeneous hornblende-biotite gneissic granite is exposed north of the migmatites (Fig. 3). Isolated stromatic migmatite units as well as occasional schollen and schlieren of migmatitic material within it indicate that the granitic rock intruded the migmatites. An earlier, light grey granite is cut by pink granite and pegmatite. A weak fabric is locally developed. Leucogranite similar to that exposed south of the Hawkeye Lake Fault is also found within the fault-bounded wedge north of the fault. The intrusion may therefore have been emplaced after final movement on the fault.

Pegmatites commonly cut migmatites and granites and are also found as coarse grained pods within granitic masses. The pegmatites are either pink or white in colour. Mineralogically they are composed of microcline, quartz, plagioclase, biotite, and muscovite. Garnets, minor amounts of apatite, and occasionally

Fig. 15 Coarse-grained fibrous sillimanite in "granitic" portion of migmatite.

Fig. 15



tourmaline crystals up to 3 cm in diameter and more than 10 cm in length are encountered in the white pegmatites. White pegmatites are commonly conformable with migmatitic layering and contain schlieren of paleosome near their edges. Pink pegmatites are later and cross-cut the layering. They, too, contain inclusions of paleosome.

Gravity modelling suggests that the gneisses and migmatites form a south-dipping, northward thickening wedge (Kehlenbeck and Cheadle, 1990).

Mylonitic and cataclastic rocks of the subvertical Quetico fault zone cut the migmatites of Block C. The fault rocks outcrop for 2.5 km along Highway 527 (Fig. 3). Feldspars in mylonitized leucosome show a characteristic brick-red alteration colour which make the fault rocks easy to identify. Recognizable stromatic migmatites in the fault zone show well-developed C-S fabric and abundant shear planes in the leucocratic layers. The fact that the migmatites have been sheared shows that final movement on the Quetico Fault post dates the migmatization and peak metamorphism, although the fault may have been initiated during an earlier period of transpression.

Mackasey et. al. (1974) attributed a dextral displacement of 100 km to the Quetico Fault. Detailed examination of the fault from Rainy Lake to Highway 527 by Kennedy (1984) found evidence to support the dextral sense of strike-slip motion. Kennedy found

that brittle deformation followed the predominantly ductile deformation within the fault zone. Purdon (1989) concluded that motion along the Quetico Fault northeast of Thunder Bay was of a complex nature. An early dip-slip component inferred from subvertical stretching lineations on foliation surfaces was overprinted by slickenfibres resulting from dextral strike-slip motion. It is not surprising, then, that metasedimentary rocks showing incipient metamorphic differentiation are adjacent to well-segregated, stromatic migmatites separated by the fault, although the initial bulk composition of the rocks on either side of the fault was likely very similar.

BLOCK D

There is great similarity between the rock types of Block D and those of Block A. The northernmost zone includes a polymetamorphic schist, a major shear zone, mafic metavolcanic rocks, and a sequence of low grade slates and greywackes. Proterozoic sedimentary rocks unconformably overlie the Archean rocks, while dikes and sills intrude both.

A series of knotted mica schists are exposed in the Smiley-deCourcey Lakes area north of the granitic intrusive rocks of Block C (Fig. 3). The strong subvertical schistosity is parallel to the regional foliation described in other units. These medium grade rocks have a polymetamorphic history which was described in detail by Kehlenbeck (1976). Inclusion trails within metamorphic

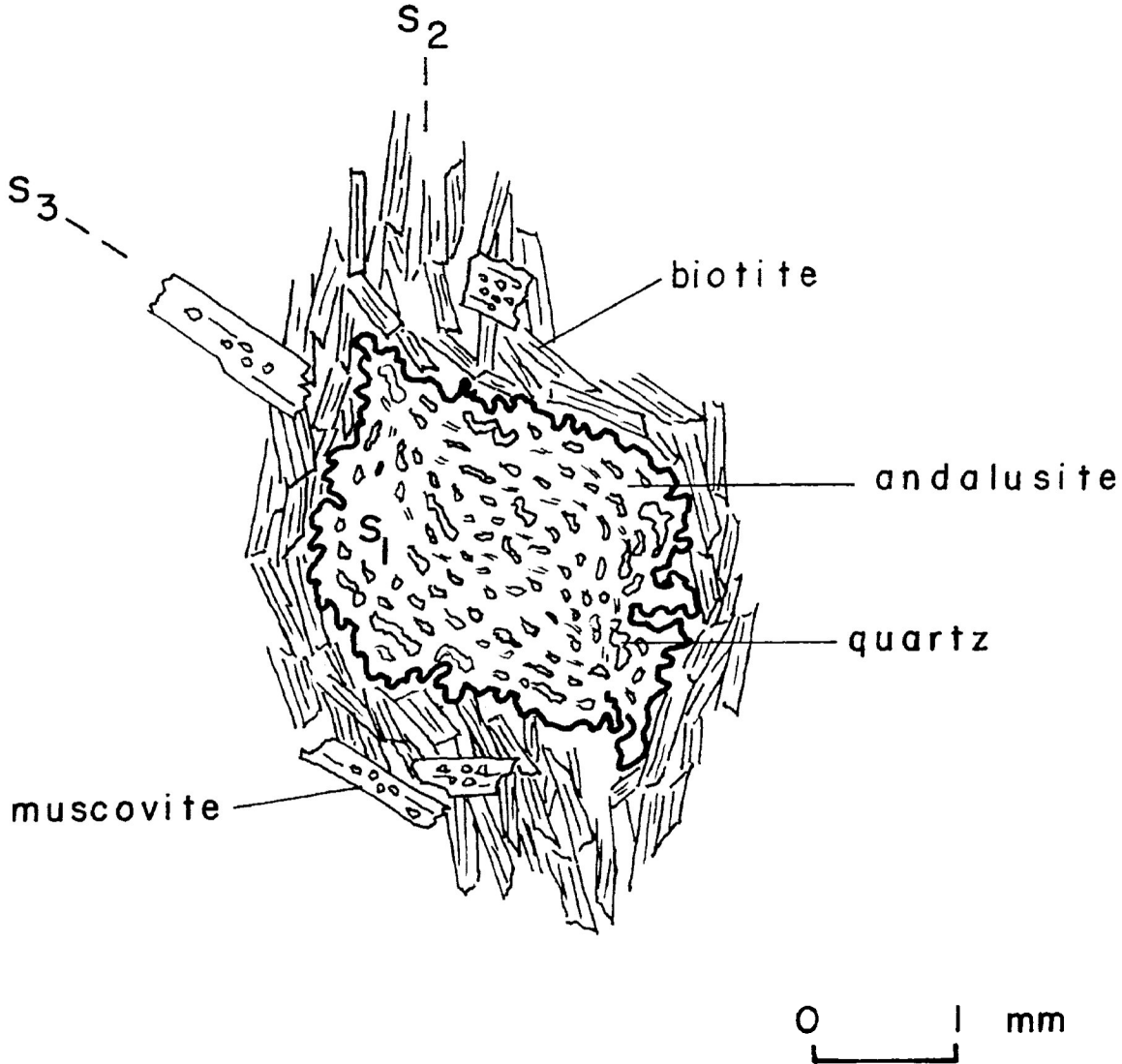
porphyroblasts of garnet, cordierite, and andalusite preserve an early fabric (S_1). The dominant schistosity, S_2 , is marked by the alignment of muscovite, biotite, and sillimanite. Porphyroblasts are often rotated and wrapped by biotite, indicating that their growth predated the development of that foliation. Late S_3 is expressed by a crenulation cleavage defined by muscovite laths overprinting the earlier fabrics (Fig. 16).

North of the schists, sheared migmatites delineate a major fault zone. The strike length of the fault is unknown; however, the 2 km outcrop width across strike of the sheared rocks is similar in magnitude to that of the Quetico Fault to the south. Coarse feldspar porphyroclasts showing the brick-red alteration colour characteristic of fault zones are wrapped by chlorite and the feldspars. Tailed porphyroclasts and bookshelf structures suggest sinistral motion; however, sense of shear is inconclusive because kinematic indicators including C-S fabrics give conflicting evidence.

A series of layered metavolcanic rocks including actinolite-grade amphibolites separates rocks of the shear zone from a thick sequence of bedded greywackes to the north. Locally, graded bedding indicates younging to the north. Staurolite, andalusite and garnet porphyroblasts indicative of medium grade regional metamorphism occur set in a matrix of quartz, plagioclase, and biotite.

Fig. 16 Typical schist from the Smiley-deCoursey Lakes area illustrating polymetamorphic fabrics.

Fig. 16



North of Starnes Lake a series of metagreywackes and arenites, possibly of volcanogenic origin, show primary sedimentary features such as graded bedding and cross-bedding. Local reversals in younging suggest that the rocks have been folded and reversals in structural facing indicate refolded folds. The rocks possess an east-west subvertical cleavage.

MINERALOGY OF METAPELITES

The lithological characteristics of the map units have been described previously. Depending on P-T conditions and the chemical composition of the rocks, a variety of metamorphic index minerals occur and commonly form porphyroblasts. For this study mineral assemblages from rocks of pelitic to semi-pelitic compositions were chosen since they are exposed over much of the area. Perry (1976) showed that samples from the central part of the area display mineralogical variation although the $\text{FeO}/(\text{FeO} + \text{MgO})$ vs MgO ratios are relatively uniform. Perry therefore concluded that the mineral assemblage present reflected changes in temperature and pressure.

Metasedimentary rocks of quartzofeldspathic composition have not been found in the study area. Most quartz-feldspar rocks formed as a result of anatexis of pelitic to semipelitic sedimentary rock. High $P(\text{H}_2\text{O})$ lowered the melting temperature of the protolith and the presence of abundant water carried by wet sediments encouraged development of hydrous minerals. Basic rocks

were altered to amphibolites by the addition of water during metamorphism.

In addition to quartz, biotite and plagioclase, the metapelites commonly contain porphyroblasts of garnet, cordierite, staurolite, or andalusite. In several samples muscovite, chlorite, staurolite and sillimanite occur. The presence of microcline and sillimanite in the absence of muscovite locally north of the Quetico Fault indicates that the reaction isograd indicative of high grade metamorphism has been crossed. Characteristic effects of local retrograde metamorphism include saussuritization of plagioclase, sericitization of potassium feldspar, chloritization of biotite and garnet, and pinitization of cordierite.

FELDSPARS

Plagioclase feldspar compositions in the metapelites of the study area most frequently lie in the oligoclase to andesine range (An_{10-50}) (Fig. 17). Plagioclase, along with quartz, makes up the bulk of the matrix of the metasedimentary rocks, schists, and gneisses. Migmatitic leucosomes are composed mainly of plagioclase, quartz, and potassium feldspar present as perthite or microcline. Microcline also occurs in central, high grade, recrystallized paleosome and is an abundant mineral in the extensive granitic rocks exposed north of the Quetico Fault.

CHLORITE

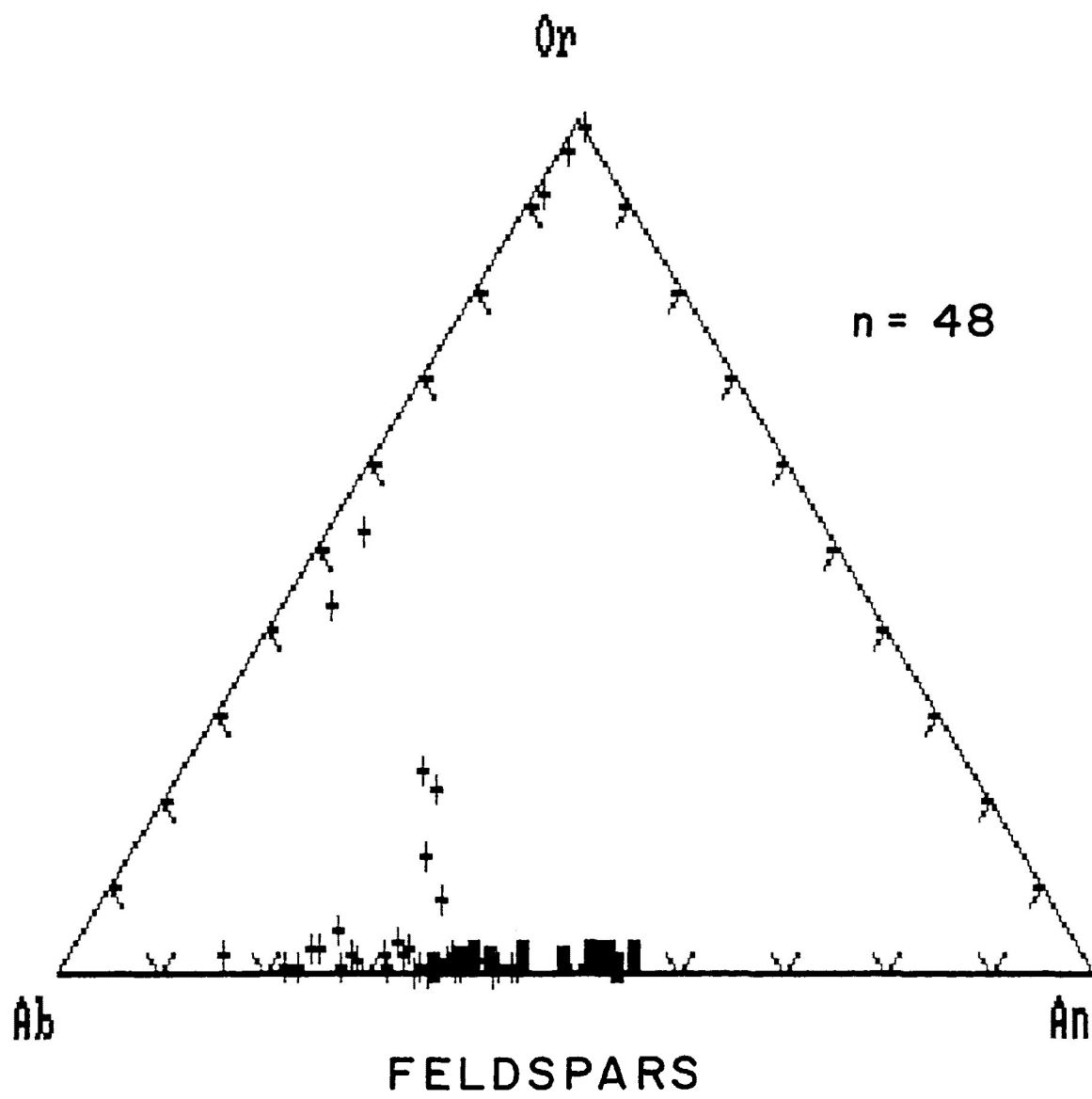
Chlorite-bearing rocks are exposed along the southern parts of Pike Lake road (as far north as P.L. 4.4), where the metasedimentary rocks are of greenschist facies. Chlorite found in higher grade rocks replaces biotite and garnet as a breakdown product of retrograde metamorphism.

BIOTITE

Biotite is at least in part the product of progressive metamorphism of chlorite-rich rocks. In some samples the biotite can be seen to replace chlorite (P.L. 5.2). In other cases the biotite defines a well developed cleavage commonly at a low angle to the primary bedding planes.

Fig. 17 Feldspars from metapelites, designated by the (+) sign, range in composition from oligoclase to andesine. Feldspars from metabasites, designated by the solid rectangle, plot in the andesine to labradorite range, reflecting the higher calcium content of the rocks. Potassium-rich feldspars are from migmatitic leucosomes. The samples which plot in the centre of the diagram are from perthitic feldspars.

Fig. 17



In the samples studied at least two generations of biotite growth can be established. Biotite is inevitably present as inclusions in porphyroblasts of garnet, cordierite, and andalusite. This early biotite is followed by a later one which envelops the porphyroblasts. In some samples even later laths of biotite which may have developed under static conditions cross-cut the planar fabric.

MUSCOVITE

Muscovite is found as a product of progressive metamorphism in rocks of the amphibolite facies. Together with biotite it defines the foliation in schists of the Smiley-deCourcey Lakes area as well as in metasedimentary rocks in the southern part of the area. In some samples from the southern metasedimentary rocks muscovite grains form clusters which give the rocks a knotted appearance, both in hand specimen and in thin section. These clusters appear to be the result of late static growth as they overprint the previous fabrics.

Small grains occur in some migmatite paleosome parallel to the biotite. In the central high grade rocks muscovite is absent. Minor amounts of muscovite result from the breakdown of alkali feldspar.

STAUROLITE

Staurolite occurs in schists and metasedimentary rocks as yellowish, lozenge-shaped poikiloblasts filled with quartz

inclusions. In the metasedimentary rocks west of Starnes Lake, small poikiloblastic staurolite fragments are contained within andalusite porphyroblasts and overgrow the biotite foliation. In schists south of the Quetico Fault, staurolite is found at the cores of cordierite porphyroblasts. This corona structure likely represents a decrease in pressure corresponding to the unroofing of the metamorphosed sequence.

GARNET

Almandine-rich pyralspite garnets are the most easily recognized and abundant metamorphic index mineral in the rocks of the Quetico subprovince. They are pinkish to deep red in colour and range in size from less than a millimetre to four centimetres in diameter and locally constitute as much as 30% of the rock. Garnets are widespread due to the common occurrence of rocks of appropriate composition. In the migmatitic rocks exposed in the central portions of the Quetico subprovince, garnets are most abundant within the biotite-rich melanosome while the largest grains are found within the pegmatitic leucosome. An inverse relationship exists between garnet size and the number of garnets per unit volume of rock.

Garnets from layered metasedimentary rocks are most easily recognized on weathered surfaces, where they stand out in relief against the finer-grained quartz-feldspar-biotite groundmass. The garnets form only in units of appropriate bulk composition. However, a nearly constant ratio of $(\text{FeO}/\text{FeO} + \text{MgO})$ vs MgO in both

garnet-bearing as well as garnet-free pelitic rocks (Perry, 1976) indicates that the iron-magnesium ratio was not a controlling factor in garnet formation. Garnets up to 2 cm in diameter are often found in pelitic tops of graded beds. In the migmatites the garnets are idioblastic. Garnets less than 1 cm in diameter occur as small crystals wrapped in biotite. Larger garnets are commonly fractured internally, although they may still show a subidioblastic outline.

Studies of thin sections confirm the variable nature of the garnets as observed in hand sample. In thin section, the garnets can be classified into four main types. The most common indicators of garnet grade metamorphism are present as subidioblastic grains and fragments. Those which reach sizes of 1mm or more are always fractured and almost always poikiloblastic, containing inclusions of quartz and sometimes of biotite. They may show incipient chlorite replacement. Other garnets are a few mm in diameter and have poikiloblastic cores and inclusion-free rims, representing two periods of garnet growth. SEM analyses have failed to show any systematic compositional variation between the rim and core of these garnets as suggested by Miyashiro (1973) and others. In such samples smaller, new, inclusion-free garnets also occur. From some medium to high grade rocks, sieve-textured garnet poikiloblasts are flattened in the plane of the foliation and wrapped by coarse biotite. More infrequent are idioblastic, inclusion-free garnets greater than 1mm in diameter from moderate to high grade rocks.

CORDIERITE

Cordierite commonly occurs with garnet, although it does occur independently. In the field altered cordierite is found as dark "knots" or augen in biotite schists in the Smiley-deCoursey Lakes area. In two other localities, both north of the Quetico Fault, clear, blue, fresh cordierite porphyroblasts up to four centimetres in diameter occur in pegmatitic leucosome. Smaller grains are present in paleosome as well. In these localities the cordierite coexists with large garnets.

Based on textural relationships observed in thin sections, it is evident that two generations of cordierite are present. An early generation has been extensively altered to greenish pinite, a matted mixture of muscovite, chlorite, and iron oxides. A later cordierite appears fresh and unaltered and contains inclusions of quartz, biotite, and sometimes sillimanite. The cordierite generally occurs as porphyroblasts which are wrapped by phyllosilicates.

ANDALUSITE

Andalusite is not as common as garnet or cordierite. It occurs as quartz-sieved poikiloblasts associated with cordierite, garnet, sillimanite, or staurolite. Andalusite occurs in rocks of the Smiley-deCoursey Lakes area, where it grew syn-tectonically with the formation of S_1 . Early quartz and biotite inclusion trails in the andalusite were subsequently rotated and wrapped by S_2 . S_2 biotite is also overgrown by later andalusite (Kehlenbeck,

1976). An occurrence of andalusite overgrowing staurolite found near the northern margin of the study area may represent a decrease in pressure of metamorphism.

SILLIMANITE

Sillimanite occurs mainly as fibrolite, commonly in close association with biotite. Sillimanite needles are also common within cordierite porphyroblasts. In such cases only, Reinhardt (1968) concluded that sillimanite is a relict phase; that is, sillimanite and its host may be regarded as a two-phase subsystem that is stable in itself but unstable for the overall system. In one location north of the Quetico Fault, coarse fibrous sillimanite is visible in an outcrop of migmatitic leucosome (Fig. 15). The fibres lie in the foliation plane of the migmatites which is crenulated. Robust sillimanite identified in thin section was confirmed by SEM analysis in a few samples from the highest grade rocks north of the Quetico Fault.

METAMORPHISM

The main objective of this study is to document variations in metamorphic grade from a series of metasedimentary rocks of pelitic composition. Metamorphic facies and baric types are used to describe regional metamorphic conditions. Peak P-T conditions can be established by a number of methods including mineral chemistry, mineral assemblages, and geothermobarometry.

A metamorphic facies designates a group of rocks characterized by a definite set of minerals formed under particular metamorphic conditions of temperature, pressure, and $P(H_2O)$ (Winkler, 1979, p. 57). Any facies is based on a set of metamorphic mineral assemblages in associated rocks of a wide range of compositions and cannot be used to classify an individual rock type (Turner, 1981). Winkler (1979) suggested the term "facies" was inappropriate because the P-T field for each is so large that, even for rocks of a constant chemical composition, many different sets of mineral parageneses are formed. Even zones or subfacies actually represent different facies, and there are too many to allow a simple means of rock classification. Winkler therefore proposed divisions of very low grade, low grade, medium grade, and high grade metamorphism, although the early facies terms remain in common use. Low grade corresponds to greenschist facies while the beginning of medium grade coincides with the beginning of the amphibolite facies. The upper part of the amphibolite facies has been reassigned to high grade metamorphism. Under high grade conditions migmatites form if water pressures are high while granulites form if water pressures are low. In this scheme of classification only the changes in mineral assemblages when passing from one metamorphic zone to the next are significant (Winkler, 1979).

In order for minerals to constitute an assemblage or a **paragenesis** an example of each mineral must be found *in contact with every other mineral* of the assemblage (Winkler, 1979). Mineral assemblages from metapelites in the study area reflect

metamorphic conditions from low to high grade. The distribution of metamorphic mineral assemblages and hence metamorphic grade is shown on Fig. 18. Perry (1976) determined that the pelitic rocks in this area and the migmatites derived from them have a relatively constant iron-magnesium ratio, so that the mineral assemblages which form should be the result of variations in temperature and pressure.

Fig. 19 is a P-T petrogenetic grid showing stability fields of mineral assemblages determined from thin section study. The dotted arrow shows the estimated path of regional metamorphism across the Quetico subprovince based on a series of metamorphic studies by Pirie and Mackasey (1978). The estimated path of regional metamorphism as determined by present study is marked by the series of numbers which correspond to the mineral assemblages shown in Fig. 20. The curve corresponds to the one set by Pirie and Mackasey (1978) but at a slightly lower pressure.

LOW GRADE METAMORPHISM IN PELITES

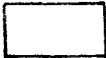
Low grade metamorphic rocks may contain chlorite, biotite, muscovite, andalusite, and garnet and are formed at temperatures between 300 and 500°C (Winkler, 1979, p. 208). In the study area the Archean metavolcanic and metasedimentary rocks of Block A as well as the metasedimentary rocks in the northern part of Block D contain assemblages which are typical of low grade metamorphism.

Fig. 18 Metamorphic assemblage map.

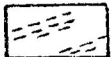
Q.F. - Quetico Fault
 E.F. - Eaglehead Fault

LOW GRADE 

1. almandine-free, chlorite + muscovite +/-
 plagioclase +/- biotite +/- quartz
 (12.6, 71.5, south of P.L.5.2)
2. almandine + chlorite + muscovite
 (12.2, 16.0, 18.8, 26.1, 28.7)

MEDIUM GRADE 

3. cordierite + almandine + biotite + muscovite +
 quartz +/- plagioclase
 (51.2)
4. cordierite + almandine + sillimanite + muscovite +
 quartz +/- plagioclase
 (62.0)
5. cordierite + almandine + sillimanite + biotite +
 muscovite + quartz +/- plagioclase
 (47.5)
6. cordierite-bearing, almandine-free
 (32.9, 52.8, 68.7, 69.9, D.L. 21.2)
7. staurolite-bearing assemblage
 (32.9, 68.7, 78.7, D.L. 21.1)

HIGH GRADE 

8. muscovite + quartz -> Kspar + sillimanite reaction
 (53.4)
9. Kspar + sillimanite + cordierite + biotite + quartz
 +/- plagioclase
 (400-4)
10. Kspar + cordierite + almandine + quartz
 (#1-2)
11. muscovite-free assemblages
 (52.3, #2-6.0, #2-8.7, 53.4, 53.9, 54.7)

Fig. 18

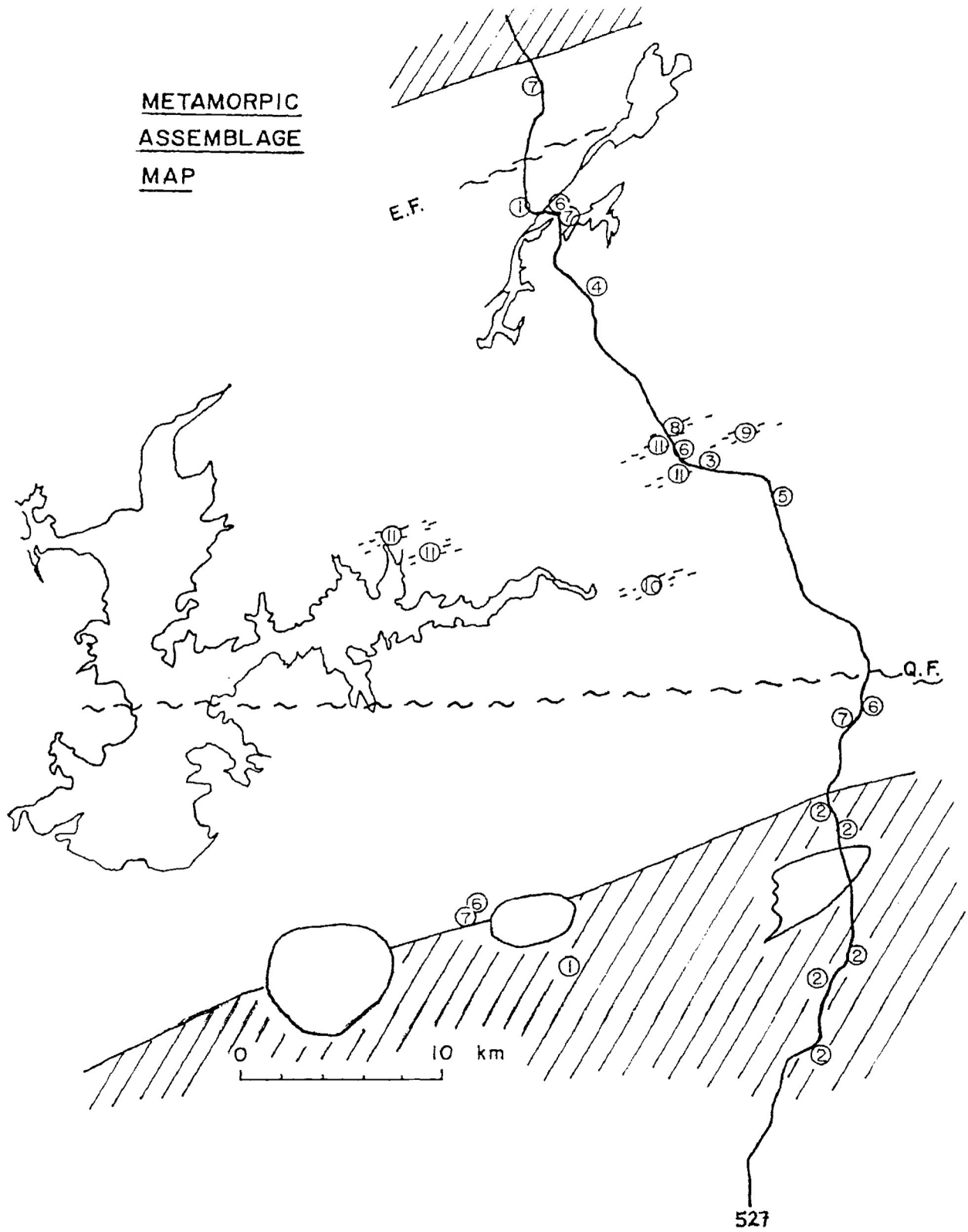
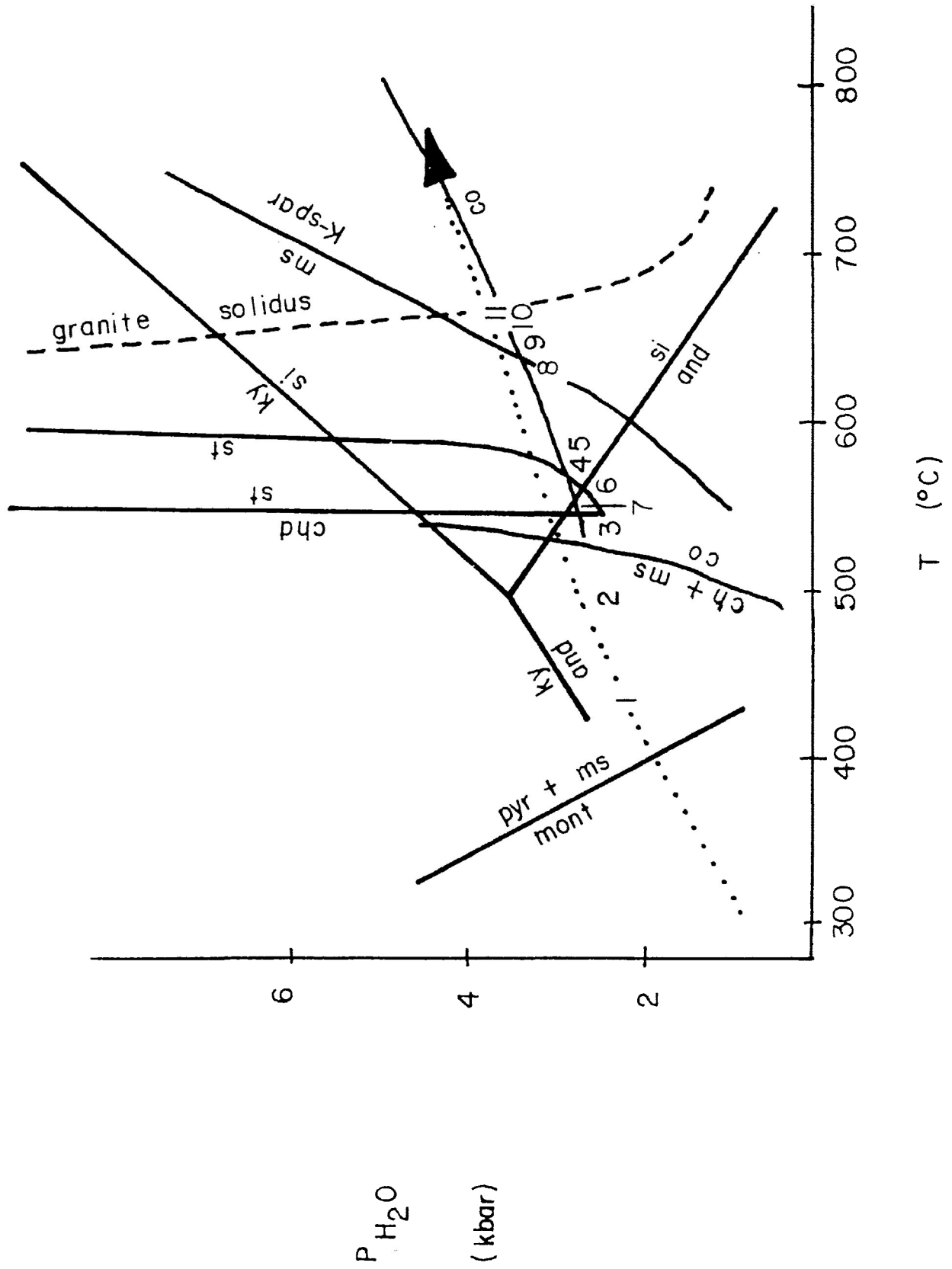


Fig. 19 P-T petrogenetic grid (after Hyndman, 1972) showing mineral assemblages of pelitic rocks of the study area numbered as in Fig. 18. The dotted arrow shows the path of regional metamorphism as determined by Pirie and Mackasey (1978). There is good agreement between the two trends although the rocks of the present study appear to have equilibrated at slightly lower pressures.

Abbreviations: and = andalusite
ch = chlorite
chd = chloritoid
co = cordierite
ky = kyanite
mont = montmorillonite
ms = muscovite
pyr = pyrophyllite
si = sillimanite
st = staurolite

Fig. 19



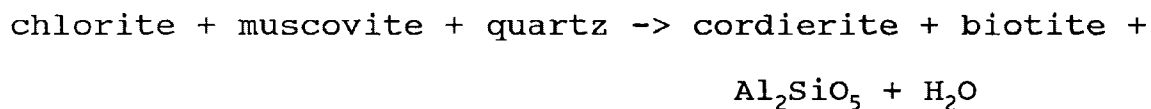
The exposures near Hazelwood Lake in Block A are folded turbidites which appear unmetamorphosed in outcrop except for an axial planar cleavage. Thin section study confirms the very fine-grained, clastic texture of these rocks but also reveals the presence of low grade metamorphic minerals chlorite and sericite. North of station P.L. 5.2 (Fig. 2), biotite is an additional phase. Along strike to the west the turbidites contain cordierite and staurolite which are indicative of medium grade metamorphism. Rather than forming as a result of regional metamorphism, field evidence indicates that these minerals have formed as the result of contact metamorphism which accompanied the emplacement of granitic to monzonitic plutons.

Almandine garnet is found in the higher temperature range of low grade metamorphism. The diagnostic assemblage of [almandine]-low grade metamorphism is almandine + chlorite + muscovite (Winkler, 1979). This assemblage, often with the additional minerals biotite, plagioclase, and quartz, are found in the metasedimentary rocks of Block A (stations 12.2, 16.0, 18.8, 26.1, and 28.7). Garnet-free low grade assemblages are found at stations 12.6, 71.5, and south of P.L. 5.2.

MEDIUM-GRADE METAMORPHISM IN PELITES

The first appearance of staurolite or cordierite (without almandine) marks the transition from low to medium-grade metamorphism in metapelites (Winkler, 1979). Andalusite is the stable Al_2SiO_5 polymorph in the low temperature part, and

sillimanite in the high temperature part. Biotite persists throughout and almandine is common. "No chlorite touching muscovite" can be used as a negative indicator of medium-grade metamorphism, since



Cordierite is observed in metasedimentary rocks of Block A along Highway 527 (at 11.0, 18.1, 18.8, 19.6). However, the close proximity of granitic intrusions to these locations suggests that the cordierite is the result of high temperature, low pressure contact effects on low grade rocks. The regional cordierite- or staurolite-in isograd strikes northeast-southwest across the study area from S.F. 10.4 to D.L. 21.2 to station 32.9. This isograd coincides with the boundary between Blocks A and B which was determined on the basis of field observations of incipient anatexis in the rocks. The earliest stages of metamorphic segregation therefore take place on the high grade side of the low to medium grade transition. Cordierite persists through Block C in the central part of the map area so that cordierite-/staurolite-free conditions (i.e low grade rocks) are not reached again until station 71.5 in Block D.

Staurolite-bearing assemblages are far less common than those in which cordierite is present. The relative paucity of staurolite does not necessarily mean that it is unstable at the prevailing P-T conditions, but rather is due to the restrictive bulk compositions

of rocks required for its formation. Winkler (1979, p. 223) estimated that the chemical composition of two-thirds of pelitic and psammitic metasedimentary rocks does not allow the formation of staurolite in medium grade metamorphism. Staurolite is restricted to rocks with low Mg/(Mg+Fe) ratios. As this ratio increases cordierite forms instead of staurolite. Formation of cordierite rims around staurolite cores at 32.9 and D.L. 21.2 in Block B may represent corresponding decreases of pressure during metamorphism. Pressure drops might be the result of uplift due to faulting or overall relaxation of stress as transpression ceased.

The following parageneses are diagnostic of the higher-temperature zone of medium grade metamorphism and occur in rocks of Block C.

cordierite + almandine + biotite + muscovite + quartz +/-
plagioclase (station 51.2)

cordierite + almandine + sillimanite + muscovite + quartz
+/- plagioclase (station 62.0)

cordierite + almandine + sillimanite + biotite + muscovite +
quartz +/- plagioclase (station 47.5)

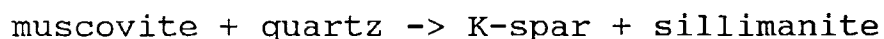
(Winkler, 1979).

Winkler (1979, p. 234) suggested that the assemblage almandine + cordierite + sillimanite + quartz is restricted to a specific range of P-T conditions: 5-7 kb at 600°C and 4-8 kb at 850°C. Almandine and cordierite coexist in the presence of muscovite in the rocks at stations 47.5, 51.2, and 62.0, as indicated above. Cordierite-

bearing, almandine-free assemblages (stations 32.9, 52.8, 68.7, 69.9, and D.L. 21.2) are stable at lower pressures. The assemblages present suggest that pressure did not exceed 6 kbar because in all assemblages containing both garnet and sillimanite, cordierite was also observed.

HIGH GRADE METAMORPHISM IN PELITES

The change from medium to high grade metamorphism is marked by the disappearance of primary muscovite in the presence of quartz and plagioclase. The reaction



which forms the boundary between medium and high grade metamorphism can be observed in a sample from station 53.4.

Parageneses diagnostic of high grade pelitic gneisses are (Winkler, 1979, p. 231):

K-spar + sillimanite/kyanite + almandine + biotite

K-spar + sillimanite + cordierite + almandine + biotite

K-spar + sillimanite + cordierite + almandine

K-spar + cordierite + almandine + quartz (station #1-2)

K-spar + sillimanite + cordierite + biotite (station 400-4)

+/- plagioclase + quartz

Fig. 20 shows typical mineral assemblages of medium to high grade rocks from the study area.

- Fig. 20 Typical mineral assemblages from medium to high grade rocks of the study area.
- a) cordierite + garnet + biotite
 - b) cordierite + sillimanite + biotite

Fig. 20a

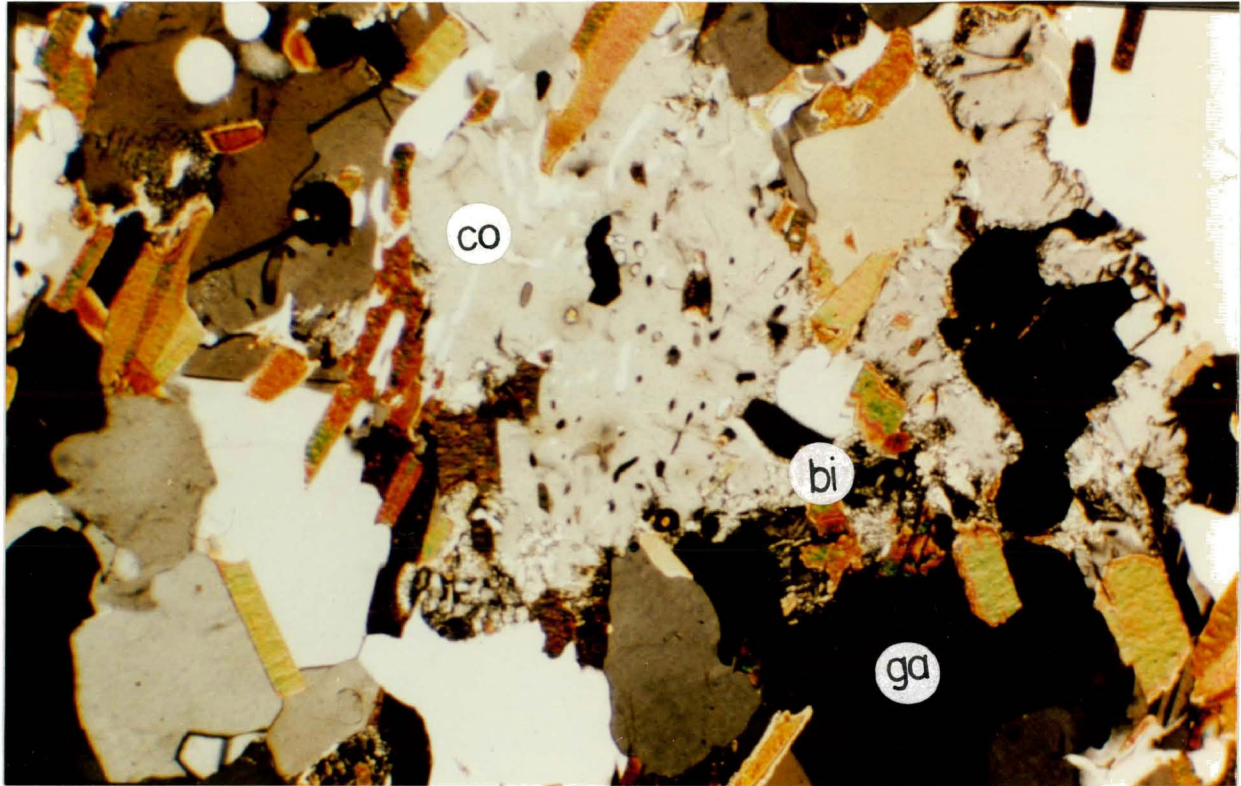
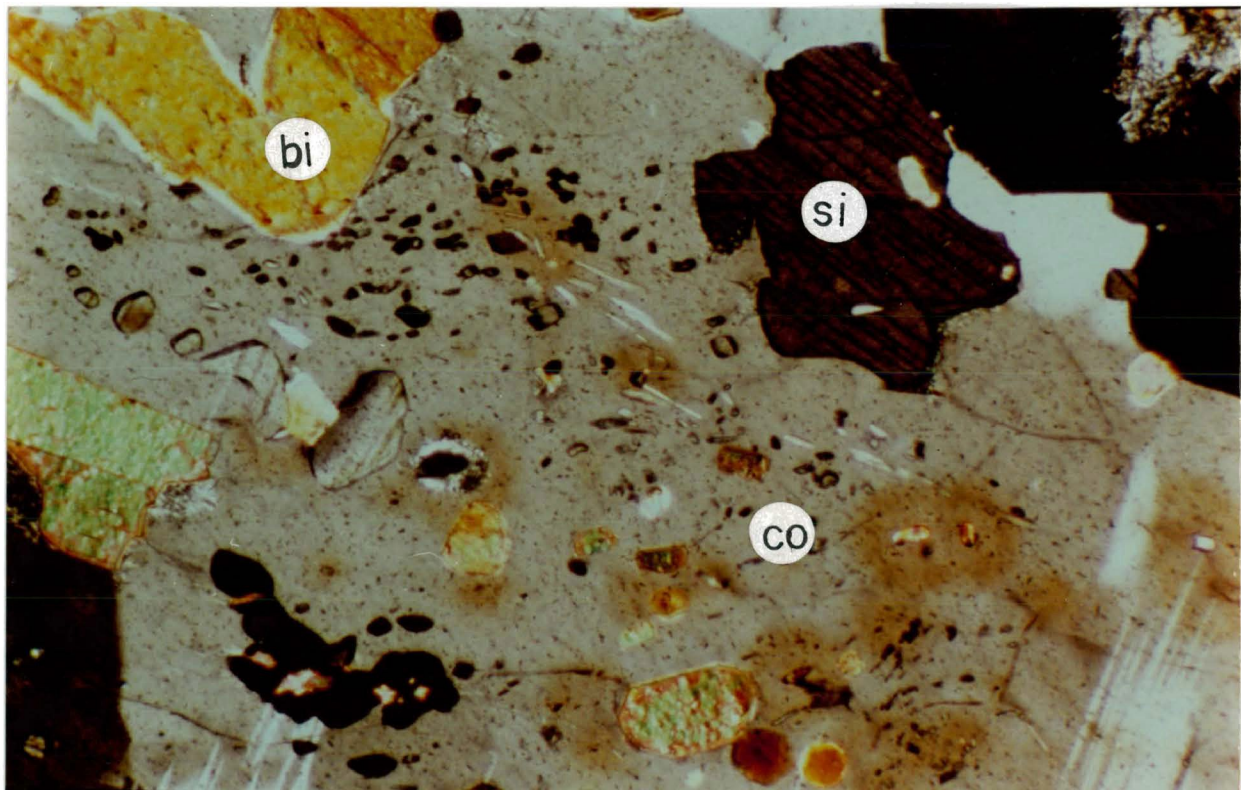


Fig. 20 b

.1 mm



At higher pressures ($P(H_2O) > 3.5\text{kb}$), anatexis in gneiss defines the beginning of high grade metamorphism (Winkler, 1979). Evidence for anatexis abounds within Block C of the study area. Quartz-feldspar leucosome segregated from biotite + quartz + plagioclase paleosome results in stromatic migmatites. Agmatitic and schlieric structures form as mobilizate envelopes paleosome. Still recognizable as former migmatite, homogeneous diatexite exhibits a nebulous texture as the paleosome becomes totally absorbed by the mobilizate and the rock takes on an igneous appearance.

The northern part of Block C is comprised mainly of gneissic granites and pegmatites. The relationship between regional metamorphism and granitic plutonism has long been recognized and it is still debated today whether uprising magmas supplied the heat for metamorphism or whether the granites result from partial fusion at the culmination of regional metamorphism (Turner, 1982).

It is possible that the potassium-rich gneissic granitic bodies of Block C were derived by large scale melting of pelitic metasedimentary rocks. The presence of accessory minerals such as muscovite, garnet, cordierite, sillimanite, tourmaline, and beryl and spodumene in pegmatites associated with the intrusions indicate they are S-type granites derived by anatexis of aluminous sedimentary rocks (Card, 1990). Based on his work in the English River subprovince Harris (1976) suggested that at conditions above 650°C and 3.5 kb the high grade muscovite-quartz breakdown reaction

results in a liquid of quartz + plagioclase + K-spar which can then migrate out of the system. Garnet and/or cordierite gneisses are therefore in fact restites of semi-pelitic sediments which have lost potassium + an aqueous phase to a granitic liquid. Harris concluded that garnet- or cordierite-bearing gneisses are indicative of temperatures in the range 650-750°C and pressures from 3.5-6.0 kb. Such high grade rocks are depleted in potassium relative to the lower grade, potassium-rich biotite gneisses which are garnet and cordierite-free. Harris (1976) suggested that the garnets in pegmatitic rocks were derived from the gneisses, possibly as restite crystals after partial melting of the gneisses. This hypothesis appears likely, since S.E.M. analyses in the present study have shown that garnets from leucosome and paleosome have almost identical chemical compositions.

GRANULITES

The highest grade assemblages found in the pelitic rocks of the study area are stable through granulite conditions. However, the pelitic assemblages do not confirm granulite facies metamorphism (granolite high grade of Winkler (1979)) because no associated hypersthene-bearing assemblages have been found. By definition (Winkler, 1979), granulites form only when $P(\text{H}_2\text{O}) \ll P(\text{tot})$. High $P(\text{H}_2\text{O})$ in the system from dehydration of wet sediments allowed partial melting, itself indicative of high grade metamorphism, to take place at relatively low temperatures. The abundance of water precluded the development of anhydrous

assemblages diagnostic of granulite facies metamorphism in the study area.

There is a considerable temperature range at any given pressure which the amphibolite -> granulite must cover (Turner, 1982) (high grade -> granulite high grade transition of Winkler). Examinations of this transition are documented by Turner (1982). Evidence for progressive increase in metamorphic grade includes characteristic systematic changes in mineral assemblages, an increase in the amount of "igneous-looking" granite, an increase in grain size of minerals, and increasing dehydration of the rock. Granulite grade pelitic gneisses contain the same mineral assemblages as their amphibolite grade counterparts although biotite is comparatively diminished in quantity. However, the presence of associated hypersthene-bearing rocks is necessary to classify pelitic assemblages within the granulite facies. This is due to the fact that a facies is defined as a series of assemblages from associated rocks of varying composition.

QUANTITATIVE ANALYSES OF MINERALS

One hundred thirty-two garnet-bearing samples were analyzed at Lakehead University using a Hitachi 570 scanning electron microscope with an attached Tracor Northern 5502 energy-dispersive X-ray spectrometer. The standardless semi-quantitative (SQ) software which normalizes each analysis to 100% was supplied with the spectrometer by Tracor Northern, with factory adjusted

standards. Correction factors were adjusted to compensate for instrument drift. The reference used to compare the garnet analyses was L.U. Geology standard block, sample my-pyrope M7 (R.H.M.).

Polished thin sections were carbon-coated before being exposed to an electron beam with an estimated resolution of one micron (A. Mackenzie, pers. comm. 1990) for a count time of 100 seconds. The instrument settings were 20 KV accelerating voltage, 28 mm working distance, and 18° takeoff angle.

The SQ analysis reports all iron as Fe²⁺. Therefore, the results of the garnet analyses were recalculated in order to determine the amount of iron present as Fe³⁺ (see Appendix A). This was done using MINFILE version 3-88, created by A.M. Afifi and E.J. Essene of the Department of Geological Sciences at the University of Michigan. This program was also used to produce the graphical illustrations of the garnet data.

The garnets of the study area cover a range of compositions. In molar proportions, the variation is from Alm₅₄₋₈₂Spess₁₋₃₃Py₂₋₂₅Gross₀₋₁₇, suggesting a parent rock composition which is relatively low in calcium and rich in iron and magnesium. Garnets from the melanosome and those from adjacent leucosome do not have appreciably different compositions. Leucosome garnets are usually larger while melanosome garnets, though smaller, are more numerous. Harris (1976) attributed the similarity of composition to

derivation from a common source during migmatite formation. Miyashiro (1976) reported decreasing MnO content from core to rim in zoned garnets. However, analyses of garnets with an inclusion-filled core and inclusion-free rim did not reveal any systematic variation in composition (Appendix B).

Folinsbee (1941) suggested that garnets which coexist with cordierite and biotite have a very limited range in composition of 71-78% almandine, 15-25% pyrope, approximately 2% spessartine, and less than 5% grossularite. Furthermore, he suggested that any garnets which fall within this compositional range should be associated with cordierite. Wynne-Edwards and Hay (1963) also found that garnet must lie within the 60-80% almandine range and have less than 10% combined spessartine and grossularite in order for it to be associated with cordierite. However, this study did not confirm these findings. Although garnets associated with cordierite are within the broad almandine range proposed by these workers, they contain up to 22% combined spessartine + grossularite. Neither is cordierite always observed in samples in which the garnet falls within the range of composition suggested by Folinsbee.

Sturt (1962) suggested that the variation in composition of a single mineral such as garnet is a better indicator of metamorphic grade than the presence or absence of index minerals, the formation of which is dependent on a number of factors. He found that garnets of pelitic schists show decreasing CaO and MnO and

increasing FeO and MgO with increasing metamorphic grade. Garnets in which the relative abundance of CaO and MnO is different due to original differences in host rock bulk composition can be compared because, among pelitic schists, it is the ratio of these oxides which is significant.

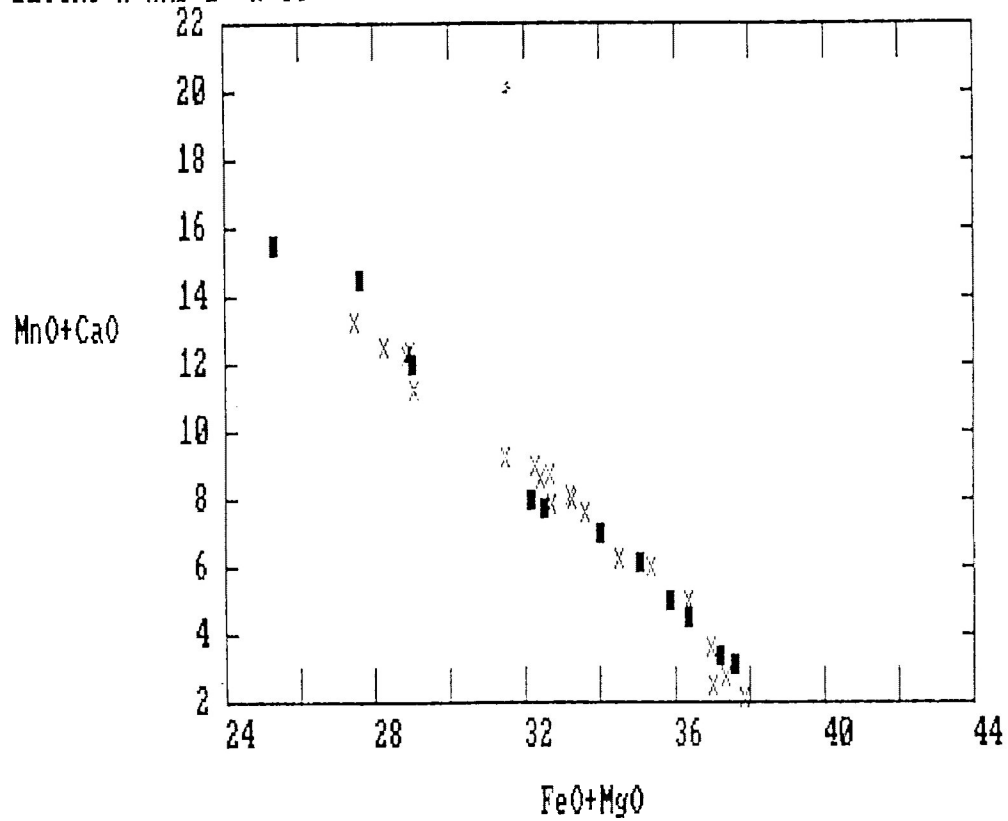
A graph of CaO+MnO vs FeO+MgO content in garnets (Sturt, 1962) should therefore plot as a straight line with a negative slope, with the higher grade rocks plotting nearer the X-axis. Such a plot for the Quetico garnets is shown in Fig. 21. The linear trend of increasing grade is evident. The fact that the garnet compositions north and south of the fault are essentially identical suggests that the present chemical compositions of the rocks now in fault contact is very similar. The samples were selected from pelitic schists, pelitic horizons of metagreywackes, and migmatitic paleosome. Garnets from vastly different rocks such as calcareous limestones or basic schists, for example, would of course be unsuitable for such an analysis since they would reflect the bulk composition of the rock and not only the metamorphic grade.

A study of garnet compositions at Broken Hill, Australia, by Stanton and Williams (1978) concluded that, since the garnet compositions varied widely on a scale of millimetres, the controlling factor in their development was parent rock composition. Overall bulk composition is indeed important in the formation of metamorphic minerals. For example, garnets only form in those parts of the parental pelite where the bulk composition is

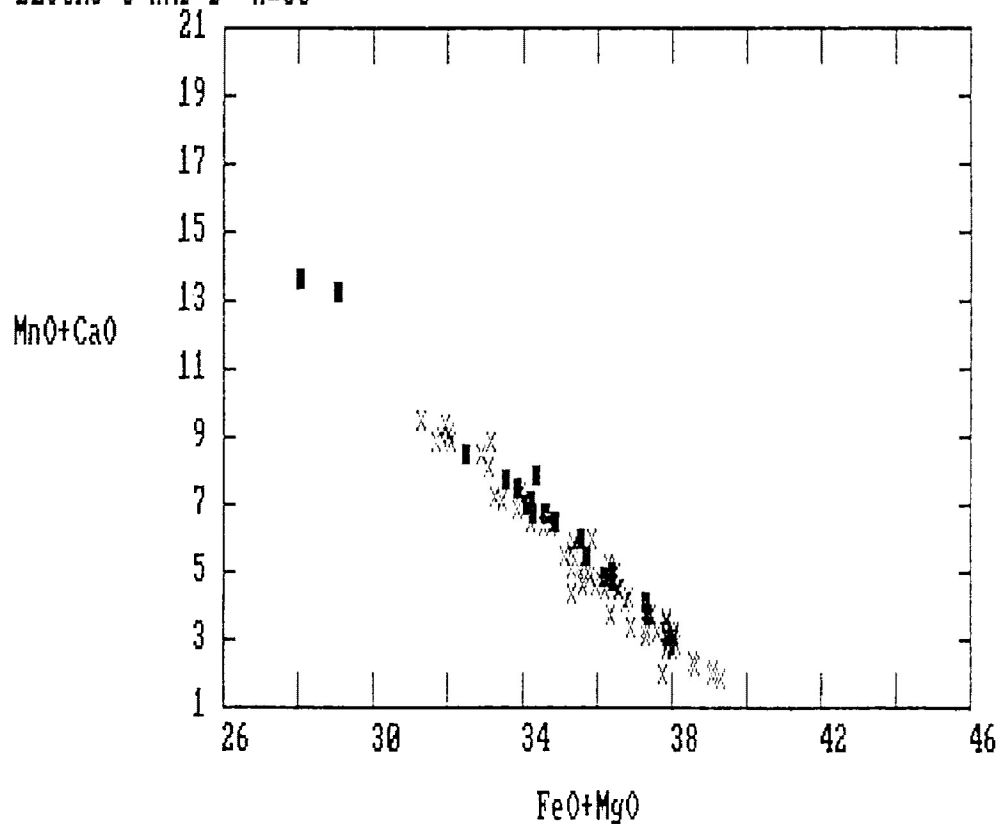
Fig. 21 Plot of (MnO + CaO) vs (FeO + MgO) of garnets from pelitic schists in the study area based on Sturt (1962). The highest grade garnets plot closest to the X-axis.

On the diagrams, samples from Blocks D and B are marked by solid squares; samples from Blocks A and C are marked by an X.

BLOCKS A AND B n=35



BLOCKS C AND D n=88



favourable. In a later paper, Stanton (1982) suggested that metapelites, which have long been considered to be of relatively constant composition, may actually vary so much on a small scale that almost the entire range of metamorphic minerals can form even without any changes or progression in metamorphic grade. However, multiple analyses of both single garnets and different garnets from a single sample revealed similar grades. Garnet analyses from different samples taken similar distances from the Quetico Fault also showed similar grades. For this reason, the metamorphic data presented here most likely represents true variations in grade and not merely variations in host rock bulk composition.

GEO THERMOBAROMETRY

Thermodynamic relationships can be used as geothermometers and geobarometers to calculate the temperature or pressure of equilibration of a rock. The analytical techniques are based on equilibrium exchange of elements between coexisting mineral phases. To obtain data suitable for such equilibrium calculations, electron microprobe analyses of biotite and additional garnet were performed at the University of Manitoba laboratory. A Cameca SX50 wavelength-dispersive probe was set at 15 KeV and 20 nA, with 20 000 times magnification (scanning raster of 5 microns). "PAP" $\phi(\rho z)$ correction procedure was applied (Pouchou and Pichoir, 1985). The microprobe results were processed for garnet-biotite geothermometry using PTMETER, a program developed by J. Maley and J. Percival at the Geological Survey of Canada.

Fig. 22 Table of results of garnet-biotite geothermometry.
For a more detailed listing see Appendix C.

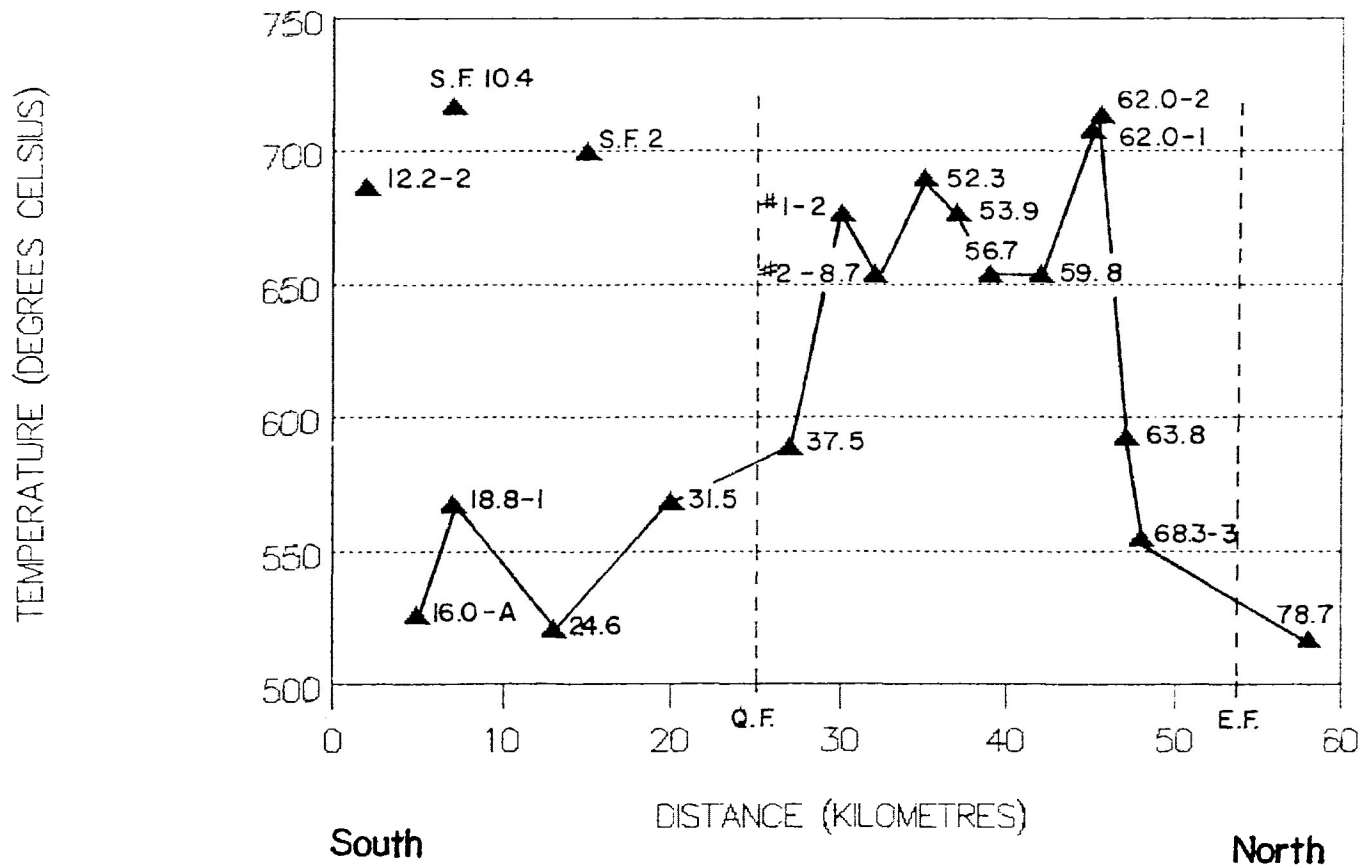
Fig. 22

<u>SAMPLE NUMBER</u>	<u>TEMPERATURE (°C)</u> <u>THOMPSON (1976)</u>	<u>BLOCK</u>
12.2-2	687	A
S.F.10.4	717	B
S.F.2	700	B
16.0-A	526	A
18.8-1	568	A
24.6	521	A
31.5	569	B
37.5	589	C
#2-8.7	654	C
#1-2	677	C
52.3	690	C
53.9	677	C
56.7	654	C
59.8	654	C
62.0-1	708	C
62.0-2	714	C
63.8	593	C
68.3-3	555	D
78.7	517	D

Fig. 23 Plot temperature variations in garnet-biotite equilibration showing the overall metamorphic asymmetry across the study area. Vertical dashed lines at 25 km and 54 km mark the locations of the Quetico and Eaglehead faults, respectively. Although schists on the south side of the Quetico Fault are adjacent to stromatic migmatites on the north, there is no abrupt temperature change across the fault. The high temperatures of samples 12.2-2, S.F. 10.4, and S.F. 2 are the result of contact metamorphism adjacent to intrusions. See Fig. 22 for a tabular presentation of the data including a list of which Block (Fig. 4) the samples are from.

Fig. 23

TEMPERATURE VARIATIONS IN A TRANSECT ACROSS STRIKE



Garnet-biotite geothermometry (Fig. 22) shows that temperatures increase from 517°C in the metasedimentary rocks of Blocks A and D to a maximum of 714°C (Thompson, 1976) in the central migmatites of Block C (Appendix C). The Ferry and Spear (1978) method gives slightly different values. Based on their method temperatures in the low pressure andalusite-bearing rocks of Blocks A and D are approximately 512°C, whereas the central migmatites of Block C yield temperatures of up to 790°C. These temperatures compare favourably with those estimated from the P-T grid (Fig. 19). In general, the pattern of steadily increasing temperatures northward is terminated by a rather sharp temperature drop north of the highest grade rocks (Fig. 23). This trend is generally reflected by the plot of (FeO + MgO) vs (MnO + CaO) for garnets (Fig. 21) and is further confirmed by mineral assemblages (Fig. 18) and textural changes in the rocks. Anomalously high temperatures reported from stations 12.2, S.F. 2, and S.F. 10.4 are attributed to the thermal effects of nearby intrusions.

The grossular-anorthite-quartz- Al_2SiO_5 geobarometer of Hodges and Spear (1982) was applied to the equilibrium assemblage garnet + plagioclase + quartz + sillimanite from one of the medium grade rocks from the central part of Block C. Given that the calculated temperature for the sample was 677°C (by Thompson, 1976) to 737°C (by Ferry and Spear, 1978), the corresponding pressure of equilibration was approximately 5 +/-1.5 kbar, consistent with the metamorphic path illustrated in Fig. 19.

Percival (1989) applied geothermobarometry to rocks from Raith, fifty km west of the present study area. His temperature estimates from Fe-Mg partitioning between garnet and biotite range from 622°C based on Thompson (1976) to 651 °C based on Ferry and Spear (1978). The pressure estimate based on Koziol and Newton's 1988 garnet-sillimanite-plagioclase-quartz-biotite assemblage was 3.3 kbar.

BARIC TYPES

Miyashiro (1973) tabulated the characteristic minerals of metapelites for low, medium, and high pressure baric type metamorphism. The rocks of the present study area fall unquestionably in the low-pressure baric type, characterized by the presence of andalusite and sillimanite and the absence of kyanite. Common minerals include biotite, cordierite, staurolite, and sillimanite, and greenschist -> amphibolite -> granulite is the common facies series. Geobarometry determined a pressure of 5 kbar near the highest grade rocks and mineral assemblages are consistent with a low pressure metamorphic regime of less than 5 kb.

The Abukuma Plateau in Japan was originally designated the type terrane for low-pressure metamorphism. Kyanite has since been found to occur there occasionally along with andalusite and sillimanite, making the area transitional between low and medium-pressure types (Miyashiro, 1973). Although no kyanite was found in the present study, kyanite in rocks 50 km to the west of the study area (Percival et. al., 1985), suggests a low to medium

pressure transitional terrane. Kyanite reported by Bauer and Tabor (1990) suggests that regions of similar rock to the southwest underwent slightly higher pressure metamorphism. The current exposure of these rocks may be due to differential uplift of parts of the subprovince and consequent unroofing of deeper structural levels.

DISCUSSION AND INTERPRETATION

A Model for Archean Crustal Evolution

Many models for the evolution of the Archean crust have been proposed. The models can be divided into two main groups: "fixist" and "mobilist" (Blackburn, 1980). Fixist models imply that all Archean rocks were primarily subjected to vertical crustal movements which resulted in their present spatial relationship. Mobilist models, on the other hand, incorporate plate tectonic theory where horizontal crustal movements juxtapose separate blocks of crust.

After examining the various models, Blackburn (1980) concluded that much of the available data were incompatible with fixist models. However, although many features remain unexplained, none of the data are incompatible with mobilist plate tectonic theory. Mobilist models have the added advantage of being uniformitarian since the processes believed to have operated in the Archean are still functioning today. A great deal of work has been done on the evolution of the Superior Province which has supported and further

developed these early theories. A recent review by Card (1990) concluded that the features of the Superior Province are best accounted for by a model of subduction-driven accretion of Archean crustal elements.

The Wabigoon and Wawa subprovinces are believed to represent the remains of former volcanic island arcs. The extrusive rocks of these terranes are pillow basalts, mafic flows, and felsic to intermediate volcanoclastic rocks. The Quetico terrane is thought to represent the remains of an accretionary prism of submarine fan and abyssal turbidites (Percival and Williams, 1989; Card, 1990). The sediments were derived from felsic and mafic material shed from the volcanic arcs (Ojakangas, 1985). Geochronological evidence appears to support the theory that the Wawa terrane approached and was accreted to the Archean protocontinent. Langford and Morin (1976) commented on the general progression of younger radiometric ages southward in the subprovinces making up the Superior province. For example, the Wabigoon volcanic and plutonic rocks formed between 2900 Ma and 2680 Ma. Major volcanism in the Wawa terrane at 2700 to 2695 Ma was followed by late plutonism at 2697 to 2675 Ma (Percival and Sullivan, 1988). Davis (1990) determined that deposition of sediments in the Quetico terrane occurred between 2698 and 2688 (+/- 5) Ma. Paleomagnetic poles from rocks of the Wabigoon, Quetico, and Wawa subprovinces coincide at about 2600 Ma (Blackburn, 1980), indicating that final docking was complete and the subprovinces had coalesced into a single unit by this time. The data gathered during this study appear to be compatible with

the proposed model of accretionary prisms, subduction zones, and volcanic island arcs.

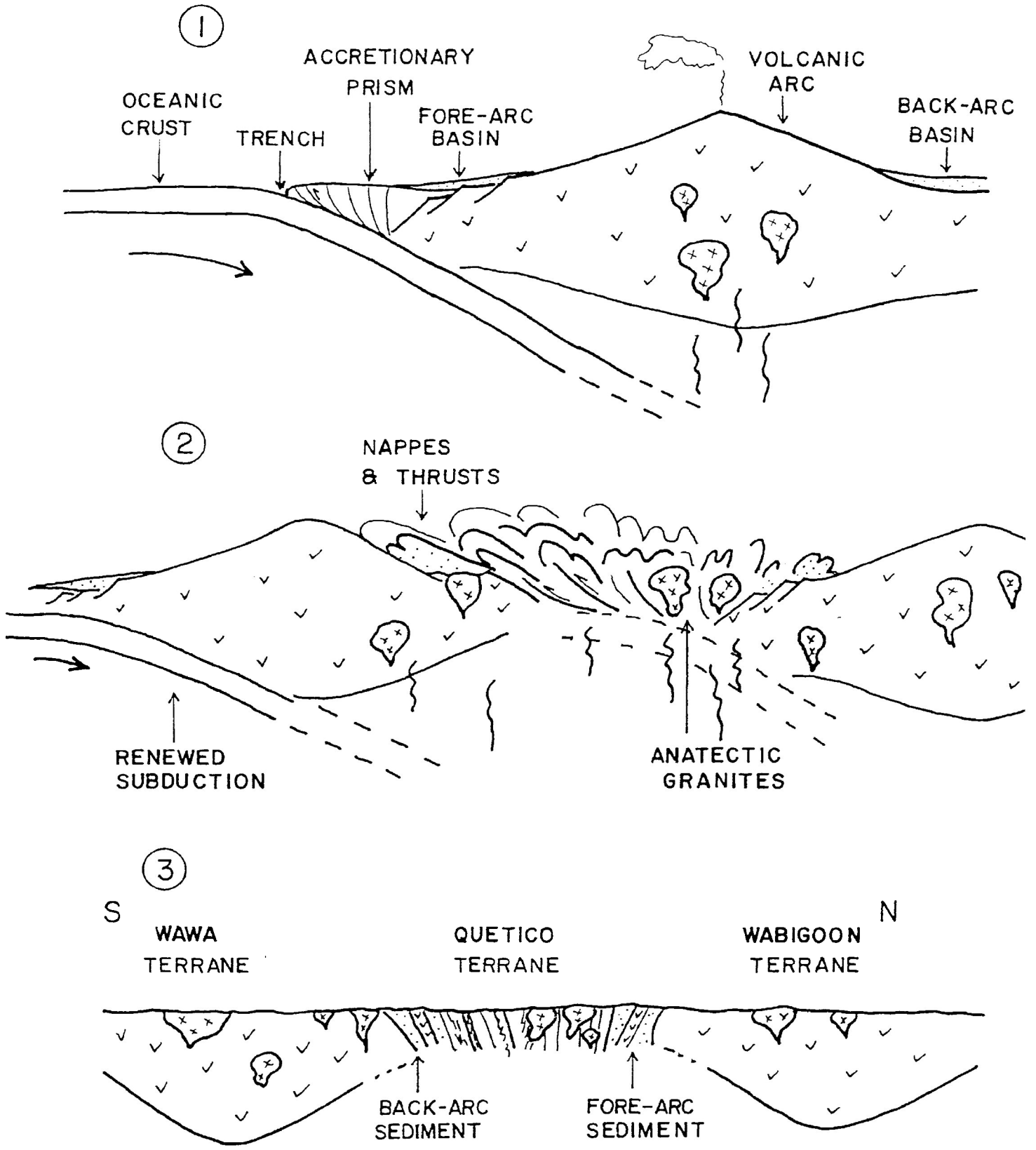
A General Model

Fig. 24 is a schematic diagram illustrating a possible evolution for the area studied. The model is based on the modern concept of plate tectonics. Hutton's principle of uniformitarianism suggests that similar crustal processes were operating throughout the earth's history although, in detail, it is likely that during Archean times they were somewhat different from today. For example, geothermal gradients are thought to have been much higher in a hot developing continental crust. Nevertheless, a model based on an Archean equivalent to plate tectonics seems to best explain the configuration of the present day Superior Province. The following discussion will explain the processes involved in accretionary tectonics and will conclude with suggestions of how the area studied conforms to such a model.

When an oceanic plate encounters continental lithosphere, the oceanic plate is subducted and a trench marks the surface expression of the subduction zone. In Fig. 24 (1) oceanic lithosphere is being subducted beneath an active volcanic arc. The volcanic terrane forms the most recently accreted part of a developing protocontinent which itself is the product of complex accretionary processes. Volcanism and granitic plutonism in the arc are the result of rising magmas generated through partial

Fig. 24 Proposed model for evolution of the Quetico subprovince:

1. Ocean - continent collision. Oceanic crust subducts beneath a volcanic arc recently accreted to a protocontinent. Sediment is deposited in back-arc and fore-arc basins and in an accretionary complex. Batholiths are emplaced in the volcanic arc.
2. Docking and transpression. The basin and accretionary prism sediments are folded, faulted, and thrust. Nappes develop. Rebounding isotherms from cessation of subduction causes partial melting and emplacement of anatectic granites. Renewed subduction takes place on the oceanic side of the docking arc and intrusions are emplaced within the arc and the deformed sediments.
3. Present erosion surface. Anatectic "roots" of the folded sedimentary sequence are exposed. Structures have been steepened by compression and faults are expressions of shear stresses. Low grade fore- and back-arc sediments are interlayered with volcanic rocks in the boundary zones due to faulting and tectonic stacking.



melting of the subducting slab of oceanic crust and the overlying upper mantle.

On the seaward side of the trench the abyssal ocean floor sediments are composed of silt, clay, and volcanic ash. As the oceanic plate is subducted beneath the protocontinent, a subduction complex or accretionary prism develops. This wedge is composed of ocean floor and trench sediments scraped off the subducting plate and tectonically accreted to the overriding plate (Reading, 1986, p. 494). Continually arriving sediments are underthrust and accreted onto the wedge and are progressively rotated into a near vertical orientation.

As the volume of the volcanic rock mass of the arc continues to increase, it gradually sinks isostatically. Thinner segments of crust adjacent to the sinking arc form extensional basins. On the continental side of the active arc, a back-arc basin forms. A fore-arc basin develops near the internally deformed accretionary prism on the seaward side. Proximal clastic sediments shed from the growing arc are deposited in these depressions. The sinking volcanic mass gradually heats up and becomes plastic and spreads laterally. The spreading is primarily directed seaward, since the bulk of the protocontinent limits expansion in that direction. The resulting horizontally directed compressive stresses are responsible for widespread folding, low angle thrusting, and formation of nappes in the rocks of the fore-arc and subduction complex.

Thus far the model has only involved the subduction of an oceanic plate beneath an active "continental" margin. However, it is conceivable that the subducting plate could be carrying a volcanic island arc that formed previously above a subduction zone in an intra-oceanic environment. This arc would have features from its earlier development similar to those already discussed; i.e. a predominantly volcanic terrane flanked by a back-arc basin on one side and by a fore-arc basin and accretionary complex on the other.

Collision of an approaching arc with the protocontinent results in compression and produces folds and thrusts at the opposing margins as well as in the intervening sediments of the extensional basins and accretionary wedge. Fig. 24 (2) schematically illustrates how thrusts and thrust nappes are tectonically emplaced onto the approaching arc. Subduction will cease when the last bit of oceanic crust has been consumed and this effectively results in the "docking" of the arc and its incorporation into the developing craton. Cessation of subduction also results in rebounding of depressed isotherms. The heat generated by the thermal relaxation beneath the sedimentary terrane causes partial melting of the overlying rock. "S"-type magmas are generated and emplaced within the deformed subduction complex.

Assuming that active sea floor spreading continues, subduction must also continue near the margins of the developing craton. Therefore, when one subduction zone becomes inactive as an arc

complex is accreted to the craton, renewed subduction is initiated beneath this newly accreted terrane as illustrated in Fig. 24 (2). Partial melting at depth of oceanic lithosphere, pelagic sediments, and overlying upper mantle results in renewed magmatism beneath the accreting arc and the deformed fore-arc.

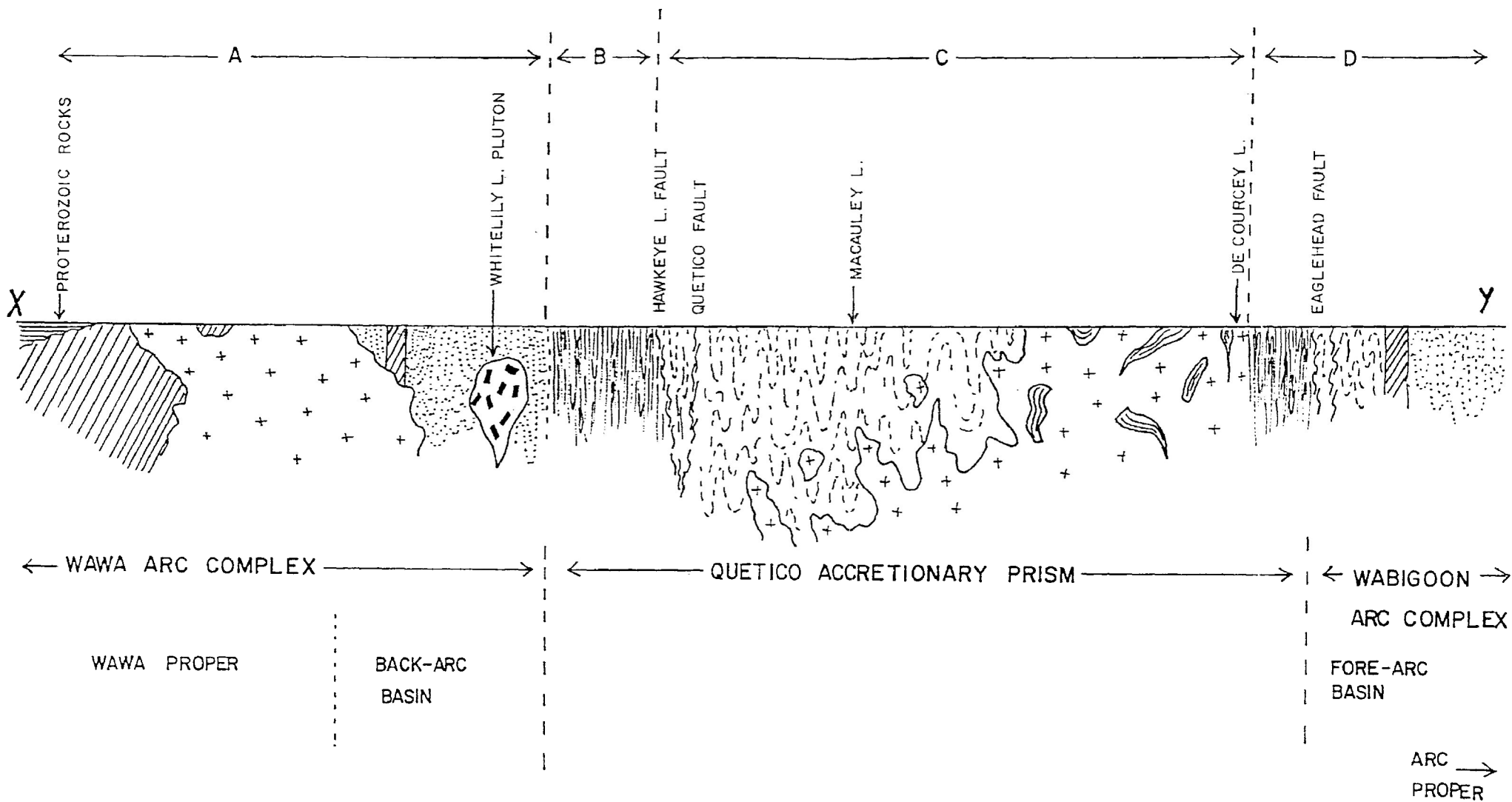
The processes described above may be repeated a number of times to produce an Archean continent composed of alternating belts of volcano-plutonic and gneiss-migmatite terranes. The present erosion surface is the product of isostatic adjustments which includes removal of vast amounts of geologically significant portions of the crust by weathering processes. In addition subsequent movements on faults have added to the difficulties in interpreting the earlier geological relationships. Therefore, when considering the present-day configuration of Archean cratons, it must be remembered that a greatly simplified model such as the one presented here cannot explain all observations.

Evolution of Rocks in the Study Area

Using the elements of the general model described above, an attempt is made here to review the data obtained from the study area with respect to this model. At the present level of erosion (Fig. 25), the volcanic and plutonic rocks of the Wabigoon subprovince may be remnants of an island arc which became accreted to and formed the margin of an Archean protocontinent. The protocontinent itself was most likely the product of complex accretionary tectonics. Rising magmas generated by partial melting

Fig. 25 Geologic cross section of the study area and its relationship to the tectonic model (Fig. 22) (see Fig. 3 for location). The Wawa arc complex is comprised of the volcanic arc proper and its back-arc basinal sediments. The Wabigoon arc complex is likewise composed of the arc proper and the fore-arc basin sediments. The Quetico accretionary prism is composed of relatively uniform subduction complex rocks. The entire sequence has been extensively deformed and metamorphosed.

Fig.25



of the subducting oceanic lithosphere and upper mantle resulted in volcanism and plutonism within the Wabigoon terrane, as shown in Fig. 24 (1).

The clastic sedimentary and volcanic rocks including conglomerates, turbidites and tuffs exposed in and north of Block D (Fig. 4) may represent deposits derived from the Wabigoon terrane and deposited in the former forearc basin (Fig. 24 (1), Fig. 25). These rocks form a low grade metamorphic sequence which may reflect their position with respect to the site of magma generation. If the fore-arc basin occupied a central position in the trench-arc gap during the approach of the Wawa terrane, then the main source of magma and heat would have been far away from the site of deposition of the sediments. Folding of the sequence as evidenced by reversals in younging and structural facing directions was due in part to seaward-directed compression from the isostatically sinking volcanic arc.

Once docked, the Wabigoon terrane formed the new protocontinental margin. The mud and clay deposited on the ocean floor was the distal counterpart to the more proximal forearc basin deposits. As accretion continued, the pelitic sediments were thrust, folded, and progressively rotated to a subvertical orientation. Ultramafic blocks preserved in the migmatites of the central part of the study area (Block C, Fig. 4) may be metamorphosed slices of ocean floor that were scraped or faulted upward into the sedimentary pile. The gneisses and migmatites of

the Quetico subprovince could be the remains of the accretionary prism on the trench side of the craton (Fig. 25).

The subducting oceanic plate was bringing with it a new volcanic arc: the Wawa terrane. The approaching Wawa arc may have had an already developed back-arc basin filled with sedimentary rocks on the side nearest the protocontinent. The turbidites and other clastic sediments of Block A (Fig. 4) may represent the material shed from the Wawa arc into the backarc basin while the volcanic rocks of Block A are the remains of the arc proper (Fig. 25). As the arc collided with the accretionary wedge at the leading edge of the continental block [Fig. 24 (2)], the intervening sediments of the forearc and backarc basins as well as the accretionary prism were compressed, folded, and thrust. Compression caused by the docking arc may have resulted in low angle thrust faults which cut earlier-formed thrusts rotated to subvertical orientations in the subduction complex. Because the sediments were water-saturated, frictional resistance could be overcome and large net slip displacements were possible along faults. Recumbent folds, if faulted during compression, could have formed nappes. Exposures with shallowly dipping layers, marked on Fig. 3 by solid circles, occur in widely separated localities. In spite of the suggested abundance of thrusts and nappes, their relative paucity of preservation today is not unexpected. The level of erosion is too deep to have preserved significant parts of the superstructure. Continued compression coupled with late diapirism steepened pre-existing planar structures and has produced

a ubiquitous penetrative cleavage. The effects of these processes have obliterated much evidence for earlier structures and stratigraphic relationships (Card, 1990).

Structures indicative of transpression have been documented by a number of workers (Bauer and Bidwell, 1990; Hudleston et. al., 1988; Spark, 1990). These structures are in general agreement with the suggestion that the Wawa arc approached the protocontinent obliquely. The Quetico Fault, initiated at this time, may have been in response to the shear component of oblique subduction. A dextral transpressive regime is suggested by kinematic indicators showing dextral displacement along the fault. Since strike-slip movement on the Quetico Fault is estimated to be on the order of tens of kilometres, no symmetry in metamorphic grade was expected across the study area. Other than separating stromatic migmatites from schists, the Quetico Fault does not appear to have a major influence on the metamorphic gradient across the strike of the rocks in the study area (Fig. 23). The reasons for this may be twofold. First, post-metamorphic movement on the fault might have juxtaposed spatially separated rocks which had equilibrated at similar conditions. This is an unlikely coincidence due to the large lateral displacement attributed to the fault. A second possibility is that the fault may have formed a barrier to fluid migration during metamorphism, so that water-saturated rocks north of the fault underwent partial melting at a relatively low temperature. Similar P-T conditions in drier rocks cut off from

metamorphic fluid circulation south of the fault were not sufficient to induce anatexis.

Docking of the Wawa terrane with the existing craton was complete as the last portions of oceanic crust were subducted. At this time subduction-generated magma production also subsided considerably. Percival (1989) suggested that cessation of subduction and consequent thermal relaxation of the depressed isotherms, together with heat generated from the decay of radioactive isotopes and the weight of the tectonically stacked accretionary wedge, could explain the low-P, high-T regime in the Quetico subprovince. High fluid pressures in the central parts of the sedimentary wedge lowered the melting temperature so that partial melting took place on a large scale as the isotherms rebounded. The granites and pegmatites of the northern part of Block C (Fig. 4, Fig. 25) may have formed at this time. Alumina-rich minerals in the granitic rocks indicate that they were derived from anatexis of aluminous sedimentary rocks. The observed metamorphic asymmetry (Fig. 23) can also be accounted for in this manner. The greatest depression of isotherms occurred beneath the subducting plate. The most substantial increase in temperature, caused by the rebounding of isotherms after cessation of subduction, was greatest beneath the subduction complex.

The docked Wawa terrane formed the new cratonic margin and the site of renewed subduction shifted [Fig. 24 (2)]. Partial melting of the subducted plate and upper mantle could have resulted in the

diapiric emplacement of late intrusions preserved in Block A (Fig. 4, Fig. 25) of the study area. The intrusions overprint the regional metamorphism with development of contact metamorphic aureoles. Subduction-driven accretion resulting in the pattern of alternating volcano-plutonic and gneiss-migmatite terranes in the Superior Province came to a halt with the docking and plutonism of the Wawa complex. This may be due to cessation of spreading at the ridge or to changes in lithospheric plate motion preventing further terrane interactions.

Late faulting possibly related to continuing transpression produced a series of pull-apart basins in the volcanic Wawa terrane. Reversals of motion along the faults caused transpression of the basin sediments and resulted in a north-south striking crenulation cleavage in the clastic sequence, a fabric which is absent in the surrounding volcanic rocks (Seemayer, 1989). A post-metamorphic crenulation cleavage observed in the high grade migmatites north of the Quetico Fault (Fig. 16) may also be related to late transpression.

Based on models using gravity data, Kehlenbeck and Cheadle (1990) suggested that the low grade metasedimentary rocks of the southern part of the study area (Block A) occupy a northward-deepening trough underlain by a basinal structure of metavolcanic rocks. This relationship might be expected if the sediments represent thrust slices or nappe-like structures which were tectonically emplaced onto the docking Wawa volcanic island arc.

Kehlenbeck and Cheadle (1990) suggest diapiric emplacement for the porphyritic plutons, since their models showed these structures to pinch out with increasing depth. Thus, the general geology, structure, and metamorphism of the study area appears to be compatible with a subduction-driven accretionary model.

If analogues of modern subduction zones existed in the Archean as suggested here, critical features such as melanges and high pressure, low temperature metamorphism are missing. Melanges, deformed and flattened mixtures of various rock types, may be the result of tectonic mixing in accretionary terranes (Spencer, 1988). It is possible that ultramafic blocks found in the rocks of the Quetico terrane are remains of melanges that have been almost completely assimilated to become part of the migmatites. The absence of high pressure-low temperature metamorphism may be attributed to high Archean geothermal gradients and long periods of metamorphism. Low temperature metamorphism was not as widespread, even in subduction settings, as it is today. Progressive deformation and heating would have transformed any former low pressure assemblages to ones of medium grade.

Based on the evidence presented here, it appears impossible to draw a definitive boundary division between the Wawa, Quetico, and Wabigoon subprovinces on the basis of differences in structure, lithology, or metamorphic grade. Deformation and tectonic stacking has produced boundary zones of complexly folded and faulted volcano-metasedimentary terranes which extend for several

kilometres between predominantly volcano-plutonic sequences and true gneiss-migmatite terranes. At the present level of erosion [Fig. 24 (3)], the lithologically varied, low grade volcanic-metasedimentary-plutonic Block A (Fig. 4) represents the transition zone between the Wawa and Quetico subprovinces in the southern part of the study area (Fig. 25). Similarly, in Block D in the north a lithologically diverse, low grade zone cut by a major shear zone represents the faulted and deformed Wabigoon-Quetico transition zone (Fig. 25).

CONCLUSIONS

Based on the data presented in this thesis together with the work of others the following conclusions appear warranted:

1. It has been agreed by most workers that the Quetico subprovince is a predominantly metasedimentary terrane (Pirie and Mackasey, 1978; Percival, 1989; Card, 1990). Schists, gneisses, and migmatites comprise the bulk of the rocks. S-type granites are intimately associated with migmatitic sections. The rocks of Blocks B and C (Fig. 4) of the present study area clearly fit the established lithological criteria of the Quetico subprovince.

2. Recent work by Percival (1989), Devaney and Williams (1989), Williams (1990), and Card (1990) has suggested that the metasedimentary sequences of the Quetico subprovince represent the remains of an accretionary prism which accumulated at the margin of the Wabigoon arc. Based on field observations in the study area, it is clear that the majority of rocks are of sedimentary origin. Because of the deformation and partial melting of significant parts of the metasedimentary terrane, it is difficult to establish stratigraphic relationships and no conclusive evidence for the former existence of an accretionary prism is available from the present study area. However, the spatial positioning of dominantly metasedimentary rocks with respect to the Wabigoon terrane makes it likely that such a prism might have existed. It has since been

significantly modified by deformation, metamorphism, and anatectic processes.

3. Boundaries between adjacent subprovinces may be clearly defined. For example, the Quetico Fault separates volcanic rocks of the Wabigoon subprovince from metasedimentary rocks of the Quetico subprovince in the Atikokan area (Mackasey et. al., 1974). In other places the boundaries may be more complex, as in the Beardmore-Geraldton area, where a fold belt (Kehlenbeck, 1986) or a thrust-imbricated supracrustal stack (Devaney and Williams, 1989) forms a transitional terrane between the Wabigoon and Quetico subprovinces.

Although the predominant lithology is sedimentary, in the present study Blocks A and D (Fig. 4) are believed to represent the complexly folded and faulted transition zones between the Wawa-Quetico and Quetico-Wabigoon subprovinces, respectively. These lithologically diverse zones may represent the deformed remains of fore-arc and back-arc basins (Fig. 25).

4. In some portions of the Quetico subprovince increases in metamorphic grade are symmetrically disposed about a thermal axis (Percival, 1989). It is commonly reported that the metamorphic grade is lowest near the margins of the Quetico subprovince and that it rises gradually toward the centre of the gneissic terrane (Pirie and Mackasey, 1974).

In the area described in this thesis the Quetico Fault lies well within the boundaries of the Quetico subprovince. Consequently, the fault zone divides the subprovince into two formerly separated parts of the terrane that have been brought into juxtaposition as a result of fault motion. Based on observations recorded here, a gradual increase in regional metamorphic grade exists from the Wawa-Quetico transition northward through the Quetico subprovince. This trend of gradual increase in grade is not interrupted by the Quetico fault zone for it continues north of the fault (Fig. 23). The highest grade rocks, as reflected by mineral assemblages, occur well north of the fault in the migmatitic part of the Quetico subprovince. From here a sharp decrease in metamorphic grade occurs toward the transition zone with the Wabigoon terrane.

5. In most outcrops a subparallelism of subvertical relict primary layering, compositional layering, and a penetrative schistosity typifies the rocks. The presently exposed rocks of the Quetico subprovince are the result of erosion and isostatic adjustment and comprise the "root" zone of an Archean orogenic belt. However, in several widely separated exposures planar structures with low dips and occasionally subvertical foliations have been found. Other workers have reported similar occurrences (Hudleston et. al., 1988; Tabor and Hudleston, 1991).

Because of low outcrop density, it was not possible to map these shallowly dipping structures for any distance in the field.

In several outcrops the subhorizontal planar elements appear to be bounded by zones of shear discontinuity. This may suggest that the structures are relicts of former larger folds which may have been detached and transported along low angle faults for some distance, likely in response to compression.

6. Several plutons in Block A of porphyritic quartz monzonite to granodiorite are unfoliated and have produced narrow but distinct contact metamorphic aureoles. Development of hornfelsic textures and static mineral growth reflects the post-tectonic emplacement of the plutons. These plutons may be representative of the final stages of subduction-driven accretionary tectonism in this part of the crust.

REFERENCES

- Ayres, L.D., 1978. Metamorphism in the Superior Province of northwestern Ontario and its relationship to crustal development. *In* Metamorphism in the Canadian Shield, Geol. Surv. Can. Paper 78-10: 25-36.
- Bauer, R.L. and Bidwell, M.E., 1990. Contrasts in the response to dextral transpression across the Quetico-Wawa subprovince boundary in northeastern Minnesota. *Can. J. Earth Sci.* **27**: 1521-1535.
- Bauer, R.L. and Tabor, J.R., 1990. Syntectonic, intermediate-pressure regional metamorphism along the northern margin of the Quetico Belt in northeastern Minnesota: contrasts with adjacent boundary areas. Abstracts, Institute on Lake Superior Geology 36th Annual Meeting, Thunder Bay, Ontario, May 9-12, 1990.
- Blackburn, C.E., 1980. Towards a mobilist tectonic model for part of the Archean of northwestern Ontario. *Geosci. Can.* **7**: 64-72.
- Borradaile, G.J., 1982. Comparison of Archean structural styles in two belts of the Canadian Superior Province. *Precamb. Res.* **19**: 179-189.
- Borradaile, G., Sarvas, P., Dutka, R., and Stewart, R., 1988. Transpression in slates along the margin of an Archean gneiss belt, northern Ontario - magnetic fabrics and petrofabrics. *Can J. Earth Sci.* **25**: 1069-1077.
- Borradaile G.J. and Spark, R., 1991. Deformation of the Archean Quetico-Shebandowan subprovince boundary in the Canadian Shield near Kashabowie, northern Ontario. *Can. J. Earth Sci.* **28**: 116-125.
- Breaks, F.W., Bond, W.D., and Stone, D., 1978. Preliminary geological synthesis of the English River Subprovince, Northwestern Ontario and its bearing upon mineral exploration. *Ont. Geol. Surv. Misc. Paper 72*, 54p.
- Brown, M., 1973. The definition of metatexis, diatexis, and migmatite. *Proc. Geol. Assoc.* **84**: 371-382.
- Card, K.D., 1990. A review of the Superior Province of the Canadian Shield, a product of Archean accretion. *Precamb. Res.* **48**: 99-156.
- Card, K.D. and Ciesielski, A., 1986. Subdivisions of the Superior Province of the Canadian Shield. *Geosci. Can.* **13**, no.1: 5-13.

- Chiew, A.S., 1976. Petrology of the metasedimentary unit at Little Dog Lake. HBS thesis, Lakehead University.
- Davis, D.W., 1990. The Seine-Coutchiching problem reconsidered: U-Pb geochronological data concerning the source and timing of Archean sedimentation in the western Superior Province. Abstracts, Institute on Lake Superior Geology 36th Annual Meeting, Thunder Bay, Ontario, May 9-12, 1990.
- Davis, D.W., Pezzutto, F., and Ojakangas, R.W., 1990. The age and provenance of metasedimentary rocks in the Quetico Subprovince, Ontario, from single zircon analyses: implications for Archean sedimentation and tectonics in the Superior Province. *Earth and Planet. Sci. Lett.* **99**: 195-205.
- Davis, D.W., Poulsen, K.H., and Kamo, S.L., 1989. New insights into Archean crustal development from geochronology in the Rainy Lake area, Superior Province, Canada. *J. Geol.* **97**: 379-398.
- Devaney, J.R. and Williams, H.R., 1989. Evolution of an Archean subprovince boundary: a sedimentological and structural study of part of the Wabigoon-Quetico boundary in northern Ontario. *Can J. Earth Sci.* **26**: 1013-1026.
- Ferry, J.M. and Spear, F.S., 1978. Experimental calibration of the partitioning of Fe and Mg between biotite and garnet. *Contrib. Min. Pet.* **66**: 113-117.
- Folinsbee, R.E., 1941. The chemical composition of garnet associated with cordierite. *Am. Min.* **26**: 50-53.
- Goodwin, A.M. and West, G.F., 1974. The Superior Geotraverse Project. *Geosci. Can.* **1**: 21-29.
- Harris, N.B.W., 1976. The significance of garnet and cordierite from the Sioux Lookout region of the English River Gneiss Belt, Northern Ontario. *Contrib. Min. Pet.* **55**: 91-104.
- Hudleston, P.J., Schultz-Ela, D., and Southwick, D.L., 1988. Transpression in an Archean greenstone belt, northern Minnesota. *Can. J. Earth Sci.* **25**: 1060-1068.
- Hyndman, D.W., 1972. Petrology of Igneous and Metamorphic Rocks. McGraw-Hill, Inc.
- Kaye, L., 1969. Map 2172: Eayrs Lake - Starnes Lake Area.
- Kehlenbeck, M.M., 1976. Nature of the Quetico-Wabigoon boundary in the De Courcey-Smiley Lakes area, Northwestern Ontario. *Can. J. Earth Sci.* **13**: 737-748.

- Kehlenbeck, M.M., 1977. The Barnum Lake pluton, Thunder Bay, Ontario. *Can. J. Earth Sci.* **14**: 2157-2167.
- Kehlenbeck, M.M., 1983. Use of stratigraphic and structural-facing directions to delineate the geometry of refolded folds near Thunder Bay, Ontario. *Geosci. Can* **11**: 23-31.
- Kehlenbeck, M.M., 1986. Folds and folding in the Beardmore-Geraldton fold belt. *Can. J. Earth Sci.* **23**: 158-171.
- Kehlenbeck, M.M. and Cheadle, S.P., 1990. Structural cross sections based on a gravity survey of parts of the Quetico and Wawa subprovinces near Thunder Bay, Ontario. *Can J. Earth Sci.* **27**: 187-199.
- Kennedy, M.C., 1980. Metamorphism and structure across the Quetico structural subprovince, Raith, Ontario. HBSc thesis, Lakehead University, Thunder Bay, Ontario.
- Kennedy, M.C., 1984. The Quetico fault in the Superior province of the southern Canadian Shield. MSc thesis, Lakehead University, Thunder Bay, Ontario.
- Koziol, A.M. and Newton, R.C., 1988. Redetermination of the anorthite breakdown reaction and improvement of the plagioclase-garnet- Al_2SiO_5 -quartz geobarometer. *Am. Min.* **73**: 216-223.
- Kyryluk, R.S., 1973. Description of structures and their significance in a migmatite complex near Thunder Bay, Ontario. BSc thesis, Lakehead University, Thunder Bay, Ontario.
- Lehto, D.A.W., 1975. Structural and petrological evolution of the Quetico gneiss belt in the Dog-Hawkeye Lakes area. HBSc thesis, Lakehead University, Thunder Bay, Ontario.
- Macdonald, R.D., 1939. Geology of Gorham Township and vicinity. O.D.M. Ann. Rpt. v.48, part 3, 18 p.
- Mackasey, W.O., Blackburn, C.E., and Trowell, N.F., 1974. A regional approach to the Wabigoon-Quetico belts and its bearing on exploration in northwestern Ontario. *Ont. Div. Mines, Misc. Paper* 58.
- Miyashiro, A., 1973. Metamorphism and Metamorphic Belts. George Allen and Unwin Ltd., London.
- Ojakangas, R.W., 1985. Review of Archean clastic sedimentation, Canadian Shield: major felsic volcanic contributions to turbidite and alluvial fan-fluvial facies associations. In Evolution of Archean Supracrustal Sequences. L.D. Ayres, P.C. Thurston, K.D. Card, and W. Weber, eds. *Geol. Assoc. of Can. Spec. Pap.* **28**: 23-47.

- Ontario Geological Survey, 1991. Bedrock geology of Ontario, west-central sheet. O.G.S., Map 2542, scale 1:1 000 000.
- Peden, K.D., 1978. The metamorphic character of the boundary between the Quetico and Shebandowan structural provinces, Shabaqua, Ontario. HBS thesis, Lakehead University, Thunder Bay, Ontario.
- Percival, J.A., 1989. A regional perspective of the Quetico metasedimentary belt, Superior Province, Canada. *Can. J. Earth Sci.* **26**: 677-693.
- Percival, J.A., Stern, R.A., and Diegel, M.R., 1985. Regional geological synthesis of Western Superior Province, Ontario. *In Current Research, Part A, Geol. Surv. Can. Paper 85-1A*: 385-397.
- Percival, J.A. and Sullivan, R.W., 1988. Age constraints on the evolution of the Quetico Belt, Superior Province, Ontario. *In Radiogenic and Isotopic Studies: Report 2, Geol. Surv. of Canada, Paper 88-2*: 97-107.
- Percival, J.A. and Williams, H.R., 1989. Late Archean Quetico accretionary complex, Superior Province, Canada.
- Perry, G.A., 1976. The relationship between metamorphism and the magnetic expression of rocks in a portion of the Quetico gneiss belt, Thunder Bay, Ontario. HBS thesis, Lakehead University, Thunder Bay, Ontario.
- Pirie, J. and Mackasey, W.O., 1978. Preliminary examination of regional metamorphism in parts of the Quetico metasedimentary belt, Superior Province, Ontario. *In Metamorphism in the Canadian Shield*. Geol. Surv. Can. Pap. 78-10: 37-48.
- Pouchou, J.L. and Pichoir, F., 1985. "PAP" ϕ (ρz) correction procedure for microanalysis. *In Microbeam Analysis*, J.T. Armstrong, ed. San Francisco Press Inc.
- Purdon, R.H., 1989. The Quetico fault zone northeast of Thunder Bay, Ontario: kinematic indicators of dextral motion. HBS thesis, Lakehead University, Thunder Bay, Ontario.
- Pye, E.G. and Fenwick, K.G., 1964. Map 2065: Atikokan-Lakehead Compilation Sheet, Geological Compilation Series.
- Reading, H.G., 1986. Sedimentary Environments and Facies, second edition. Blackwell Scientific Publications, London.
- Reinhardt, E.W., 1968. Phase relations in cordierite-bearing gneisses from the Gananoque area, Ontario. *Can. J. Earth Sci.* **5**: 455-482.

- Sawyer, E.W., 1983. The structural history of a part of the Archean Quetico metasedimentary belt, Superior Province, Canada. *Precamb. Res.* **22**: 271-294.
- Seemayer, B.E., 1989. Contact of a late Archean clastic sequence. HBSc thesis, Lakehead University, Thunder Bay, Ontario.
- Spark, R.N., 1990. Magnetic fabrics and boundary structure at the Quetico/Shebandowan subprovince boundary, near Kashabowie, NW Ontario. MSc thesis, Lakehead University, Thunder Bay, Ontario.
- Spencer, E.W., 1988. Introduction to the Structure of the Earth, third edition. McGraw-Hill, Inc.
- Stanton, R.L., 1982. Metamorphism of a stratiform sulphide orebody at Mount Misery, Einasleigh, Queensland, Australia: 2 - implications. *Trans. Inst. Mining and Metallurgy* **91**: B72-79.
- Stanton, R.L. and Williams, K.L., 1978. Garnet compositions at Broken Hill, New South Wales, as indicators of metamorphic processes. *J. Petrol.* **19**: 514-529.
- Sturt, B.A., 1962. The composition of garnets from pelitic schists in relation to the grade of regional metamorphism. *J. Pet.* **3**: 181-191.
- Tabor, J.R. and Hudleston, P.J., 1991. Deformation at an Archean subprovince boundary, northern Minnesota. *Can. J. Earth Sci.* **28**: 292-307.
- Thompson, A.B., 1976. Mineral reactions in pelitic schists II. Calculations of some P-T-x phase relations. *Am. J. Sci.* **276**: 425-454.
- Turner, F.J., 1981. Metamorphic Petrology: Mineralogical, Field, and Tectonic Aspects, second edition. Hemisphere Publishing Corporation.
- Williams, H.R., 1990. Subprovince accretion tectonics in the south-central Superior Province. *Can. J. Earth Sci.* **27**: 570-581.
- Winkler, H.G.F., 1979. Petrogenesis of Metamorphic Rocks, fourth edition. Springer-Verlag, New York.
- Wynne-Edwards, H.R. and Hay, P.W., 1963. Coexisting cordierite and garnet in regionally metamorphosed rocks from the Westport area, Ontario. *Can. Min.* **7**: 453-478.

APPENDIX A

SEM ANALYSES

GARNETS
FELDSPARS

nqfault.tot
88 samples, 30 elements, Date: 02-28-1991

Page 1

	62.0-1	.0-1-2	.0-1-2	62.0-1	#2-8.7	62.0-1	62.0-1	62.0-2	62.0-2	centr
SiO2	35.03	35.92	35.92	34.48	37.22	35.18	35.18	34.42	34.11	34.50
TiO2	-	-	-	-	-	-	-	-	-	0.19
Al2O3	19.33	18.99	18.99	19.00	19.39	18.71	18.71	18.16	18.41	18.65
Cr2O3	-	-	-	-	-	-	-	0.06	-	-
Fe2O3	4.93	4.29	4.29	5.93	2.84	5.65	5.65	7.10	7.14	5.99
FeO	35.97	35.83	35.83	35.76	34.27	35.00	35.00	34.79	34.96	35.19
MnO	0.80	0.94	0.94	0.85	0.87	1.14	1.14	1.62	1.64	2.08
MgO	3.34	3.29	3.29	3.30	4.32	3.55	3.55	3.29	3.11	2.87
CaO	1.10	1.17	1.17	1.17	1.39	1.27	1.27	1.27	1.35	1.13
Total	100.49	100.43	100.43	100.49	100.29	100.51	100.50	100.71	100.71	100.60
#Si IV	5.69	5.84	5.84	5.62	5.98	5.72	5.72	5.62	5.58	5.64
#Al IV	0.31	0.16	0.16	0.38	0.02	0.28	0.28	0.38	0.42	0.36
T site	6.00	6.00	6.00	6.00	6.00	6.00	6.00	6.00	6.00	6.00
#Al VI	3.40	3.48	3.48	3.27	3.66	3.31	3.31	3.12	3.12	3.24
#Ti VI	-	-	-	-	-	-	-	-	-	0.02
#Cr	-	-	-	-	-	-	-	0.01	-	-
#Fe +3	0.60	0.52	0.52	0.73	0.34	0.69	0.69	0.87	0.88	0.74
O site	4.00	4.00	4.00	4.00	4.00	4.00	4.00	4.00	4.00	4.00
#Fe +2	4.89	4.87	4.87	4.88	4.61	4.76	4.76	4.75	4.78	4.81
#Mn +2	0.11	0.13	0.13	0.12	0.12	0.16	0.16	0.22	0.23	0.29
#Mg	0.81	0.80	0.80	0.80	1.04	0.86	0.86	0.80	0.76	0.70
#Ca	0.19	0.20	0.20	0.20	0.24	0.22	0.22	0.22	0.24	0.20
A site	6.00	6.00	6.00	6.00	6.00	6.00	6.00	6.00	6.00	6.00
#O	23.85	23.92	23.92	23.81	23.99	23.86	23.86	23.81	23.79	23.83
FeO+MgO	39.31	39.12	39.12	39.06	38.59	38.55	38.55	38.08	38.07	38.06
MnO+CaO	1.90	2.11	2.11	2.02	2.26	2.41	2.41	2.89	2.99	3.21
alm	81.48	81.16	81.16	81.27	76.78	79.35	79.35	79.21	79.64	80.23
spess	1.84	2.16	2.16	1.96	1.97	2.62	2.62	3.74	3.78	4.80
py	13.49	13.29	13.29	13.37	17.25	14.35	14.35	13.35	12.63	11.66
gross	3.19	3.40	3.40	3.41	3.99	3.69	3.69	3.70	3.94	3.30

	62.0-2	53.9	mi34	62.0-2	62.0-2	62.0-2	62.0-2	62.0-2	54.7	#2-0.8
SiO2	34.02	36.42	35.19	34.16	33.98	34.15	34.34	33.55	36.02	35.69
TiO2	-	-	-	-	-	-	-	-	-	-
Al2O3	18.08	19.01	19.27	18.38	18.61	18.42	18.38	18.41	19.18	19.36
Cr2O3	0.10	-	0.09	0.18	-	-	-	0.08	0.20	0.20
Fe2O3	7.29	4.29	4.12	7.03	6.95	7.26	7.07	7.18	4.01	4.46
FeO	35.34	33.44	34.74	34.66	34.93	34.46	34.42	35.65	33.94	33.54
MnO	2.06	1.91	2.58	1.60	2.08	1.65	1.76	2.58	2.21	1.17
MgO	2.71	4.54	3.24	3.30	3.00	3.45	3.47	2.22	3.91	4.31
CaO	1.12	0.82	0.54	1.39	1.16	1.34	1.26	1.05	0.93	1.63
Total	100.72	100.43	99.77	100.70	100.71	100.73	100.70	100.72	100.40	100.36
#Si IV	5.59	5.87	5.76	5.58	5.56	5.57	5.60	5.53	5.83	5.75
#Al IV	0.41	0.13	0.24	0.42	0.44	0.43	0.40	0.47	0.17	0.25
T site	6.00	6.00	6.00	6.00	6.00	6.00	6.00	6.00	6.00	6.00
#Al VI	3.09	3.48	3.48	3.11	3.14	3.11	3.13	3.10	3.49	3.43
#Ti VI	-	-	-	-	-	-	-	-	-	-
#Cr	0.01	-	0.01	0.02	-	-	-	0.01	0.03	0.03
#Fe +3	0.90	0.52	0.51	0.86	0.86	0.89	0.87	0.89	0.49	0.54
O site	4.00	4.00	4.00	4.00	4.00	4.00	4.00	4.00	4.00	4.00
#Fe +2	4.85	4.51	4.76	4.73	4.78	4.70	4.69	4.91	4.59	4.52
#Mn +2	0.29	0.26	0.36	0.22	0.29	0.23	0.24	0.36	0.30	0.16
#Mg	0.66	1.09	0.79	0.80	0.73	0.84	0.84	0.55	0.94	1.04
#Ca	0.20	0.14	0.09	0.24	0.20	0.23	0.22	0.19	0.16	0.28
A site	6.00	6.00	6.00	6.00	6.00	6.00	6.00	6.00	6.00	6.00
#O	23.79	23.93	23.88	23.79	23.78	23.78	23.80	23.76	23.91	23.88
FeO+MgO	38.05	37.98	37.98	37.96	37.93	37.91	37.89	37.87	37.85	37.85
MnO+CaO	3.18	2.73	3.12	2.99	3.24	2.99	3.02	3.63	3.14	2.80
alm	80.88	75.12	79.28	78.88	79.62	78.32	78.22	81.83	76.55	75.38
spess	4.78	4.35	5.96	3.69	4.80	3.80	4.05	6.00	5.05	2.66
py	11.06	18.18	13.18	13.39	12.19	13.98	14.06	9.08	15.72	17.27
gross	3.28	2.36	1.58	4.05	3.39	3.90	3.67	3.09	2.69	4.69

nqfault.tot

Page 3

88 samples, 30 elements, Date: 02-28-1991

	2 edge	62.0-2	62.0-2	check	#1-2	check	68.3-3	47.5	62.0-2	68.3-3
SiO2	34.06	33.95	34.26	34.79	36.30	36.32	34.25	36.68	34.04	35.06
TiO2	-	-	-	-	0.26	-	-	-	-	-
Al2O3	18.89	18.80	18.66	19.22	19.27	19.20	19.06	19.27	18.99	19.37
Cr2O3	0.09	0.14	-	-	-	-	-	-	0.07	0.09
Fe2O3	6.31	6.81	6.68	4.96	3.50	3.61	5.51	3.67	6.14	4.50
FeO	35.00	34.53	34.67	32.94	33.54	33.94	35.30	32.86	33.40	35.20
MnO	2.30	1.74	1.86	0.89	2.19	2.41	0.49	2.22	1.96	0.49
MgO	2.85	3.31	3.16	4.83	4.04	3.49	2.03	4.45	3.90	2.09
CaO	1.14	1.42	1.39	1.12	1.10	1.28	3.32	1.21	1.17	3.58
Total	100.63	100.69	100.68	98.75	100.20	100.25	99.96	100.37	99.66	100.38
#Si IV	5.57	5.53	5.59	5.69	5.87	5.89	5.63	5.90	5.57	5.72
#Al IV	0.43	0.47	0.41	0.31	0.13	0.11	0.37	0.10	0.43	0.28
T site	6.00	6.00	6.00	6.00	6.00	6.00	6.00	6.00	6.00	6.00
#Al VI	3.21	3.15	3.18	3.39	3.54	3.56	3.32	3.56	3.23	3.44
#Ti VI	-	-	-	-	0.03	-	-	-	-	-
#Cr	0.01	0.02	-	-	-	-	-	-	0.01	0.01
#Fe +3	0.78	0.83	0.82	0.61	0.43	0.44	0.68	0.44	0.76	0.55
O site	4.00	4.00	4.00	4.00	4.00	4.00	4.00	4.00	4.00	4.00
#Fe +2	4.79	4.71	4.73	4.50	4.54	4.60	4.85	4.42	4.57	4.80
#Mn +2	0.32	0.24	0.26	0.12	0.30	0.33	0.07	0.30	0.27	0.07
#Mg	0.69	0.80	0.77	1.18	0.97	0.84	0.50	1.07	0.95	0.51
#Ca	0.20	0.25	0.24	0.20	0.19	0.22	0.58	0.21	0.21	0.63
A site	6.00	6.00	6.00	6.00	6.00	6.00	6.00	6.00	6.00	6.00
#O	23.79	23.77	23.80	23.84	23.95	23.94	23.81	23.95	23.79	23.86
FeO+MgO	37.85	37.84	37.83	37.77	37.58	37.43	37.33	37.31	37.30	37.29
MnO+CaO	3.44	3.16	3.25	2.01	3.29	3.69	3.81	3.43	3.13	4.07
alm	79.78	78.45	78.85	75.06	75.59	76.71	80.84	73.69	76.19	79.99
spess	5.31	4.00	4.28	2.05	5.00	5.52	1.14	5.04	4.53	1.13
py	11.58	13.41	12.81	19.62	16.23	14.06	8.29	17.79	15.86	8.47
gross	3.33	4.13	4.05	3.27	3.18	3.71	9.74	3.48	3.42	10.42

nqfault.tot

Page 4

88 samples, 30 elements, Date: 02-28-1991

	52.3	56.7	59.8	#1-1	59.8	56.8-3	68.3-1	68.3-1	56.8-3	50.5
SiO2	37.66	37.20	34.47	36.10	34.79	34.98	35.16	34.91	34.92	37.51
TiO2	0.19	-	0.13	-	-	-	-	0.11	-	-
Al2O3	19.36	19.49	18.89	19.78	18.51	18.95	19.05	18.72	18.60	19.34
Cr2O3	0.09	-	-	-	0.08	0.10	-	-	-	0.13
Fe2O3	2.76	2.43	6.14	3.26	6.17	4.91	4.90	5.54	4.95	3.04
FeO	32.93	33.17	33.06	32.85	33.20	33.84	34.47	34.19	34.13	30.85
MnO	2.20	3.37	3.44	3.51	3.68	4.67	1.19	1.18	4.82	2.02
MgO	3.95	3.69	3.70	3.74	3.36	2.68	1.94	2.22	2.24	5.50
CaO	1.13	0.89	0.74	1.03	0.84	0.37	3.78	3.58	0.35	1.78
Total	100.27	100.24	100.56	100.27	100.63	100.50	100.49	100.44	100.02	100.16
#Si IV	6.00	6.00	5.61	5.84	5.67	5.73	5.74	5.70	5.77	5.98
#Al IV	-	-	0.39	0.16	0.33	0.27	0.26	0.30	0.23	0.02
T site	6.00	6.00	6.00	6.00	6.00	6.00	6.00	6.00	6.00	6.00
#Al VI	3.64	3.70	3.23	3.60	3.23	3.38	3.40	3.31	3.38	3.62
#Ti VI	0.02	-	0.02	-	-	-	-	0.01	-	-
#Cr	0.01	-	-	-	0.01	0.01	-	-	-	0.02
#Fe +3	0.33	0.30	0.75	0.40	0.76	0.60	0.60	0.68	0.62	0.36
O site	4.00	4.00	4.00	4.00	4.00	4.00	4.00	4.00	4.00	4.00
#Fe +2	4.39	4.47	4.50	4.44	4.53	4.63	4.70	4.67	4.71	4.12
#Mn +2	0.30	0.46	0.47	0.48	0.51	0.65	0.16	0.16	0.67	0.27
#Mg	0.94	0.89	0.90	0.90	0.82	0.65	0.47	0.54	0.55	1.31
#Ca	0.19	0.15	0.13	0.18	0.15	0.06	0.66	0.63	0.06	0.30
A site	5.82	5.98	6.00	6.00	6.00	6.00	6.00	6.00	6.00	6.00
#O	23.83	23.98	23.81	23.92	23.84	23.86	23.87	23.86	23.88	23.99
FeO+MgO	36.88	36.86	36.76	36.59	36.56	36.52	36.41	36.41	36.37	36.35
MnO+CaO	3.33	4.26	4.18	4.54	4.52	5.04	4.97	4.76	5.17	3.80
alm	73.12	74.57	74.99	74.00	75.46	77.23	78.38	77.83	78.55	68.58
spess	4.95	7.67	7.90	8.01	8.47	10.79	2.74	2.72	11.23	4.55
py	15.64	14.79	14.96	15.02	13.62	10.90	7.86	9.01	9.19	21.80
gross	3.21	2.56	2.15	2.97	2.45	1.08	11.01	10.44	1.03	5.07

nqfault.tot

Page 5

88 samples, 30 elements, Date: 02-28-1991

	56.8-3	0W 5	43.6	0.9-2A	43.6	mi34+	43.6	43.6	51.2	68.3-5
SiO2	34.58	35.53	36.74	34.99	36.05	35.66	36.40	36.40	35.49	35.27
TiO2	-	-	-	-	-	-	-	-	-	0.28
Al2O3	18.89	18.61	19.92	18.94	20.00	18.57	18.86	18.86	19.03	17.32
Cr2O3	-	-	-	0.11	-	-	0.09	0.09	-	0.08
Fe2O3	5.46	5.26	2.89	5.64	3.71	4.39	4.36	4.36	4.79	6.33
FeO	33.80	33.33	31.76	32.24	31.41	33.68	31.85	31.85	32.32	33.19
MnO	4.94	2.55	2.62	3.78	2.71	5.67	2.83	2.83	4.24	4.56
MgO	2.50	2.87	4.42	3.85	4.56	2.16	3.96	3.96	3.40	2.51
CaO	0.37	2.37	1.93	1.01	1.95	0.30	2.10	2.10	1.14	1.00
Total	100.54	100.53	100.28	100.55	100.39	100.43	100.45	100.45	100.41	100.54
#Si IV	5.67	5.78	5.89	5.68	5.78	5.86	5.87	5.87	5.77	5.81
#Al IV	0.33	0.22	0.11	0.32	0.22	0.14	0.13	0.13	0.23	0.19
T site	6.00	6.00	6.00	6.00	6.00	6.00	6.00	6.00	6.00	6.00
#Al VI	3.33	3.36	3.65	3.30	3.55	3.46	3.46	3.46	3.41	3.17
#Ti VI	-	-	-	-	-	-	-	-	-	0.03
#Cr	-	-	-	0.01	-	-	0.01	0.01	-	0.01
#Fe +3	0.67	0.64	0.35	0.69	0.45	0.54	0.53	0.53	0.59	0.78
O site	4.00	4.00	4.00	4.00	4.00	4.00	4.00	4.00	4.00	4.00
#Fe +2	4.64	4.54	4.26	4.37	4.21	4.63	4.30	4.30	4.39	4.57
#Mn +2	0.69	0.35	0.36	0.52	0.37	0.79	0.39	0.39	0.58	0.64
#Mg	0.61	0.70	1.06	0.93	1.09	0.53	0.95	0.95	0.82	0.62
#Ca	0.07	0.41	0.33	0.18	0.33	0.05	0.36	0.36	0.20	0.18
A site	6.00	6.00	6.00	6.00	6.00	6.00	6.00	6.00	6.00	6.00
#O	23.84	23.89	23.94	23.84	23.89	23.93	23.94	23.94	23.88	23.92
FeO+MgO	36.30	36.20	36.18	36.09	35.97	35.84	35.81	35.81	35.72	35.70
MnO+CaO	5.31	4.92	4.55	4.79	4.66	5.97	4.93	4.93	5.38	5.56
alm	77.28	75.64	70.95	72.90	70.14	77.15	71.63	71.63	73.23	76.19
spess	11.44	5.86	5.93	8.66	6.13	13.15	6.45	6.45	9.73	10.60
py	10.19	11.61	17.60	15.52	18.15	8.82	15.88	15.88	13.73	10.27
gross	1.08	6.89	5.52	2.93	5.58	0.88	6.05	6.05	3.31	2.94

nqfault.tot

88 samples, 30 elements, Date: 02-28-1991

	i24.65	68.3-2	0.9-2A	40.9-1	43.6-2	43.6-2	59.8	56.8-1	EB 4	68.3-2
SiO2	37.74	36.75	34.54	35.53	35.96	35.96	32.69	37.19	36.19	35.79
TiO2	-	-	-	0.06	-	-	-	-	-	-
Al2O3	19.68	19.82	19.45	19.21	19.12	19.12	18.48	19.20	19.25	19.55
Cr2O3	-	-	-	-	-	-	-	-	0.17	-
Fe2O3	2.61	2.14	5.33	4.38	5.04	5.04	10.20	3.04	4.23	3.64
FeO	31.77	33.52	31.52	32.17	30.67	30.67	29.34	31.07	30.71	32.73
MnO	0.31	1.83	4.05	4.88	2.88	2.88	3.59	4.40	3.45	2.69
MgO	3.82	2.03	3.97	3.19	4.64	4.64	5.95	4.22	4.39	2.14
CaO	4.33	4.13	1.10	1.04	2.21	2.21	0.78	1.18	2.02	3.83
Total	100.26	100.22	99.96	100.46	100.52	100.51	101.03	100.31	100.41	100.36
#Si IV	6.00	5.95	5.62	5.78	5.77	5.77	5.26	5.99	5.82	5.81
#Al IV	-	0.05	0.38	0.22	0.23	0.23	0.74	0.01	0.18	0.19
T site	6.00	6.00	6.00	6.00	6.00	6.00	6.00	6.00	6.00	6.00
#Al VI	3.69	3.74	3.35	3.46	3.39	3.39	2.77	3.63	3.47	3.56
#Ti VI	-	-	-	0.01	-	-	-	-	-	-
#Cr	-	-	-	-	-	-	-	-	0.02	-
#Fe +3	0.31	0.26	0.65	0.54	0.61	0.61	1.23	0.37	0.51	0.44
O site	4.00	4.00	4.00	4.00	4.00	4.00	4.00	4.00	4.00	4.00
#Fe +2	4.22	4.54	4.29	4.37	4.12	4.12	3.95	4.18	4.13	4.45
#Mn +2	0.04	0.25	0.56	0.67	0.39	0.39	0.49	0.60	0.47	0.37
#Mg	0.91	0.49	0.96	0.77	1.11	1.11	1.43	1.01	1.05	0.52
#Ca	0.74	0.72	0.19	0.18	0.38	0.38	0.13	0.20	0.35	0.67
A site	5.91	6.00	6.00	6.00	6.00	6.00	6.00	6.00	6.00	6.00
#O	23.91	23.98	23.81	23.89	23.89	23.89	23.63	23.99	23.91	23.91
FeO+MgO	35.59	35.55	35.49	35.36	35.31	35.31	35.29	35.29	35.10	34.87
MnO+CaO	4.64	5.96	5.15	5.92	5.09	5.09	4.37	5.58	5.47	6.52
alm	70.40	75.69	71.46	72.90	68.63	68.63	65.81	69.73	68.83	74.09
spess	0.70	4.19	9.30	11.20	6.53	6.53	8.16	10.00	7.83	6.17
py	15.09	8.17	16.04	12.89	18.51	18.51	23.79	16.88	17.54	8.64
gross	12.29	11.95	3.20	3.02	6.34	6.34	2.24	3.39	5.80	11.11

nqfault.tot

Page 7

88 samples, 30 elements, Date: 02-28-1991

	63.8	QW 34	0.9-2A	71.1-1	QW 3-2	68.3-2	EB 32	QW 3	40.9-1	.3-2-2
SiO2	35.12	34.93	34.33	34.39	35.17	36.37	36.47	35.46	35.14	36.10
TiO2	-	-	-	-	-	0.07	-	-	-	-
Al2O3	18.75	18.83	18.46	19.58	18.95	19.68	19.13	18.64	19.24	18.95
Cr2O3	0.10	-	-	-	-	-	-	-	-	-
Fe2O3	6.10	5.40	7.03	4.06	5.30	2.84	4.03	5.31	4.81	3.91
FeO	31.26	31.92	30.96	33.09	31.52	31.90	30.17	31.59	30.79	32.12
MnO	4.31	5.44	5.34	7.71	3.80	3.07	4.22	3.35	6.44	3.25
MgO	3.47	2.66	3.58	1.26	2.75	2.32	4.02	2.50	3.14	1.74
CaO	2.02	1.35	1.00	0.22	3.00	4.03	2.27	3.61	0.91	4.31
Total	101.13	100.53	100.70	100.31	100.49	100.27	100.31	100.46	100.47	100.38
#Si IV	5.67	5.71	5.59	5.68	5.72	5.89	5.88	5.77	5.72	5.88
#Al IV	0.33	0.29	0.41	0.32	0.28	0.11	0.12	0.23	0.28	0.12
T site	6.00	6.00	6.00	6.00	6.00	6.00	6.00	6.00	6.00	6.00
#Al VI	3.25	3.34	3.14	3.50	3.35	3.65	3.51	3.35	3.41	3.52
#Ti VI	-	-	-	-	-	0.01	-	-	-	-
#Cr	0.01	-	-	-	-	-	-	-	-	-
#Fe +3	0.74	0.66	0.86	0.50	0.65	0.35	0.49	0.65	0.59	0.48
O site	4.00	4.00	4.00	4.00	4.00	4.00	4.00	4.00	4.00	4.00
#Fe +2	4.22	4.36	4.22	4.57	4.29	4.32	4.07	4.30	4.19	4.38
#Mn +2	0.59	0.75	0.74	1.08	0.52	0.42	0.58	0.46	0.89	0.45
#Mg	0.84	0.65	0.87	0.31	0.67	0.56	0.97	0.61	0.76	0.42
#Ca	0.35	0.24	0.17	0.04	0.52	0.70	0.39	0.63	0.16	0.75
A site	6.00	6.00	6.00	6.00	6.00	6.00	6.00	6.00	6.00	6.00
#O	23.84	23.85	23.80	23.84	23.86	23.95	23.94	23.89	23.86	23.94
FeO+MgO	34.73	34.58	34.54	34.35	34.27	34.22	34.19	34.09	33.93	33.86
MnO+CaO	6.33	6.79	6.34	7.93	6.80	7.10	6.49	6.96	7.35	7.56
alm	70.41	72.71	70.32	76.19	71.45	71.99	67.77	71.69	69.86	72.94
spess	9.83	12.55	12.28	17.98	8.72	7.02	9.60	7.70	14.80	7.47
py	13.93	10.80	14.49	5.17	11.11	9.33	16.10	10.11	12.70	7.04
gross	5.83	3.94	2.91	0.65	8.71	11.65	6.53	10.50	2.65	12.54

nqfault.tot

Page 8

88 samples, 30 elements, Date: 02-28-1991

	.3-2-2	37.5	68.3-2	68.3-2	37.5	37.5	dump	63.8	40.9-1	QW 60
SiO2	36.10	35.96	35.50	35.50	35.22	35.23	34.90	35.29	35.09	35.26
TiO2	-	-	-	-	-	-	0.06	-	-	-
Al2O3	18.95	19.09	18.82	18.82	18.95	19.07	19.19	18.63	19.04	18.68
Cr2O3	-	0.06	-	-	0.10	-	0.14	-	-	-
Fe2O3	3.91	4.42	4.96	4.96	5.74	5.84	4.14	5.44	4.99	5.70
FeO	32.12	30.16	31.52	31.52	29.50	29.04	31.37	30.32	30.13	29.33
MnO	3.25	4.60	3.38	3.38	4.51	4.55	8.37	6.00	7.39	6.04
MgO	1.74	3.68	2.02	2.02	3.97	4.20	1.79	2.76	2.79	3.16
CaO	4.31	2.33	4.31	4.31	2.58	2.67	0.45	2.10	1.08	2.41
Total	100.38	100.30	100.51	100.51	100.56	100.61	100.40	100.55	100.51	100.58
#Si IV	5.88	5.82	5.78	5.78	5.69	5.67	5.74	5.75	5.73	5.73
#Al IV	0.12	0.18	0.22	0.22	0.31	0.33	0.26	0.25	0.27	0.27
T site	6.00	6.00	6.00	6.00	6.00	6.00	6.00	6.00	6.00	6.00
#Al VI	3.52	3.45	3.39	3.39	3.29	3.29	3.46	3.33	3.39	3.30
#Ti VI	-	-	-	-	-	-	0.01	-	-	-
#Cr	-	0.01	-	-	0.01	-	0.02	-	-	-
#Fe +3	0.48	0.54	0.61	0.61	0.70	0.71	0.51	0.67	0.61	0.70
O site	4.00	4.00	4.00	4.00	4.00	4.00	4.00	4.00	4.00	4.00
#Fe +2	4.38	4.08	4.29	4.29	3.98	3.91	4.32	4.13	4.11	3.98
#Mn +2	0.45	0.63	0.47	0.47	0.62	0.62	1.17	0.83	1.02	0.83
#Mg	0.42	0.89	0.49	0.49	0.96	1.01	0.44	0.67	0.68	0.77
#Ca	0.75	0.40	0.75	0.75	0.45	0.46	0.08	0.37	0.19	0.42
A site	6.00	6.00	6.00	6.00	6.00	6.00	6.00	6.00	6.00	6.00
#O	23.94	23.91	23.89	23.89	23.84	23.84	23.87	23.88	23.86	23.86
FeO+MgO	33.86	33.84	33.54	33.54	33.47	33.24	33.16	33.08	32.92	32.49
MnO+CaO	7.56	6.93	7.69	7.69	7.09	7.22	8.82	6.10	8.47	6.45
alm	72.94	67.98	71.53	71.53	66.36	65.18	71.92	68.90	68.52	66.41
spess	7.47	10.50	7.77	7.77	10.28	10.34	19.44	13.81	17.02	13.85
py	7.04	14.79	8.17	8.17	15.92	16.80	7.32	11.18	11.31	12.75
gross	12.54	6.73	12.54	12.53	7.44	7.68	1.32	6.11	3.15	6.99

ngfault.tot
88 samples, 30 elements, Date: 02-28-1991

Page 9

	39.3-2	EB 13	EB 12	39.3-2	37.5	37.5	.5-2#2	71.5-2
SiO2	35.27	36.20	35.99	35.15	35.45	35.63	33.91	31.47
TiO2	-	-	-	-	0.15	-	-	-
Al2O3	19.30	18.83	19.36	19.10	18.79	19.38	18.52	17.16
Cr2O3	0.09	-	-	0.08	-	-	-	-
Fe2O3	4.87	4.21	3.71	5.36	5.49	4.71	5.28	9.60
FeO	28.79	29.03	28.70	28.39	27.85	27.65	28.61	27.55
MnO	6.51	7.04	8.50	6.65	6.14	6.62	13.16	13.64
MgO	3.33	3.02	3.24	3.48	3.84	3.64	0.42	0.51
CaO	2.33	2.05	0.87	2.33	2.70	2.85	0.12	-
Total	100.49	100.38	100.37	100.54	100.41	100.47	100.02	99.92
#Si IV	5.71	5.88	5.84	5.69	5.73	5.75	5.68	5.34
#Al IV	0.29	0.12	0.16	0.31	0.27	0.25	0.32	0.66
T site	6.00	6.00	6.00	6.00	6.00	6.00	6.00	6.00
#Al VI	3.40	3.48	3.55	3.34	3.31	3.43	3.33	2.77
#Ti VI	-	-	-	-	0.02	-	-	-
#Cr	0.01	-	-	0.01	-	-	-	-
#Fe +3	0.59	0.52	0.45	0.65	0.67	0.57	0.67	1.23
O site	4.00	4.00	4.00	4.00	4.00	4.00	4.00	4.00
#Fe +2	3.90	3.94	3.90	3.84	3.77	3.73	4.01	3.91
#Mn +2	0.89	0.97	1.17	0.91	0.84	0.90	1.87	1.96
#Mg	0.80	0.73	0.78	0.84	0.93	0.88	0.10	0.13
#Ca	0.40	0.36	0.15	0.40	0.47	0.49	0.02	-
A site	6.00	6.00	6.00	6.00	6.00	6.00	6.00	6.00
#O	23.86	23.94	23.92	23.85	23.88	23.87	23.84	23.67
FeO+MgO	32.12	32.05	31.94	31.87	31.69	31.29	29.03	28.06
MnO+CaO	8.84	9.09	9.37	8.98	8.84	9.47	13.28	13.64
alm	64.98	65.72	64.93	64.06	62.76	62.14	66.78	65.17
spess	14.88	16.14	19.48	15.20	14.02	15.07	31.11	32.68
py	13.40	12.19	13.07	14.00	15.43	14.58	1.75	2.15
gross	6.74	5.95	2.25	6.74	7.80	8.21	0.36	-

sqfault.tot

Page 1

44 samples, 30 elements, Date: 02-28-1991

	12.2-2	0.4 -2	12.7-3	10.4	12.7-3	12.6-2	19.6	31.5	10.5-2	124.65
SiO2	37.30	36.67	36.10	35.68	35.40	36.83	36.94	35.53	35.47	37.74
TiO2	-	-	-	0.15	-	0.07	-	-	-	-
Al2O3	20.22	19.49	20.26	18.78	19.91	20.59	19.63	18.88	19.58	19.68
Cr2O3	0.07	0.07	-	-	0.22	-	0.12	-	0.22	-
Fe2O3	2.69	3.42	4.27	5.38	4.37	0.84	2.16	5.25	4.32	2.61
FeO	31.45	33.05	30.94	32.74	30.74	32.74	32.96	32.65	31.66	31.77
MnO	0.97	1.66	1.91	1.86	1.72	2.30	4.06	2.69	3.97	0.31
MgO	6.41	4.55	6.41	4.44	6.28	4.23	3.39	3.70	4.20	3.82
CaO	1.16	1.43	0.81	1.50	0.81	1.34	0.95	1.81	1.01	4.33
Total	100.27	100.34	100.70	100.53	99.46	98.93	100.22	100.52	100.42	100.26
#Si IV	5.90	5.89	5.71	5.76	5.68	5.96	5.98	5.76	5.72	6.00
#Al IV	0.10	0.11	0.29	0.24	0.32	0.04	0.02	0.24	0.28	-
T site	6.00	6.00	6.00	6.00	6.00	6.00	6.00	6.00	6.00	6.00
#Al VI	3.67	3.58	3.49	3.33	3.44	3.89	3.72	3.36	3.45	3.69
#Ti VI	-	-	-	0.02	-	0.01	-	-	-	-
#Cr	0.01	0.01	-	-	0.03	-	0.02	-	0.03	-
#Fe +3	0.32	0.41	0.51	0.65	0.53	0.10	0.26	0.64	0.52	0.31
O site	4.00	4.00	4.00	4.00	4.00	4.00	4.00	4.00	4.00	4.00
#Fe +2	4.16	4.44	4.09	4.42	4.13	4.43	4.46	4.42	4.27	4.22
#Mn +2	0.13	0.23	0.26	0.25	0.23	0.32	0.56	0.37	0.54	0.04
#Mg	1.51	1.09	1.51	1.07	1.50	1.02	0.82	0.89	1.01	0.91
#Ca	0.20	0.25	0.14	0.26	0.14	0.23	0.16	0.31	0.17	0.74
A site	6.00	6.00	6.00	6.00	6.00	6.00	6.00	6.00	6.00	5.91
#O	23.95	23.94	23.86	23.89	23.84	23.99	23.99	23.88	23.86	23.91
FeO+MgO	37.86	37.60	37.35	37.18	37.02	36.97	36.35	36.35	35.86	35.59
MnO+CaO	2.13	3.09	2.72	3.36	2.53	3.64	5.01	4.50	4.98	4.64
alm	69.36	73.98	68.24	73.64	68.75	73.86	74.35	73.72	71.21	70.40
spess	2.17	3.76	4.27	4.24	3.90	5.26	9.27	6.15	9.04	0.70
py	25.20	18.15	25.20	17.80	25.03	17.01	13.63	14.89	16.84	15.09
gross	3.28	4.10	2.29	4.32	2.32	3.87	2.75	5.24	2.91	12.29

sqfault.tot
44 samples, 30 elements, Date: 02-28-1991

Page 2

	H-41-1	EB 4	mi20.7	26.1	EB 32	F. 7.5	16.0-2	23.5-1	18.8-1	11.6-2
SiO2	35.58	36.19	35.97	35.86	36.47	35.78	36.01	35.73	36.01	34.85
TiO2	-	-	-	0.16	-	-	-	-	0.07	-
Al2O3	18.73	19.25	19.68	19.23	19.13	18.78	19.55	19.53	20.04	18.81
Cr2O3	0.07	0.17	-	0.08	-	-	-	0.07	-	0.23
Fe2O3	4.81	4.23	3.50	4.40	4.03	4.84	3.55	3.85	2.91	4.59
FeO	32.34	30.71	31.66	30.73	30.17	30.40	30.34	29.89	29.70	29.48
MnO	4.86	3.45	4.53	3.48	4.22	5.78	6.21	6.78	7.02	6.58
MgO	3.00	4.39	3.40	3.79	4.02	3.58	3.28	3.38	3.50	3.21
CaO	1.09	2.02	1.58	2.72	2.27	1.19	1.41	1.16	1.05	1.29
Total	100.48	100.41	100.32	100.45	100.31	100.36	100.35	100.40	100.30	99.04
#Si IV	5.80	5.82	5.82	5.78	5.88	5.81	5.83	5.79	5.82	5.75
#Al IV	0.20	0.18	0.18	0.22	0.12	0.19	0.17	0.21	0.18	0.25
T site	6.00	6.00	6.00	6.00	6.00	6.00	6.00	6.00	6.00	6.00
#Al VI	3.40	3.47	3.57	3.44	3.51	3.41	3.57	3.52	3.64	3.40
#Ti VI	-	-	-	0.02	-	-	-	-	0.01	-
#Cr	0.01	0.02	-	0.01	-	-	-	0.01	-	0.03
#Fe +3	0.59	0.51	0.43	0.53	0.49	0.59	0.43	0.47	0.35	0.57
O site	4.00	4.00	4.00	4.00	4.00	4.00	4.00	4.00	4.00	4.00
#Fe +2	4.41	4.13	4.28	4.14	4.07	4.13	4.11	4.05	4.01	4.06
#Mn +2	0.67	0.47	0.62	0.48	0.58	0.80	0.85	0.93	0.96	0.92
#Mg	0.73	1.05	0.82	0.91	0.97	0.87	0.79	0.82	0.84	0.79
#Ca	0.19	0.35	0.27	0.47	0.39	0.21	0.24	0.20	0.18	0.23
A site	6.00	6.00	6.00	6.00	6.00	6.00	6.00	6.00	6.00	6.00
#O	23.90	23.91	23.91	23.90	23.94	23.91	23.92	23.90	23.91	23.87
FeO+MgO	35.34	35.10	35.06	34.52	34.19	33.98	33.62	33.27	33.20	32.69
MnO+CaO	5.95	5.47	6.11	6.20	6.49	6.97	7.62	7.94	8.07	7.87
alm	73.49	68.83	71.42	69.06	67.77	68.84	68.51	67.52	66.90	67.74
spess	11.19	7.83	10.35	7.92	9.60	13.26	14.20	15.51	16.02	15.31
py	12.15	17.54	13.67	15.18	16.10	14.45	13.20	13.61	14.05	13.15
gross	3.17	5.80	4.57	7.83	6.53	3.45	4.08	3.36	3.03	3.80

sqfault.tot
44 samples, 30 elements, Date: 02-28-1991

Page 3

	mi13.0	S.F. 1	S.F. 1	17.9	17.9-2	17.9-2	F. 1-2	F. 1-2	-82 -2	EB 13
SiO2	35.46	35.90	35.90	35.31	36.04	36.04	36.29	36.29	34.91	36.20
TiO2	-	-	-	-	0.15	0.15	-	-	-	-
Al2O3	18.53	19.48	19.48	18.86	18.44	18.44	19.04	19.04	18.59	18.83
Cr2O3	0.09	0.19	0.19	0.10	0.21	0.21	-	-	-	-
Fe2O3	5.03	4.57	4.57	5.16	4.34	4.34	5.07	5.07	4.64	4.21
FeO	30.97	27.91	27.91	29.34	29.55	29.55	27.33	27.33	29.80	29.03
MnO	4.86	4.62	4.62	6.70	7.11	7.11	4.52	4.52	8.30	7.04
MgO	1.69	4.58	4.58	3.07	2.71	2.71	4.80	4.80	2.30	3.02
CaO	3.88	3.16	3.16	1.97	1.88	1.88	3.44	3.44	0.75	2.05
Total	100.51	100.42	100.41	100.51	100.43	100.43	100.50	100.49	99.29	100.38
#Si IV	5.80	5.75	5.75	5.74	5.88	5.88	5.80	5.80	5.79	5.88
#Al IV	0.20	0.25	0.25	0.26	0.12	0.12	0.20	0.20	0.21	0.12
T site	6.00	6.00	6.00	6.00	6.00	6.00	6.00	6.00	6.00	6.00
#Al VI	3.37	3.42	3.42	3.36	3.42	3.42	3.39	3.39	3.42	3.48
#Ti VI	-	-	-	-	0.02	0.02	-	-	-	-
#Cr	0.01	0.02	0.02	0.01	0.03	0.03	-	-	-	-
#Fe +3	0.62	0.55	0.55	0.63	0.53	0.53	0.61	0.61	0.58	0.52
O site	4.00	4.00	4.00	4.00	4.00	4.00	4.00	4.00	4.00	4.00
#Fe +2	4.24	3.74	3.74	3.99	4.03	4.03	3.65	3.65	4.13	3.94
#Mn +2	0.67	0.63	0.63	0.92	0.98	0.98	0.61	0.61	1.17	0.97
#Mg	0.41	1.09	1.09	0.74	0.66	0.66	1.14	1.14	0.57	0.73
#Ca	0.68	0.54	0.54	0.34	0.33	0.33	0.59	0.59	0.13	0.36
A site	6.00	6.00	6.00	6.00	6.00	6.00	6.00	6.00	6.00	6.00
#O	23.90	23.87	23.87	23.87	23.95	23.95	23.90	23.90	23.89	23.94
FeO+MgO	32.66	32.49	32.49	32.41	32.26	32.26	32.13	32.13	32.10	32.05
MnO+CaO	8.74	7.78	7.78	8.67	8.99	8.99	7.96	7.96	9.05	9.09
alm	70.59	62.30	62.30	66.50	67.18	67.18	60.91	60.91	68.88	65.72
spess	11.22	10.44	10.44	15.38	16.37	16.37	10.20	10.20	19.43	16.14
py	6.87	18.22	18.22	12.40	10.98	10.98	19.07	19.07	9.48	12.19
gross	11.33	9.04	9.04	5.72	5.47	5.47	9.82	9.82	2.22	5.95

sqfault.tot

Page 4

44 samples, 30 elements, Date: 02-28-1991

	EB 12	D-82	D-1	18.1	26.5-2	24.6	. 23.1	17.9	17.9	.5-1#2
SiO2	35.99	35.47	35.30	34.78	35.63	34.84	36.00	34.87	34.87	35.28
TiO2	-	-	-	-	-	0.07	0.22	0.14	0.14	-
Al2O3	19.36	18.65	19.35	19.07	18.79	18.91	18.87	18.77	18.77	19.17
Cr2O3	-	0.08	-	-	0.15	0.30	-	-	-	-
Fe2O3	3.71	4.25	5.07	4.91	5.68	5.21	4.27	5.34	5.34	4.96
FeO	28.70	30.07	28.16	28.11	26.93	25.55	26.75	26.49	26.49	26.52
MnO	8.50	9.66	5.58	8.34	5.35	7.94	7.34	10.68	10.68	7.99
MgO	3.24	1.64	3.43	3.34	3.91	3.48	2.27	2.47	2.47	2.33
CaO	0.87	0.61	3.51	0.95	4.12	3.29	4.67	1.67	1.67	4.24
Total	100.37	100.43	100.40	99.50	100.56	99.59	100.39	100.43	100.42	100.49
#Si IV	5.84	5.84	5.70	5.71	5.73	5.68	5.84	5.71	5.71	5.73
#Al IV	0.16	0.16	0.30	0.29	0.27	0.32	0.16	0.29	0.29	0.27
T site	6.00	6.00	6.00	6.00	6.00	6.00	6.00	6.00	6.00	6.00
#Al VI	3.55	3.46	3.38	3.39	3.29	3.31	3.45	3.33	3.33	3.39
#Ti VI	-	-	-	-	-	0.01	0.03	0.02	0.02	-
#Cr	-	0.01	-	-	0.02	0.04	-	-	-	-
#Fe +3	0.45	0.53	0.62	0.61	0.69	0.64	0.52	0.66	0.66	0.61
O site	4.00	4.00	4.00	4.00	4.00	4.00	4.00	4.00	4.00	4.00
#Fe +2	3.90	4.14	3.80	3.86	3.62	3.48	3.63	3.62	3.62	3.60
#Mn +2	1.17	1.35	0.76	1.16	0.73	1.10	1.01	1.48	1.48	1.10
#Mg	0.78	0.40	0.83	0.82	0.94	0.85	0.55	0.60	0.60	0.56
#Ca	0.15	0.11	0.61	0.17	0.71	0.57	0.81	0.29	0.29	0.74
A site	6.00	6.00	6.00	6.00	6.00	6.00	6.00	6.00	6.00	6.00
#O	23.92	23.92	23.85	23.85	23.87	23.84	23.93	23.86	23.86	23.86
FeO+MgO	31.94	31.71	31.59	31.45	30.84	29.03	29.02	28.96	28.96	28.85
MnO+CaO	9.37	10.27	9.09	9.29	9.47	11.23	12.01	12.35	12.35	12.23
alm	64.93	69.03	63.39	64.29	60.39	58.05	60.50	60.41	60.41	60.00
spess	19.48	22.46	12.72	19.32	12.15	18.27	16.82	24.67	24.67	18.31
py	13.07	6.71	13.76	13.62	15.63	14.10	9.15	10.04	10.04	9.40
gross	2.52	1.79	10.12	2.78	11.83	9.58	13.53	4.88	4.88	12.29

sqfault.tot
44 samples, 30 elements, Date: 02-28-1991

Page 5

	mi12.7	32.9-1	16.0-A	.L.0.8
SiO2	35.86	34.66	35.33	33.40
TiO2	0.10	-	-	0.22
Al2O3	18.58	18.55	19.54	17.63
Cr2O3	-	-	-	-
Fe2O3	5.17	4.38	4.90	8.84
FeO	25.79	26.93	24.79	23.51
MnO	6.92	14.02	7.44	10.35
MgO	2.46	0.66	2.65	1.77
CaO	5.54	0.48	5.83	5.16
Total	100.42	99.68	100.48	100.89
#Si IV	5.81	5.79	5.69	5.48
#Al IV	0.19	0.21	0.31	0.52
T site	6.00	6.00	6.00	6.00
#Al VI	3.36	3.45	3.41	2.88
#Ti VI	0.01	-	-	0.03
#Cr	-	-	-	-
#Fe +3	0.63	0.55	0.59	1.09
O site	4.00	4.00	4.00	4.00
#Fe +2	3.49	3.76	3.34	3.22
#Mn +2	0.95	1.99	1.02	1.44
#Mg	0.59	0.16	0.64	0.43
#Ca	0.96	0.09	1.01	0.91
A site	6.00	6.00	6.00	6.00
#O	23.91	23.90	23.85	23.75
FeO+MgO	28.25	27.59	27.44	25.28
MnO+CaO	12.46	14.50	13.27	15.51
alm	58.24	62.74	55.68	53.73
spess	15.83	33.09	16.93	23.95
py	9.90	2.74	10.61	7.21
gross	16.03	1.43	16.78	15.11

fsp.rec

Page 1

48 samples, 23 elements, Date: 02-28-1991

	16.0-1	32.9-1	23.8-2	16.0-E	16.0-E	mi34+	12.7-1	53.9	mi34	mi20.7
Si+4	26.83	30.39	29.10	26.48	28.92	29.87	28.41	28.43	29.48	28.64
Al+3	7.89	9.47	9.22	15.16	11.96	12.19	12.87	12.37	12.66	11.51
Fe+2	0.56	0.08	-	0.34	0.30	0.18	-	-	-	0.26
Mn+2	-	-	0.06	-	-	0.06	-	-	-	-
Mg+2	0.21	-	0.15	-	0.28	-	-	-	0.19	-
Ca+2	0.17	0.12	0.15	0.51	0.69	2.14	3.45	3.91	3.09	3.82
K+1	21.48	13.97	14.76	7.09	6.27	0.34	0.15	0.15	0.42	3.83
Na+1	0.39	-	0.75	3.59	4.44	6.94	7.21	7.54	5.76	4.98
Ti+4	-	-	0.61	0.06	-	-	0.10	-	-	-
Cr+3	-	-	-	0.07	0.13	-	-	-	0.06	-
#Si+4	2.90	3.01	2.97	2.59	2.82	2.82	2.71	2.72	2.79	2.78
#Al+3	0.89	0.98	0.98	1.54	1.22	1.20	1.28	1.23	1.25	1.16
#Ca+2x100	1.30	0.84	1.07	3.48	4.69	14.16	23.10	26.23	20.51	25.99
#K+1x100	166.67	99.54	108.11	49.86	43.94	2.31	1.02	1.03	2.82	26.71
#Na+1x100	5.19	-	9.33	42.94	52.99	80.19	84.11	88.15	66.61	59.09
#TOTAL	5.52	5.00	5.13	5.10	5.05	4.99	5.07	5.11	4.94	5.06
#O-2	8.00	8.00	8.00	8.00	8.00	8.00	8.00	8.00	8.00	8.00
totcat	173.16	-	118.52	96.28	101.62	96.65	108.23	115.40	89.94	111.80
totcat / 100	1.73	1.00	1.19	0.96	1.02	0.97	1.08	1.15	0.90	1.12
An	0.75	0.84	0.90	3.62	4.62	14.65	21.34	22.73	22.81	23.25
Or	96.25	99.16	91.22	51.78	43.24	2.39	0.95	0.89	3.14	23.90
Ab	3.00	-	7.88	44.60	52.14	82.96	77.71	76.38	74.06	52.86

fsp.rec
48 samples, 23 elements, Date: 02-28-1991

Page 2

	11.0-1	15.4-1	mi20.7	18.8-1	47.5	16.0-1	mi20.7	11.6-1	400-4	11.0-1
Si+4	28.31	28.87	28.34	29.15	28.06	28.19	27.54	29.07	28.83	28.80
Al+3	13.27	13.15	11.55	12.77	12.45	11.35	11.86	11.21	12.81	11.30
Fe+2	0.51	0.16	0.16	-	-	0.42	0.35	0.10	-	-
Mn+2	0.09	-	-	0.13	0.16	-	0.18	-	-	0.13
Mg+2	0.23	-	-	-	-	0.59	0.16	-	-	-
Ca+2	3.36	3.46	4.39	3.82	4.60	4.97	4.94	5.17	4.43	5.32
K+1	0.44	0.64	3.50	0.10	0.38	0.21	2.33	0.32	0.30	0.55
Na+1	5.93	5.62	5.12	5.84	6.80	7.06	5.73	6.58	5.61	6.42
Ti+4	-	-	0.05	-	0.09	-	0.17	-	-	-
Cr+3	-	-	-	-	-	-	-	-	-	0.07
#Si+4	2.71	2.74	2.76	2.76	2.70	2.75	2.71	2.79	2.74	2.77
#Al+3	1.32	1.30	1.17	1.26	1.25	1.15	1.21	1.12	1.27	1.13
#Ca+2x100	22.56	22.99	29.93	25.36	31.01	33.97	34.02	34.73	29.47	35.87
#K+1x100	3.03	4.35	24.50	0.68	2.64	1.45	16.47	2.17	2.04	3.79
#Na+1x100	69.41	65.15	60.87	67.50	80.02	84.20	68.77	77.11	65.02	75.48
#TOTAL	4.99	4.96	5.08	4.95	5.09	5.10	5.11	5.05	4.97	5.06
#O-2	8.00	8.00	8.00	8.00	8.00	8.00	8.00	8.00	8.00	8.00
totcat	95.00	92.49	115.31	93.54	113.67	119.62	119.26	114.01	96.53	115.14
totcat / 100	0.95	0.92	1.15	0.94	1.14	1.20	1.19	1.14	0.97	1.15
An	23.75	24.85	25.96	27.11	27.28	28.40	28.52	30.46	30.53	31.16
Or	3.19	4.71	21.25	0.72	2.32	1.22	13.81	1.91	2.11	3.29
Ab	73.06	70.44	52.79	72.17	70.40	70.39	57.67	67.63	67.36	65.55

fsp.rec

Page 3

48 samples, 23 elements, Date: 02-28-1991

	69.9	H-41-1	EB12	mi20.7	12.6-1	11.0-1	31.5	16.0-1	L.23.1	OW 34
Si+4	28.82	29.12	28.78	30.70	27.84	27.90	28.08	28.26	28.65	28.82
Al+3	12.71	12.63	12.52	11.71	13.48	13.30	12.66	11.62	12.63	12.71
Fe+2	0.05	0.10	-	0.58	0.17	-	0.28	0.26	0.10	0.12
Mn+2	-	-	-	-	-	0.07	-	-	0.05	-
Mg+2	-	-	-	0.26	-	-	-	-	-	-
Ca+2	4.57	4.48	4.80	3.55	5.07	5.26	5.54	6.18	5.25	5.16
K+1	0.11	0.30	0.38	0.91	0.14	-	0.10	-	0.07	0.05
Na+1	5.64	5.26	5.47	3.67	5.49	5.76	5.76	6.38	5.34	5.10
Ti+4	0.07	-	0.06	-	0.05	-	-	-	-	-
Cr+3	-	-	0.09	-	-	0.05	-	-	-	-
	-	-	-	-	-	-	-	-	-	-
#Si+4	2.74	2.76	2.74	2.90	2.66	2.66	2.69	2.73	2.73	2.74
#Al+3	1.26	1.25	1.24	1.15	1.34	1.32	1.26	1.17	1.25	1.26
#Ca+2x100										
	30.46	29.76	32.02	23.50	33.95	35.20	37.24	41.76	35.01	34.34
#K+1x100										
	0.74	2.03	2.61	6.19	0.97	-	0.69	-	0.51	0.34
#Na+1x100										
	65.46	60.89	63.65	42.35	64.11	67.16	67.57	75.22	62.15	59.22
#TOTAL	4.96	4.93	4.97	4.77	4.99	5.01	5.01	5.06	4.96	4.93
#O-2	8.00	8.00	8.00	8.00	8.00	8.00	8.00	8.00	8.00	8.00
totcat	96.66	92.68	98.29	72.04	99.03	102.36	105.50	116.98	97.68	93.90
totcat / 100										
	0.97	0.93	0.98	0.72	0.99	1.02	1.06	1.17	0.98	0.94
An	31.51	32.11	32.58	32.62	34.28	34.39	35.30	35.70	35.85	36.57
Or	0.76	2.19	2.66	8.60	0.98	-	0.65	-	0.52	0.36
Ab	67.72	65.70	64.76	58.79	64.74	65.61	64.05	64.30	63.63	63.07

fsp.rec
48 samples, 23 elements, Date: 02-28-1991

Page 4

	11.6-1	.4-3 ?	11.0-1	F. 7.5	23.8-1	17.8-1	17.8-1	26.1	68.7-1	OW 60
Si+4	28.57	28.52	28.70	28.49	27.84	28.29	27.88	28.54	27.80	28.37
Al+3	11.34	12.86	11.12	12.81	13.53	11.32	11.51	13.26	13.21	12.95
Fe+2	0.19	0.16	-	0.13	0.15	0.28	0.18	-	0.11	0.12
Mn+2	-	-	-	-	-	-	-	-	-	0.07
Mg+2	-	-	0.13	-	-	-	-	-	-	-
Ca+2	6.30	5.30	6.47	5.47	5.52	6.75	7.21	5.59	6.17	6.04
K+1	0.20	0.28	0.15	0.19	0.15	0.34	0.25	0.04	0.08	0.08
Na+1	6.05	4.99	6.04	5.00	5.01	5.83	5.82	4.46	4.83	4.47
Ti+4	-	-	-	-	-	-	0.09	-	-	-
Cr+3	-	-	-	0.05	-	-	-	-	0.12	-
#Si+4	2.75	2.72	2.76	2.72	2.66	2.74	2.71	2.70	2.66	2.70
#Al+3	1.14	1.28	1.12	1.27	1.34	1.14	1.16	1.31	1.32	1.28
#Ca+2x100	42.56	35.35	43.66	36.52	36.96	45.80	49.04	37.11	41.39	40.33
#K+1x100	1.38	1.93	1.03	1.31	1.02	2.37	1.74	0.28	0.57	0.57
#Na+1x100	71.17	58.10	71.07	58.23	58.49	68.94	68.96	51.61	56.50	52.08
#TOTAL	5.04	4.95	5.04	4.95	4.97	5.05	5.07	4.90	4.96	4.92
#O-2	8.00	8.00	8.00	8.00	8.00	8.00	8.00	8.00	8.00	8.00
totcat	115.10	95.38	115.76	96.06	96.47	117.11	119.73	88.99	98.47	92.97
totcat / 100	1.15	0.95	1.16	0.96	0.96	1.17	1.20	0.89	0.98	0.93
An	36.97	37.06	37.72	38.02	38.31	39.11	40.96	41.69	42.04	43.38
Or	1.20	2.02	0.89	1.36	1.06	2.02	1.45	0.32	0.58	0.61
Ab	61.83	60.91	61.39	60.62	60.63	58.87	57.59	57.99	57.38	56.01

fsp.rec

Page 5

48 samples, 23 elements, Date: 02-28-1991

	39.3-1	F.10.4	400-1	400-1	17.8-3	39.3-1	26.5-2	400-1
Si+4	27.28	28.27	26.80	26.81	26.58	27.98	27.55	27.13
Al+3	11.84	13.01	13.56	13.51	13.77	11.52	13.27	11.55
Fe+2	0.14	0.08	0.18	0.21	-	0.23	0.12	0.16
Mn+2	-	-	-	0.09	0.12	-	-	0.09
Mg+2	-	-	-	-	-	-	-	-
Ca+2	7.91	6.18	7.47	7.58	7.85	8.47	7.61	9.58
K+1	0.39	0.11	0.22	0.32	0.30	0.39	0.11	0.42
Na+1	5.60	4.47	4.52	4.13	4.18	4.28	3.71	4.36
Ti+4	-	-	-	0.07	-	-	-	-
Cr+3	-	-	-	0.05	-	-	0.05	-
	-	-	-	-	-	-	-	-
#Si+4	2.66	2.69	2.59	2.59	2.57	2.71	2.64	2.65
#Al+3	1.20	1.29	1.36	1.36	1.38	1.16	1.32	1.18
#Ca+2x100								
	53.99	41.23	50.54	51.38	53.12	57.46	51.13	65.60
#K+1x100								
	2.73	0.74	1.55	2.19	2.07	2.71	0.74	2.97
#Na+1x100								
	66.63	52.08	53.29	48.86	49.37	50.63	43.44	52.09
#TOTAL	5.09	4.92	5.00	4.98	5.00	4.98	4.92	5.03
#O-2	8.00	8.00	8.00	8.00	8.00	8.00	8.00	8.00
totcat	123.35	94.05	105.39	102.43	104.56	110.80	95.32	120.67
totcat / 100								
	1.23	0.94	1.05	1.02	1.05	1.11	0.95	1.21
An	43.77	43.84	47.95	50.16	50.80	51.86	53.64	54.37
Or	2.21	0.79	1.48	2.14	1.98	2.45	0.78	2.46
Ab	54.02	55.37	50.57	47.70	47.22	45.69	45.58	43.17

APPENDIX B
SEM ANALYSES
ZONED GARNETS

gnt62.CAT

Page 1

7 samples, 24 elements, Date: 12-11-1991

	Core -2 (3)	rim -2 (2)	core -2 (2)	rim 62.0-2	rim 62.0-2	core 62.0-2	core 62.0-2
SiO2	36.35	36.82	37.31	38.40	38.28	37.80	38.23
TiO2	-	-	-	0.14	-	-	-
Al2O3	20.36	20.60	20.31	20.08	20.43	20.65	20.44
Cr2O3	0.08	-	0.20	-	-	-	-
Fe2O3	1.33	1.65	1.19	2.43	1.92	1.15	1.86
FeO	31.79	33.85	33.91	32.54	32.56	33.47	33.10
MnO	1.68	1.57	1.59	1.58	1.73	1.58	1.47
MgO	5.20	4.24	3.98	3.76	4.15	4.29	3.94
CaO	1.01	1.35	1.63	1.31	1.14	1.18	1.16
Total	97.80	100.09	100.12	100.24	100.20	100.11	100.20
#Si IV	5.92	5.91	5.99	6.00	6.00	6.00	6.00
#Al IV	0.08	0.09	0.01	-	-	-	-
T site	6.00	6.00	6.00	6.00	6.00	6.00	6.00
#Al VI	3.83	3.80	3.83	3.70	3.77	3.86	3.78
#Ti VI	-	-	-	0.02	-	-	-
#Cr	0.01	-	0.03	-	-	-	-
#Fe +3	0.16	0.20	0.14	0.29	0.23	0.14	0.22
O site	4.00	4.00	4.00	4.00	4.00	4.00	4.00
#Fe +2	4.33	4.54	4.55	4.25	4.27	4.44	4.34
#Mn +2	0.23	0.21	0.22	0.21	0.23	0.21	0.20
#Mg	1.26	1.01	0.95	0.88	0.97	1.02	0.92
#Ca	0.18	0.23	0.28	0.22	0.19	0.20	0.20
A site	6.00	6.00	6.00	5.56	5.66	5.87	5.66
#O	23.96	23.95	23.99	23.56	23.66	23.87	23.66

All analyses from 62.0-2

APPENDIX C

GARNET-BIOTITE GEOTHERMOMETRY

GEOBAROMETRY

Garnet

Sample id : ga

Analysis- 37.65 .00 21.50 .06 35.06 2.03 4.12 1.05 .00
.00

Biotite

Sample id : bi

Analysis- 35.49 2.67 18.06 .11 20.78 .00 9.26 .00 .09
9.60

1*****

#1-2

=====

==> GARNET-BIOTITE THERMOMETER <==

A.B.Thompson 1976 temperature (C): 677.

Assumed pressure in bars

	2000.	3000.	4000.	5000.	6000.	7000.	8000.	
TEMP.	724.	728.	733.	737.	742.	746.	751.	*1
	737.	742.	746.	751.	755.	760.	764.	*2
(C)	736.	741.	745.	750.	754.	759.	763.	*3
	573.	578.	582.	587.	591.	596.	600.	*4
	647.	656.	665.	674.	683.	692.	701.	*5
	764.	769.	773.	778.	783.	787.	792.	*6

1 - Ferry & Spear 1978

2 - Hodges & Spear 1982, using revised equilibrium constant

3 - Ganguly & Saxena, Am. Min. 69, Ca-Mn correction

4 - Indares & Martignole, Am. Min. 70, Bio Al Ti correction

5 - Perchuk et al, J. Metamorphic Geol. 1985

6 - Hoinkes, C.M.P. (1986)

Garnet
 Sample id : ga
 Analysis- 38.60 .07 21.69 .04 32.01 1.17 6.11 1.18 .00
 .00
 Biotite
 Sample id : bi
 Analysis- 36.53 2.55 18.29 .14 16.55 .03 11.62 .00 .14
 9.48
 1*****
 12.2-2

=====
 =====

==> GARNET-BIOTITE THERMOMETER <==

A.B.Thompson 1976 temperature (C): 687.

Assumed pressure in bars

	2000.	3000.	4000.	5000.	6000.	7000.	8000.	
TEMP.	738.	743.	747.	752.	757.	761.	766.	*1
	754.	758.	763.	768.	772.	777.	782.	*2
(C)	690.	695.	699.	704.	709.	713.	718.	*3
	575.	579.	584.	588.	593.	598.	602.	*4
	655.	664.	673.	683.	692.	701.	710.	*5
	785.	790.	795.	799.	804.	809.	814.	*6

- 1 - Ferry & Spear 1978
- 2 - Hodges & Spear 1982, using revised equilibrium constant
- 3 - Ganguly & Saxena, Am. Min. 69, Ca-Mn correction
- 4 - Indares & Martignole, Am. Min. 70, Bio Al Ti correction
- 5 - Perchuk et al, J. Metamorphic Geol. 1985
- 6 - Hoinkes, C.M.P. (1986)

Garnet

Sample id : ga

Analysis- 37.26 .14 20.85 .07 27.28 6.33 2.24 5.36 .00
.00

Biotite

Sample id : biav

Analysis- 36.80 2.23 16.50 .11 19.56 .21 10.51 .00 .06
9.67

1*****

16.0-A

=====

==> GARNET-BIOTITE THERMOMETER <==

A.B.Thompson 1976 temperature (C): 526.

Assumed pressure in bars

	2000.	3000.	4000.	5000.	6000.	7000.	8000.	
TEMP.	520.	523.	527.	530.	534.	537.	541.	*1
	566.	570.	573.	577.	581.	585.	589.	*2
(C)	602.	605.	609.	613.	616.	620.	623.	*3
	540.	543.	547.	550.	554.	558.	561.	*4
	602.	610.	618.	626.	634.	642.	649.	*5
	627.	631.	635.	640.	644.	648.	652.	*6

1 - Ferry & Spear 1978

2 - Hodges & Spear 1982, using revised equilibrium constant

3 - Ganguly & Saxena, Am. Min. 69, Ca-Mn correction

4 - Indares & Martignole, Am. Min. 70, Bio Al Ti correction

5 - Perchuk et al, J. Metamorphic Geol. 1985

6 - Hoinkes, C.M.P. (1986)

Garnet

Sample id : ga

Analysis- 37.79 .00 21.30 .05 30.41 6.85 3.64 .83 .00
.00

Biotite

Sample id : biav

Analysis- 36.25 1.58 18.51 .11 17.73 .17 11.72 .01 .18
8.27

1*****

18.8-1

=====

==> GARNET-BIOTITE THERMOMETER <==

A.B.Thompson 1976 temperature (C): 568.

Assumed pressure in bars

	2000.	3000.	4000.	5000.	6000.	7000.	8000.	
TEMP.	574.	577.	581.	585.	589.	593.	597.	*1
	581.	585.	589.	593.	597.	601.	604.	*2
(C)	612.	616.	619.	623.	627.	631.	635.	*3
	530.	534.	538.	541.	545.	549.	553.	*4
	569.	577.	585.	593.	602.	610.	618.	*5
	597.	601.	605.	609.	613.	617.	621.	*6

1 - Ferry & Spear 1978

2 - Hodges & Spear 1982, using revised equilibrium constant

3 - Ganguly & Saxena, Am. Min. 69, Ca-Mn correction

4 - Indares & Martignole, Am. Min. 70, Bio Al Ti correction

5 - Perchuk et al, J. Metamorphic Geol. 1985

6 - Hoinkes, C.M.P. (1986)

Garnet

Sample id : ga

Analysis- 37.89 .00 21.28 .02 35.22 .84 4.43 1.26 .00
.00

Biotite

Sample id : bi

Analysis- 36.24 1.61 18.29 .06 19.57 .18 10.03 .00 .14
9.39

1*****

#2-8.7

=====
=====

==> GARNET-BIOTITE THERMOMETER <==

A.B.Thompson 1976 temperature (C): 654.

Assumed pressure in bars

	2000.	3000.	4000.	5000.	6000.	7000.	8000.	
TEMP.	691.	696.	700.	704.	709.	713.	717.	*1
	706.	711.	715.	720.	724.	729.	733.	*2
(C)	691.	695.	699.	704.	708.	712.	717.	*3
	553.	557.	562.	566.	571.	575.	579.	*4
	635.	643.	652.	661.	670.	679.	688.	*5
	736.	741.	746.	750.	755.	759.	764.	*6

1 - Ferry & Spear 1978

2 - Hodges & Spear 1982, using revised equilibrium constant

3 - Ganguly & Saxena, Am. Min. 69, Ca-Mn correction

4 - Indares & Martignole, Am. Min. 70, Bio Al Ti correction

5 - Perchuk et al, J. Metamorphic Geol. 1985

6 - Hoinkes, C.M.P. (1986)

Garnet

Sample id : ga

Analysis- 37.60 .10 21.20 .04 26.94 7.84 2.30 5.02 .00
.00

Biotite

Sample id : biav

Analysis- 36.56 2.07 18.27 .09 18.44 .21 10.52 .00 .15
9.36

1*****

24.6

=====

==> GARNET-BIOTITE THERMOMETER <==

A.B.Thompson 1976 temperature (C): 521.

Assumed pressure in bars

	2000.	3000.	4000.	5000.	6000.	7000.	8000.	
TEMP.	513.	517.	520.	524.	528.	531.	535.	*1
	555.	559.	562.	566.	570.	574.	577.	*2
(C)	598.	601.	605.	608.	612.	615.	619.	*3
	539.	543.	546.	550.	553.	557.	561.	*4
	592.	600.	608.	616.	624.	632.	639.	*5
	614.	618.	622.	626.	630.	634.	638.	*6

1 - Ferry & Spear 1978

2 - Hodges & Spear 1982, using revised equilibrium constant

3 - Ganguly & Saxena, Am. Min. 69, Ca-Mn correction

4 - Indares & Martignole, Am. Min. 70, Bio Al Ti correction

5 - Perchuk et al, J. Metamorphic Geol. 1985

6 - Hoinkes, C.M.P. (1986)

Garnet
 Sample id : ga
 Analysis- 38.03 .02 21.41 .09 31.55 2.68 3.83 .09 .00
 .00
 Biotite
 Sample id : biav
 Analysis- 37.53 1.53 17.40 .09 17.73 .06 11.81 .02 .08
 9.43
 1*****
 31.5

=====
 =====

==> GARNET-BIOTITE THERMOMETER <==

A.B.Thompson 1976 temperature (C): 569.

Assumed pressure in bars

	2000.	3000.	4000.	5000.	6000.	7000.	8000.	
TEMP.	575.	579.	583.	587.	591.	595.	599.	*1
	576.	580.	584.	588.	592.	596.	600.	*2
(C)	582.	586.	590.	594.	597.	601.	605.	*3
	468.	472.	476.	479.	483.	487.	491.	*4
	559.	567.	576.	584.	592.	601.	609.	*5
	578.	582.	586.	590.	594.	598.	601.	*6

- 1 - Ferry & Spear 1978
- 2 - Hodges & Spear 1982, using revised equilibrium constant
- 3 - Ganguly & Saxena, Am. Min. 69, Ca-Mn correction
- 4 - Indares & Martignole, Am. Min. 70, Bio Al Ti correction
- 5 - Perchuk et al, J. Metamorphic Geol. 1985
- 6 - Hoinkes, C.M.P. (1986)

Garnet
 Sample id : ga
 Analysis- 38.03 .00 21.44 .05 30.05 5.47 3.71 2.40 .00
 .00
 Biotite
 Sample id : biav
 Analysis- 37.18 2.13 17.28 .14 18.56 .14 11.69 .00 .20
 8.97
 1*****
 37.5

=====
 =====

==> GARNET-BIOTITE THERMOMETER <==

A.B.Thompson 1976 temperature (C): 589.

Assumed pressure in bars

	2000.	3000.	4000.	5000.	6000.	7000.	8000.	
TEMP.	601.	605.	609.	613.	617.	621.	625.	*1
	625.	629.	634.	638.	642.	646.	650.	*2
(C)	642.	646.	650.	654.	658.	662.	666.	*3
	558.	562.	566.	570.	574.	578.	582.	*4
	606.	614.	623.	631.	640.	648.	656.	*5
	670.	674.	678.	682.	687.	691.	695.	*6

- 1 - Ferry & Spear 1978
- 2 - Hodges & Spear 1982, using revised equilibrium constant
- 3 - Ganguly & Saxena, Am. Min. 69, Ca-Mn correction
- 4 - Indares & Martignole, Am. Min. 70, Bio Al Ti correction
- 5 - Ferchuk et al, J. Metamorphic Geol. 1985
- 6 - Hoinkes, C.M.P. (1986)

Garnet

Sample id : ga

Analysis- 37.88 .00 21.41 .02 33.39 3.06 3.86 1.05 .00
 .00

Biotite

Sample id : biav

Analysis- 35.32 2.52 18.34 .11 21.24 .12 8.95 .00 .10
 9.09

1*****

52.3 ga-bi

=====

==> GARNET-BIOTITE THERMOMETER <==

A.B.Thompson 1976 temperature (C): 690.

Assumed pressure in bars

	2000.	3000.	4000.	5000.	6000.	7000.	8000.	
TEMP.	743.	747.	752.	757.	761.	766.	771.	*1
	757.	762.	766.	771.	776.	780.	785.	*2
(C)	766.	770.	775.	779.	784.	788.	793.	*3
	610.	615.	619.	624.	628.	633.	638.	*4
	656.	665.	674.	683.	692.	701.	710.	*5
	786.	791.	795.	800.	805.	810.	815.	*6

1 - Ferry & Spear 1978

2 - Hodges & Spear 1982, using revised equilibrium constant

3 - Ganguly & Saxena, Am. Min. 69, Ca-Mn correction

4 - Indares & Martignole, Am. Min. 70, Bio Al Ti correction

5 - Perchuk et al, J. Metamorphic Geol. 1985

6 - Hoinkes, C.M.P. (1986)

Garnet
 Sample id : ga
 Analysis- 38.40 .00 21.41 .04 34.09 2.10 4.39 .85 .00
 .00
 Biotite
 Sample id : biav
 Analysis- 36.17 2.94 18.61 .14 19.09 .11 9.33 .00 .13
 9.62
 1*****
 53.9

=====
 =====

==> GARNET-BIOTITE THERMOMETER <==

A.B.Thompson 1976 temperature (C): 677.

Assumed pressure in bars

	2000.	3000.	4000.	5000.	6000.	7000.	8000.	
TEMP.	723.	728.	732.	737.	741.	746.	750.	*1
	734.	739.	743.	748.	753.	757.	762.	*2
(C)	726.	731.	735.	740.	744.	748.	753.	*3
	556.	561.	565.	570.	574.	579.	583.	*4
	644.	653.	662.	671.	680.	689.	698.	*5
	757.	761.	766.	771.	775.	780.	785.	*6

- 1 - Ferry & Spear 1978
- 2 - Hodges & Spear 1982, using revised equilibrium constant
- 3 - Ganguly & Saxena, Am. Min. 69, Ca-Mn correction
- 4 - Indares & Martignole, Am. Min. 70, Bio Al Ti correction
- 5 - Perchuk et al, J. Metamorphic Geol. 1985
- 6 - Hoinkes, C.M.P. (1986)

Garnet

Sample id : ga

Analysis- 37.56 .04 21.39 .10 33.45 3.59 4.13 .10 .00
.00

Biotite

Sample id : biav

Analysis- 35.98 1.93 18.38 .13 19.79 .13 9.97 .01 .11
9.32

1*****

56.7

=====
=====

==> GARNET-BIOTITE THERMOMETER <==

A.B.Thompson 1976 temperature (C): 654.

Assumed pressure in bars

	2000.	3000.	4000.	5000.	6000.	7000.	8000.	
TEMP.	691.	695.	699.	704.	708.	712.	717.	*1
	692.	696.	701.	705.	709.	714.	718.	*2
(C)	702.	706.	710.	715.	719.	723.	727.	*3
	567.	572.	576.	580.	585.	589.	594.	*4
	617.	626.	635.	643.	652.	661.	670.	*5
	694.	699.	703.	707.	712.	716.	721.	*6

1 - Ferry & Spear 1978

2 - Hodges & Spear 1982, using revised equilibrium constant

3 - Ganguly & Saxena, Am. Min. 69, Ca-Mn correction

4 - Indares & Martignole, Am. Min. 70, Bio Al Ti correction

5 - Perchuk et al, J. Metamorphic Geol. 1985

6 - Hoinkes, C.M.P. (1986)

Garnet
 Sample id : ga
 Analysis- 38.02 .01 21.32 .01 32.17 2.87 4.45 .88 .00
 .00
 Biotite
 Sample id : biav
 Analysis- 36.12 2.06 18.97 .10 18.30 .11 10.33 .00 .19
 9.42
 1*****
 59.8

=====
 =====

==> GARNET-BIOTITE THERMOMETER <==

A.B.Thompson 1976 temperature (C): 654.

Assumed pressure in bars

	2000.	3000.	4000.	5000.	6000.	7000.	8000.	
TEMP.	690.	695.	699.	704.	708.	712.	717.	*1
	701.	706.	710.	715.	719.	723.	728.	*2
(C)	693.	697.	702.	706.	710.	715.	719.	*3
	564.	569.	573.	577.	582.	586.	590.	*4
	629.	638.	647.	656.	664.	673.	682.	*5
	723.	728.	732.	737.	741.	746.	750.	*6

- 1 - Ferry & Spear 1978
- 2 - Hodges & Spear 1982, using revised equilibrium constant
- 3 - Ganguly & Saxena, Am. Min. 69, Ca-Mn correction
- 4 - Indares & Martignole, Am. Min. 70, Bio Al Ti correction
- 5 - Perchuk et al, J. Metamorphic Geol. 1985
- 6 - Hoinkes, C.M.P. (1986)

Garnet

Sample id : ga

Analysis- 37.71 .00 21.34 .00 36.80 .81 3.25 1.14 .00
.00

Biotite

Sample id : biav

Analysis- 34.87 2.23 19.36 .11 22.54 .05 6.90 .00 .08
9.59

1*****

62.0-1

=====

==> GARNET-BIOTITE THERMOMETER <==

A.B.Thompson 1976 temperature (C): 708.

Assumed pressure in bars

	2000.	3000.	4000.	5000.	6000.	7000.	8000.	
TEMP.	768.	772.	777.	782.	787.	791.	796.	*1
	784.	789.	793.	798.	803.	808.	813.	*2
(C)	800.	805.	809.	814.	819.	823.	828.	*3
	590.	595.	600.	604.	609.	614.	619.	*4
	668.	677.	687.	696.	705.	714.	723.	*5
	816.	821.	826.	831.	836.	841.	846.	*6

1 - Ferry & Spear 1978

2 - Hodges & Spear 1982, using revised equilibrium constant

3 - Ganguly & Saxena, Am. Min. 69, Ca-Mn correction

4 - Indares & Martignole, Am. Min. 70, Bio Al Ti correction

5 - Perchuk et al, J. Metamorphic Geol. 1985

6 - Hoinkes, C.M.F. (1986)

Garnet

Sample id : ga

Analysis- 37.90 .01 21.17 .01 34.64 1.91 3.47 1.27 .00
.00

Biotite

Sample id : biav

Analysis- 34.76 2.19 18.80 .09 22.53 .07 7.69 .02 .20
8.93

1*****

62.0-2

=====

==> GARNET-BIOTITE THERMOMETER <==

A.B.Thompson 1976 temperature (C): 714.

Assumed pressure in bars

	2000.	3000.	4000.	5000.	6000.	7000.	8000.	
TEMP.	777.	782.	786.	791.	796.	801.	805.	*1
	795.	800.	805.	810.	815.	820.	824.	*2
(C)	807.	812.	817.	821.	826.	831.	836.	*3
	628.	633.	638.	642.	647.	652.	657.	*4
	675.	684.	693.	702.	712.	721.	730.	*5
	832.	837.	842.	847.	853.	858.	863.	*6

1 - Ferry & Spear 1978

2 - Hodges & Spear 1982, using revised equilibrium constant

3 - Ganguly & Saxena, Am. Min. 69, Ca-Mn correction

4 - Indares & Martignole, Am. Min. 70, Bio Al Ti correction

5 - Ferchuk et al, J. Metamorphic Geol. 1985

6 - Hoinkes, C.M.F. (1986)

Garnet

Sample id : ga

Analysis- 37.49 .00 21.44 .00 31.37 4.46 3.18 3.05 .00
 .00

Biotite

Sample id : biav

Analysis- 36.04 1.93 16.77 .10 20.34 .10 10.36 .01 .28
 8.92

1*****

63.8

=====

==> GARNET-BIOTITE THERMOMETER <==

A.B.Thompson 1976 temperature (C): 593.

Assumed pressure in bars

	2000.	3000.	4000.	5000.	6000.	7000.	8000.	
TEMP.	607.	611.	615.	619.	623.	627.	631.	*1
	638.	642.	646.	650.	654.	658.	663.	*2
(C)	659.	663.	667.	671.	675.	679.	683.	*3
	566.	570.	573.	577.	581.	585.	589.	*4
	618.	627.	635.	643.	652.	660.	668.	*5
	692.	696.	701.	705.	710.	714.	718.	*6

1 - Ferry & Spear 1978

2 - Hodges & Spear 1982, using revised equilibrium constant

3 - Ganguly & Saxena, Am. Min. 69, Ca-Mn correction

4 - Indares & Martignole, Am. Min. 70, Bio Al Ti correction

5 - Perchuk et al, J. Metamorphic Geol. 1985

6 - Hoinkes, C.M.P. (1986)

Garnet

Sample id : ga

Analysis- 37.49 .00 21.23 .03 37.10 .28 2.20 2.79 .00
.00

Biotite

Sample id : biav

Analysis- 36.50 1.41 17.47 .06 24.12 .06 8.31 .00 .16
8.82

1*****

68.3-3

=====

==> GARNET-BIOTITE THERMOMETER <==

A.B.Thompson 1976 temperature (C): 555.

Assumed pressure in bars

	2000.	3000.	4000.	5000.	6000.	7000.	8000.	
TEMP.	556.	560.	564.	568.	571.	575.	579.	*1
	582.	586.	590.	593.	597.	601.	605.	*2
(C)	612.	616.	619.	623.	627.	631.	634.	*3
	465.	469.	473.	477.	480.	484.	488.	*4
	587.	595.	604.	612.	620.	628.	636.	*5
	627.	631.	635.	639.	643.	647.	651.	*6

1 - Ferry & Spear 1978

2 - Hodges & Spear 1982, using revised equilibrium constant

3 - Ganguly & Saxena, Am. Min. 69, Ca-Mn correction

4 - Indares & Martignole, Am. Min. 70, Bio Al Ti correction

5 - Perchuk et al, J. Metamorphic Geol. 1985

6 - Hoinkes, C.M.P. (1986)

Garnet
 Sample id : ga
 Analysis- 37.40 .00 21.31 .06 31.59 7.39 2.76 .95 .00
 .00
 Biotite
 Sample id : bi
 Analysis- 36.49 1.47 19.45 .05 18.03 .18 10.70 .00 .36
 8.82
 1*****
 78.7

=====
 =====

==> GARNET-BIOTITE THERMOMETER <==

A.B.Thompson 1976 temperature (C): 517.

Assumed pressure in bars

	2000.	3000.	4000.	5000.	6000.	7000.	8000.	
TEMP.	508.	512.	516.	519.	523.	526.	530.	*1
	516.	520.	523.	527.	530.	534.	537.	*2
(C)	564.	568.	571.	575.	578.	582.	585.	*3
	472.	475.	479.	482.	486.	490.	493.	*4
	534.	542.	550.	558.	565.	573.	581.	*5
	531.	535.	538.	542.	546.	549.	553.	*6

- 1 - Ferry & Spear 1978
- 2 - Hodges & Spear 1982, using revised equilibrium constant
- 3 - Ganguly & Saxena, Am. Min. 69, Ca-Mn correction
- 4 - Indares & Martignole, Am. Min. 70, Bio Al Ti correction
- 5 - Perchuk et al, J. Metamorphic Geol. 1985
- 6 - Hoinkes, C.M.P. (1986)

Garnet

Sample id : GA

Analysis- 37.50 .05 21.65 .00 34.31 1.53 4.94 1.35 .00
.00

Biotite

Sample id : BIAV

Analysis- 35.79 3.55 18.93 .11 18.45 .06 8.97 .01 .06
9.65

1*****

S.F. 10.4

=====

==> GARNET-BIOTITE THERMOMETER <==

A.B.Thompson 1976 temperature (C): 717.

Assumed pressure in bars

	2000.	3000.	4000.	5000.	6000.	7000.	8000.	
TEMP.	782.	787.	791.	796.	801.	806.	810.	*1
	801.	806.	811.	815.	820.	825.	830.	*2
(C)	772.	777.	782.	786.	791.	796.	800.	*3
	583.	588.	593.	598.	603.	607.	612.	*4
	677.	686.	696.	705.	714.	723.	733.	*5
	839.	844.	849.	854.	859.	864.	869.	*6

1 - Ferry & Spear 1978

2 - Hodges & Spear 1982, using revised equilibrium constant

3 - Ganguly & Saxena, Am. Min. 69, Ca-Mn correction

4 - Indares & Martignole, Am. Min. 70, Bio Al Ti correction

5 - Perchuk et al, J. Metamorphic Geol. 1985

6 - Hoinkes, C.M.P. (1986)

Garnet

Sample id : GA

Analysis- 37.79 .00 21.54 .07 34.04 1.61 4.70 1.10 .00
 .00

Biotite

Sample id : BIAV

Analysis- 36.46 2.53 17.62 .10 17.48 .06 11.81 .00 .13
 9.57

1*****

S.F. 2

=====

==> GARNET-BIOTITE THERMOMETER <==

A.B.Thompson 1976 temperature (C): 600.

Assumed pressure in bars

	2000.	3000.	4000.	5000.	6000.	7000.	8000.	
TEMP.	616.	620.	625.	629.	633.	637.	641.	*1
	628.	632.	636.	640.	644.	648.	652.	*2
(C)	611.	615.	619.	623.	627.	631.	635.	*3
	484.	488.	492.	496.	500.	505.	509.	*4
	595.	604.	612.	621.	629.	638.	646.	*5
	650.	654.	659.	663.	667.	671.	675.	*6

1 - Ferry & Spear 1978

2 - Hodges & Spear 1982, using revised equilibrium constant

3 - Ganguly & Saxena, Am. Min. 69, Ca-Mn correction

4 - Indares & Martignole, Am. Min. 70, Bio Al Ti correction

5 - Perchuk et al, J. Metamorphic Geol. 1985

6 - Hoinkes, C.M.P. (1986)

Garnet

Sample id : ga

Analysis- 38.40 .00 21.41 .04 34.09 2.10 4.39 .85 .00
.00

Plagioclase

Sample id : plag

Analysis- 60.82 .00 23.37 .00 .00 .00 .00 5.47 10.16
.18

==> Cationic charge deficiency = .339

Biotite

Sample id : biav

Analysis- 36.17 2.94 18.61 .14 19.09 .11 9.33 .00 .13
9.62

1*****

53.9 ga-bi-pl-als-q

=====

=====

==> GRD-AN-QZ-ALS BAROMETER <==

Assumed Temperature (C)

	700.	400.	500.	600.	700.	800.	900.
Press.	4344.	280.	1635.	2989.	4344.	5698.	7053.
*1							
(bars)	4905.	969.	2281.	3593.	4905.	6217.	7528.
*2							
	5723.	1970.	3225.	4476.	5723.	6966.	8206.
*3							
	5704.	1724.	3051.	4377.	5704.	7031.	8358.
*4							

==> Simultaneous solution of gt-bi & gt-pl

736. C at 4834. bars

714. C at 5093. bars

714. C at 5901. bars (Koziol & Newton

recalibration)

==> With Ganguly and Saxena mn corr, to gro activity

Assumed Temperature (C)

	700.	400.	500.	600.	700.	800.	900.
Press.	3113.	-571.	657.	1885.	3113.	4341.	5569.
*1							
(bars)	2953.	-381.	730.	1842.	2953.	4064.	5176.

*2
 | 3771. 620. 1674. 2725. 3771. 4814. 5853. |
 *3

==> Simultaneous solution of gt-bi & gt-pl

730. C at 3482. bars

714. C at 3112. bars

714. C at 3921. bars (Koziol & Newton

recalibration)

/1 - Ghent et al, 1979 gro-an-qz-als barometer

2 - Newton and Haselton, 1981 gro-an-qz-als barometer

3 - Newton and Haselton, 1981 gro-an-qz-als barometer with
 Koziol & Newton

recalibration of end member reaction

4 - Hodges and Spear, 1982 Barometer with anorthite activity
 modification

of Hodges & Royden(1984))

=====
 =====

==> GARNET-BIOTITE THERMOMETER <==

A.B.Thompson 1976 temperature (C): 677.

Assumed pressure in bars

	2000.	3000.	4000.	5000.	6000.	7000.	8000.	
TEMP.	723.	728.	732.	737.	741.	746.	751.	*1
	734.	739.	743.	748.	753.	757.	762.	*2
(C)	726.	731.	735.	740.	744.	749.	753.	*3
	556.	561.	565.	570.	574.	579.	583.	*4
	644.	653.	662.	671.	680.	689.	698.	*5
	757.	761.	766.	771.	775.	780.	785.	*6

1 - Ferry & Spear 1978

2 - Hodges & Spear 1982, using revised equilibrium constant

3 - Ganguly & Saxena, Am. Min. 69, Ca-Mn correction

4 - Indares & Martignole, Am. Min. 70, Bio Al Ti correction

5 - Perchuk et al, J. Metamorphic Geol. 1985

6 - Hoinkes, C.M.P. (1986)

Garnet

Sample id : ga

Analysis- 38.40 .00 21.41 .04 34.09 2.10 4.39 .85 .00
 .00

Plagioclase

Sample id : plag

Analysis- 60.82 .00 23.37 .00 .00 .00 .00 5.47 10.16
 .18

==> Cationic charge deficiency = .339

|*****|

53.9 ga-pl-als-q

=====

==> GRO-AN-QZ-ALS BAROMETER <==

Assumed Temperature (C)

	700.	400.	500.	600.	700.	800.	900.
Press.	4344.	280.	1635.	2989.	4344.	5698.	7053.
*1							
(bars)	4905.	969.	2281.	3593.	4905.	6217.	7528.
*2							
	5723.	1970.	3225.	4476.	5723.	6966.	8206.
*3							
	5704.	1724.	3051.	4377.	5704.	7031.	8358.
*4							

==> With Ganguly and Saxena mn corr, to gro activity

Assumed Temperature (C)

	700.	400.	500.	600.	700.	800.	900.
Press.	3113.	-571.	657.	1885.	3113.	4341.	5569.
*1							
(bars)	2953.	-381.	730.	1842.	2953.	4064.	5176.
*2							
	3771.	620.	1674.	2725.	3771.	4814.	5853.
*3							

/1 - Ghent et al,1979 gro-an-qz-als barometer

2 - Newton and Haselton,1981 gro-an-qz-als barometer

3 - Newton and Haselton,1981 gro-an-qz-als barometer with
Koziol & Newton

recalibration of end member reaction

4 - Hodges and Spear,1982 Barometer with anorthite activity
modification of Hodges & Royden(1984))